# Windtunnel modelling of torch fires

Final report


Referencenumber 91-422
Filenumber 112324-18767/22863-TOR
Date November 1991
NP



Author
F.J. Verheij
N.J. Duijm



Keywords:
- dispersion
- fires
- windtunnels
- scaling

ST-code:
G.10


A data diskette containing the experimental data can be obtained from the author


Intended for:
CEC programme 'Major Technological Hazards'
Theme EV4T16
Project FG: 'Physical modelling of Torch Fires'

## Summary

Five European Institutes have been cooperating in the project 'Physical Modelling of Torch Fires' in which the influence of flames on its surroundings is studied. In the framework of this project TNO Institute of Environmental and Energy Technology has applied small scale modelling of flames in one of their windtunnels.

The aim of the experiments is to find proper scaling rules with respect to temperature and heat flux of flames. To this end 7 out of the 10 field measurements performed by Risø, Denmark have been repeated in the windtunnel on scales 1:10 and 1:25 (3 out of these 7).

The shape of the flames, temperature profiles and heat fluxes of both model and field scale have been compared. The field scale mean wind velocities range from 2.2 to 5.2 m/s. The ratio between the gas exit velocity and the mean wind velocity range from 4 to 32.

The following can be concluded:

- flame lengths are modelled well down to scale 1:25 applying the Froude number similarity;
- the shape of the flame is modelled well down to scale 1:25 applying the Froude number similarity except for the difference in the buoyancy between the field and the windtunnel measurements;
- temperature profiles are modelled well down to scale 1:25 applying Froude number similarity. This holds only for the mean values. However, there is a difference in the buoyancy between the open air and the windtunnel configuration. This results in a difference of the shift of the 'tail' of the flame in vertical direction;
- heat fluxes can not be scaled applying the Boltzmann number. This is probably due to a higher formation of soot in the windtunnel flames compared to the field flames. The heat flux sensors therefore 'see' lower temperatures in the former flames resulting in lower heat fluxes. Though the comparison between the 1:10 and the 1:25 scale measurements is very good.

# Table of contents

## List of symbols

| | | |
|---|---|---|
| Bo | Boltzmann number, $\varepsilon_{max}.\sigma(T_{max}^4-T_\infty^4)/\rho.C_p.U.T_{max}$ | (-) |
| $C_p$ | specific heat | (J/kgK) |
| D | diameter of the burner exit | (m) |
| Fr | Froude number, $U^2/g.D$ | (-) |
| g | acceleration of gravity | ($m/s^2$) |
| H | height of the burner outlet above ground level | (m) |
| Q | heat flux | ($W/m^2$) |
| Re | Reynolds number, $U_f.D/\nu_f$ | (-) |
| $T_f$ | temperature of the fuel | (°C) |
| $T_{max}$ | maximum temperature of the flame | (°C) |
| U | mean wind speed | (m/s) |
| $U_a$ | wind speed at level 2.H | (m/s) |
| $U_f$ | fuel speed at burner outlet | (m/s) |
| $u_*$ | friction velocity | (m/s) |
| z | height | (m) |
| $z_0$ | roughness length | (m) |
| $\kappa$ | von Karman constant, $\kappa$=0.4 | (-) |
| $\varepsilon_{max}$ | maximum emissivity | (-) |
| $\rho$ | density | ($kg/m^3$) |
| $\sigma$ | Stefan-Boltzmann constant, $\sigma=5.67x10^{-8}$ | ($J/smK^4$) |
| $\sigma_u$ | standard deviation of the wind speed fluctuations | (m/s) |

**Subscripts:**

| | |
|---|---|
| a | ambient |
| f | fuel |
| fs | field scale |
| m | model scale |

# 1 Introduction

A considerable part of the project 'Physical modelling of torch fires' consists of windtunnel experiments. Aim of these experiments is to investigate the influence of scaling on the shape, the temperature and the heat flux of flames.

The windtunnel experiments consist of two series. The first series has been carried out in May/June 1989. Basic idea of these series was to model field experiments at scales of 1:10 and 1:25 applying the Froude number similarity on wind speed and burner sizes (see Duijm and Bisgaard '88). The field experiments were expected to be carried out with a burner exit diameter of 0.10 m and low wind velocities. Finally these boundary conditions turned out to be somewhat different. The first series of the windtunnel experiments therefore only can be compared mutually and can not be used for comparison with the field experiments and the second series of the windtunnel experiments.
From the former experiments it appeared that applying Froude number similarity and correcting the heat flux by the difference in Boltzmann numbers (assuming equal emissivities) a correct way of scaling is obtained for scaling factors up to 2.5. The results of the first series of experiments have been described in a separate TNO report (Verheij and Duijm '89).

The aim of the second series of experiments, described in this report and carried out in the period February/April 1991, is to apply the aforementioned scaling rules on larger scaling factors. To this end 7 out of the 10 field measurements performed by Risø, Denmark (Ott '91) have been repeated in the windtunnel on scales 1:10 and 1:25 (3 out of these 7).
The experiments have been performed at the largest atmospheric boundary layer windtunnel (number 4) at TNO Institute for Environmental and Energy Technology, Apeldoorn. The windtunnel lay-out has been described in Verheij and Duijm '89. A brief description of the measuring device used is written in chapter 2. In this chapter an overview of the performed experiments and a description of the simulated atmospheric boundary layer are also given.

The general data processing and the results of the experiments are described and discussed in chapter 3. Comparisons between model and field scale have been made on the shape of the flames, temperature profiles and heat fluxes.

In chapter 4 concluding remarks including recommendations for future experiments are given.

# 2 Description of the experiments

## 2.1 The windtunnel lay-out

The flame experiments have been performed at windtunnel number 4 (also called LIA, Large Industrial Aerodynamics windtunnel) being the largest windtunnel at TNO Institute for Environmental and Energy Technology. This tunnel is a so-called atmospheric boundary layer windtunnel.
A description of the windtunnel lay-out is to be found in Verheij & Duijm '89; the basis for the modelling can be found in Duijm & Bisgaard '88.

The fuel used for the experiments is Dutch natural gas. The gas supply can be regulated between 0 and approximately $4.10^{-3}$ $m^3/s$. A description of the gas control unit is to be found in the same report.

## 2.2 The measuring equipment

The measuring equipment for the windtunnel flame experiments comprise:
- one pyrometer for temperature measurements;
- two heat flux sensors;
- one flow meter;
- several temperature transducers;
- two pressure transducers;
- one velocity transducer;
- two data samplers.

Except for the pyrometer and the heat flux sensors the devices are the same as used for the first series of experiments. These have already been described in Verheij and Duijm '89.
In appendix A technical data of the pyrometer and the heat flux sensors is given.

*Pyrometer*
At the TNO Institute for Environmental and Energy Technology laboratories an improved pyrometer is manufactured especially for the 1991 windtunnel flame experiments (see figure 2). This pyrometer consist of a 10% PtRh-Pt thermocouple. Its sizes are smaller than the one used in the 1989 experiments. The diameter of the wires is only 0.2 mm and the weld is approximately 0.5 to 1 mm. The wires are enveloped by a small two holes ceramic tube but the weld is unprotected. The reason for this new measuring strategy was that both the mass and the size of the weld of the present pyrometer are so small and the sucked gas and/or air volume of the previous pyrometer is relative large that it was expected to obtain:
- a better spatial resolution, and thus measuring higher temperatures in the narrow high temperature zones and at the edges;
- a better temporal resolution, and thus measuring more realistic temperature fluctuations.

In principle a passive, i.e. without suction, pyrometer will underestimate temperatures due to radiation from the hot pyrometer to the cold surroundings.

Theoretically it can be shown that this systematic error decreases when the size of the instrument decreases.
The ceramic tube is on its turn enveloped by a stainless steel tube with another ceramic tube at the end.

In order to test the new equipment one of the 1989 experiments has been repeated (D=10 mm, $U_a$=0.8 m/s, $U_f$=5.0 m/s). With the new pyrometer we measured higher mean temperatures and more pronounced vertical profiles of the rms-values of the temperature. The maximum temperature measured now was 1260 °C.
The results confirm our expectations and proved the correctness of the new strategy.

*Heat flux sensors*
Two heat flux sensors are used to measure the heat flux at the windtunnel ground floor surface. These heat flux sensors consist of a thermopile, formed by a large number of thermocouples, embedded into a filling and enclosing material. The thermopile generates an output signal in the millivolt range. In figure 3 a heat flux sensor and its principle is shown.
The sensors used for the 1991 measurements have been developed by TNO Technical Physical Services Laboratories especially for the windtunnel measurements based on the experience of the former 1989 experiments. The sizes of the sensors are 24 mm diameter and 4 mm height. The other transport of heat in the sensors is negligible compared to the radiation.

From the repeated experiment (see also under *pyrometer*) it appeared that the measured heat fluxes are now about 20 to 30% higher.

## 2.3 The boundary layer profile

The experiments have been performed at two different scales compared to the field experiments, i.e. 1:10 and 1:25. For the experiments carried out during the period of February/April 1991 a smooth windtunnel floor partially covered with small blocks has been used simulating the Risø site with an average terrain roughness of $3.8 \times 10^{-4}$ m.
The profile measurements were focused on the 1:10 scale experiments in the lower part of the boundary layer. We therefore tried to create a roughness length of the tunnel floor of $3.8 \times 10^{-5}$. Both the mean wind speed and the turbulence profile have been measured at two different wind speeds of 1.0 and 2.0 m/s respectively at a reference height of 1.0 m. The wind speeds and reference height correspond to 3.2 and 6.4 m/s and 10 m field scale.
The profiles are shown in figures 4 (windspeed) and figure 5 (turbulence). In these figures also the profiles according to the following formulas have been drawn:

mean wind speed: $U = u_*/\kappa \ln(z/z_0)$
turbulence: $\sigma_u/U = 2.2.\kappa/\ln(z/z_0)$

in which: U = mean wind speed (m/s);
$u_*$ = friction wind speed (m/s);
$\kappa$ = von Karman constant (-);
z = height (m);
$z_0$ = roughness length (m);
$\sigma_u$ = standard deviation of the wind speed fluctuations (m/s).

A proper scaling of the profiles turned out to be very difficult for the combination low roughness and low wind speeds. Especially the turbulence profile shows great dependency on the mean wind speed. The final results as shown in the figures were satisfying sufficiently regarding the torch fires experiments.

## 2.4 Overview of the performed experiments

As already mentioned the experiments have been performed at scales 1:10 and 1:25 compared to the Risø field experiments. The experiments are restricted to certain boundaries as to the mean wind speed and the gas flow. In order to keep the model flame burning at higher wind and/or gas velocities a heated filament was placed about 1 cm behind the burner exit. We were therefore not able to measure the flame temperature in the vicinity of the burner exit (see the results of the experiments).
The layout of the burner configuration, similar to the Risø experiments, is shown in figure 6.

An overview of the performed experiments is given in table 1. In this table the mean wind speed $U_a$ (at 5 m height field scale), the gas velocity at the burner exit $U_f$, the ratio between these velocities and the Froude number Fr at both model and field scale are presented. The Froude number is defined as:

$$Fr = U_a^2/g.D$$

The velocity ratio $U_f/U_a$ ranges from approximately 4 to 32, the Froude number ranges from 10 to 55.

In table 1 the mean velocities of both the air and the fuel (gas), the ratio between these velocities and the Froude number are given. The first two columns represent the experiments numbers defined by Risø and TNO respectively, the third and fourth column the Risø field scale values, the fifth and sixth column the TNO model scale values and the latter two contain values which are scale independent. For experiments 11 and 12 only temperature measurements have been performed. The experiments are ranked on $U_f$.

*Table 1 Performed experiments, February/March 1991*

*a) overall parameters*

| | H (m) | $z_0$ (m) | D (m) |
|---|---|---|---|
| field scale | 2.50 | 3.8E-04 | 0.050 |
| 1:10 model scale | 0.25 | 3.8E-05 | 0.005 |
| 1:25 model scale | 0.10 | 1.5E-05 | 0.002 |

*b) scale 1:10 experiments*

| Exp. number | | Field scale | | Model scale (1:10) | | | |
|---|---|---|---|---|---|---|---|
| Risø | TNO | $U_a$ | $U_f$ | $U_a$ | $U_f$ | $U_f/U_a$ | Fr |
| R6a | 2 | 2.2 | 19 | 0.70 | 6.0 | 8.6 | 10 |
| R5c | 1 | 4.4 | 20 | 1.39 | 6.3 | 4.5 | 39 |
| R6b | 9 | 2.5 | 39 | 0.79 | 12.3 | 15.6 | 13 |
| R5b | 8 | 5.2 | 40 | 1.64 | 12.6 | 7.7 | 55 |
| R6c | 7 | 2.6 | 83 | 0.82 | 26.2 | 31.9 | 14 |
| R7c | 3 | 3.9 | 83 | 1.23 | 26.2 | 21.3 | 31 |
| R5a | 6 | 4.8 | 83 | 1.52 | 26.2 | 17.3 | 47 |

*c) scale 1:25 experiments*

| Exp. number | | Field scale | | Model scale (1:25) | | | |
|---|---|---|---|---|---|---|---|
| Risø | TNO | $U_a$ | $U_f$ | $U_a$ | $U_f$ | $U_f/U_a$ | Fr |
| R5b | 12 | 5.2 | 40 | 1.04 | 8.0 | 7.7 | 55 |
| R6c | 11 | 2.6 | 83 | 0.52 | 16.6 | 31.9 | 14 |
| R5a | 10 | 4.8 | 83 | 0.96 | 16.6 | 17.3 | 47 |

# 3 Results

## 3.1 General data processing

Primarily the data were stored in files containing no more than 100 measurements. These files have been translated into data files per experiment and subdivided into files containing temperature data measured in the plane along the wind direction (A-series), same for the plane perpendicular to the wind direction at a distance of 4.1 m field scale (B-series) and heat flux data (C-series).
The code of these data files is as follows: TOFnnX.DAT, where nn is the experiment number (see paragraph 2.4) and X is the above mentioned series number.

The contour plots of the flame temperatures has been made using the plot program SURFER and arbitrary grid sizes.
The temperature profiles have been made using the spread sheet program LOTUS-123. This program has also been used to draw the graphs concerning the heat flux measurements.

For all figures the numbers along the axes describe the field scale dimensions. This means that as far as the temperature measurements are concerned the Froude number similarity has been applied (see par. 2.4) and that the Boltzmann number similarity has been applied on the heat flux measurements (see par. 3.4). All distances are expressed in distances from the burner exit.

## 3.2 Flame shape

The shape of the windtunnel flames are shown by pointing out its edges. The definition of the flame edges are arbitrary. We defined the 100 °C mean temperature level to be the flame edge. The 100 °C level is found by means of interpolation between points on a calculation grid. In this way we were able to draw contour plots showing the flame shape. Although the density of the measurement grid is relatively high interpolation between data points sometimes show a somewhat rectangular flame shape.
The resulting contour plots are given in Appendix B. From these plots the flame lengths are determined which have been compared with the flame lengths of the field scale experiments. These comparisons proved that flame lengths can be modelled well down to scale 1:25 applying the Froude number similarity. An overview of the flame lengths is given in table 2. (In table 2 the lengths of the windtunnel flames are multiplied with 10 and 25 respectively in accordance to the Froude number scaling).

*Table 2 Comparison of flame length*

| Exp. number | | Field scale | | Flame length (in m) | | | | |
|---|---|---|---|---|---|---|---|---|
| Risø | TNO | $U_a$ | $U_f$ | field | 1:10 | 1:25 | $U_f/U_a$ | Fr |
| R6a | 2 | 2.2 | 19 | 4.9 | 5.4 | | 8.6 | 10 |
| R5c | 1 | 4.4 | 20 | | 5.3 | | 4.5 | 39 |
| R6b | 9 | 2.5 | 39 | 6.0 | 7.1 | | 15.6 | 13 |
| R5b | 8 | 5.2 | 40 | | 6.9 | 7.0 | 7.7 | 55 |
| R6c | 7 | 2.6 | 83 | 8.9 | 9.1 | 8.9 | 31.9 | 14 |
| R7c | 3 | 3.9 | 83 | 9.1 | 10.0 | | 21.3 | 31 |
| R5a | 6 | 4.8 | 83 | | 8.9 | 9.2 | 17.3 | 47 |

However, from the contour plots it can be seen that there is a difference in the buoyancy between the field scale and windtunnel scale flames. The latter therefore show a larger vertical shift of the hindmost part of the flames.

The following can also be seen from several contour plots and table 2:
- increasing the burner exit velocity increases the size of the flame both in along wind and in vertical direction;
- increasing the wind velocity doesn't cause a significant difference in size but results in a more horizontal flame.

## 3.3 Flame temperature

Temperature measurements have been carried out for all experiments mentioned in table 1. Mean and rms-values of the temperature have been measured in the plane along the wind direction in all cases and in the plane perpendicular to the wind direction at a distance of 4.1 m field scale of the experiments.
The field scale and the windtunnel scale flame temperatures can only be compared by comparing the vertical temperature profiles at a distance of 4.1 m field scale. Vertical mean temperature profiles of all windtunnel measurements are included in Appendix C. The results of the comparison with field data are shown in figures 7 to 13. Apart from the difference in the vertical shift mentioned in par 3.2 the mean temperature profiles are in good accordance. In some cases although the maximum temperature of the windtunnel scale flames appears to be somewhat higher. This is in agreement with the UPM calculations (Crespo '91).
The rms-values of the flame temperatures show large differences. This is most probably caused by the different measurement techniques used by TNO and Risø.

As far as the windtunnel experiments are concerned the contour plots of the 1:10 and the 1:25 scale temperature measurements can be compared (see appendix B). The similarity between the different plots is striking. A qualitative comparison can also be made between the contour plots on the one hand and the infra red figures of the experiments shown in the Risø report (Ott '91) on the other hand. There seems to be a good agreement between the part of the flames where the highest temperatures occur.

For a few experiments the temperatures of a cross section at 4.1 m field scale have been measured. The results are shown in figures Appendix D.
In a few occasions, the kidney shaped double vortex appears (TOF07, TOF11).

## 3.4 Heat flux

The heat flux measurements have been carried out for all experiments mentioned in table 1 except numbers 11 and 12. The measurements concern the heat flux to the windtunnel ground floor surface at the centre-line of the burner exit and at a distance of 2.5 m field scale lateral from the centre-line. In the latter case a heat flux sensor (Q2) was positioned at an angle of 45° to the windtunnel floor.
The windtunnel experiments enables us to show the course of the heat flux as a function of the along wind distance from the burner exit. Regarding the field scale heat flux measurements comparisons can be made with the 'Q2' experiments performed at a distance of 4.1 m field scale from the burner exit. Results of the experiments are shown in Appendix E.
The comparisons can be made using the Boltzmann number similarity. This means that additional to the Froude number similarity the heat fluxes have to be multiplied with the velocity ratio of the different scales. In previous reports the Boltzmann number has been given as:

$$Bo = \frac{\sigma . T_f^3}{\rho_f . C_{p,f} . U_f}$$

in which $\sigma$ is the Stefan-Boltzmann constant, $\sigma=5.67 \cdot 10^{-8}$ (in $J/smK^4$);
$T_f$ is the temperature of the fuel (in °C);
$\rho_f$ is the density of the fuel (in $kg/m^3$);
$C_{p,f}$ is the specific heat (in J/kgK);
$U_f$ is the velocity of the fuel (in m/s).

It can be argued that the emissivity $\varepsilon$ should be included:

$$Bo = \frac{\sigma . \varepsilon . T_f^4}{\rho_f . C_{p,f} . U_f . T_f}$$

In Duijm & Bisgaard '88 only independent parameters have been included in the analysis; $\varepsilon$ was thought to be similar for correctly scaled flames of different size. However, for opaque flames $\varepsilon$ depends on the ratio of the absorption length to the size of the flame. The emissivity therefore should be included in the definition of the Boltzmann number.
In first order neglecting changes in the emissivity, application of the Froude number similarity implies a reduction of the total heat flux $\rho_f.C_{p,f}.U_f.T_f$ by the square root of the geometric scale factor. If at the same time the ratio between radiant heat and convection heat remains equal, the radiative heat flux will also be reduced by the square root of the scale factor.

Comparing the previous (1989) and the present windtunnel results using this 'U-scaling' approach, on scale 1:10 and 1:25 this theory seems to be valid (figure 14). Compared to field scale results (Ott '91, figure 11) the windtunnel results Q2 are about a factor 3 to 4 lower. The findings of Risø that the heatflux is independent of windvelocity are supported by the windtunnel results (figure 15 and 16).
The windtunnel flames contain more soot as appears from the more yellow colour of these flames compared to the field scale flames. The emissivity therefore will be lower and thus will the radiative heat flux. The reason for the higher formation of soot in the windtunnel flames is thought to be caused by the impossibility to scale the smallest sizes of the turbulence.

# 4 Conclusions

Comparisons have been made between low pressure flame experiments carried out at Risø (field scale) and TNO (windtunnel scale). The following results have been studied in detail:

- flame shape;
- flame temperature;
- heat flux.

*Flame shape.*
Comparing the results it appears that applying the Froude number similarity a correct way of scaling is obtained, at least to scaling ratios up to 25. This holds for the flame lengths and the flame shape in general. The only difference is the vertical shift of the 'tail' of the flame. The windtunnel scale flames show a larger shift which is due to a difference in buoyancy.

*Flame temperature.*
Mean flame temperatures are modelled well using the Froude-number similarity up to scaling ratios up to 25. In some cases the maximum temperatures of the windtunnel scale flames are somewhat higher.
There is a difference between the rms-values of the temperatures comparing the different scale flames. This is due to different measuring techniques used by Risø (field scale) and TNO (windtunnel scale).

*Heat flux.*
In order to compare the heat flux measurements the windtunnel values are multiplied by the square root of the geometric scale factor.
Comparing the previous (1989) and the present windtunnel results on scale 1:10 and 1:25 this theory seems to be valid. However, comparing the windtunnel results with the field scale results (Ott '91) the former show an underestimation of the latter. This is due not only to the effects of length scales and emisitivity but probably also to a higher formation of soot in the windtunnel flames. Compared to the field scale flames the emissivity therefore will be lower and thus will the radiative heat flux.

*Future experiments.*
In the near future also experiments will be performed using other burner diameters. These experiments must prove that using equal velocity ratios and equal Froude numbers both temperature profiles and heat fluxes are not sensible for different sizes of the burner diameter.

# 5 References

[1] Duijm, N.J. and Bisgaard;
Small scale cold and hot modelling of torch fires;
MT-TNO 88-130, May 1988, Apeldoorn, The Netherlands.

[2] Verheij, F.J. and Duijm, N.J.;
Torch Fires - Data Report no. 1;
MT-TNO 89-359, November 1989, Apeldoorn, The Netherlands.

[3] Ott, S.;
An experimental study of large natural gas flames;
Risø, 1991, Roskilde, Denmark.

[4] Crespo, A. et al.;
One-dimensional model of torch firs: UPMFIRE;
UPM, July 1991, Madrid, Spain.

[5] Crespo, A. and Hernández, J.;
Numerical three-dimensionla model of torch fires;
UPM, July 1991, Madrid, Spain.

[6] Duijm, N.J., Crespo, A., Biardi, G. and Højholt, P.;
Modelization of torch fires;
Eurotherm Seminar No. 14, May 15-17, 1990, Louvain la Neuve, Belgium.

# 6 Authentication

Name and address of the principal
CEC programme 'Major Technological Hazards'
Theme EV4T16
Project FG: 'Physical modelling of Torch Fires'

Names and functions of the cooperators
ir. N.J. Duijm - research coordinator
ir. F.J. Verheij - scientïst
F.C. Balster - technician

Names of establishments to which part of the research was put out to contract
-

Date upon which, or period in which, the research took place
January 1988 - November 1991

Signature

N.J. Duijm
research coordinator

Approved by

ir. B. Stork
section leader

# Appendix A Technical data of the measuring equipment

*Sunction pyrometer*
The type S (platinum 10% rhodium - platinum or Pt10Rh-Pt) thermocouple used in the pyrometer can withstand temperatures up to 1700 °C. The thickness of the wires is 0.2 mm. The accuracy of the thermocouple is 1.5 °C.

*Heat flux sensors*
Q1 : heat flux sensor at positions Y=0
Q2 : heat flux sensor at positions Y=2.5 m (45° sight angle).

Sizes : diameter 24 mm, thickness 4 mm.

| | |
|---|---|
| Calibration value C (at 20 °C) | : 0.73 (Q1) and 0.70 (Q2) $W/m^2.\mu V$ |
| Temperature correction | : negligible |
| Internal electrical resistance | : 1380 (Q1) and 1417 (Q2) |
| Thermal conductivity | : approximately 50 W/m.K |
| Accuracy of calibration value | : 5% |

Heat flow ($W/m^2$) = C x measured voltage (mV).

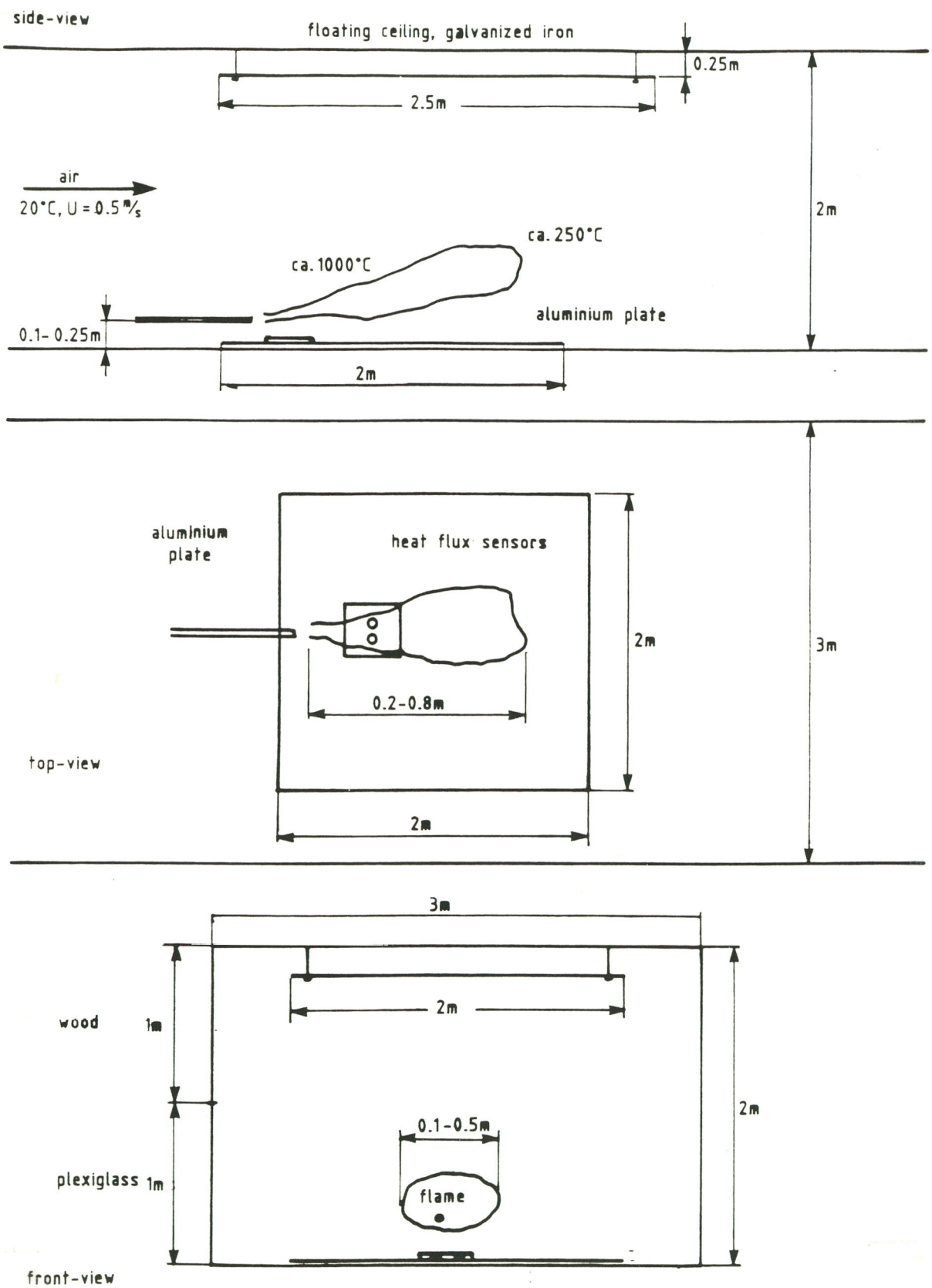


Diagram of the measuring section of LIA during the "Torch Fire Experiments"

IMET – TNO
91 – 422

Fig. 1

Side view

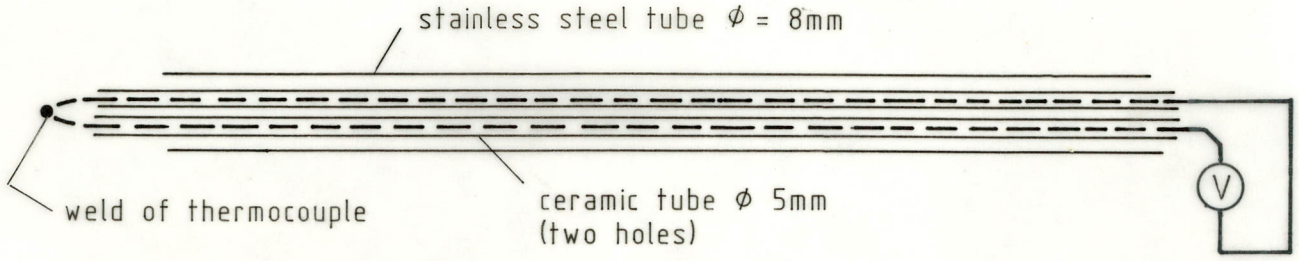


Front view

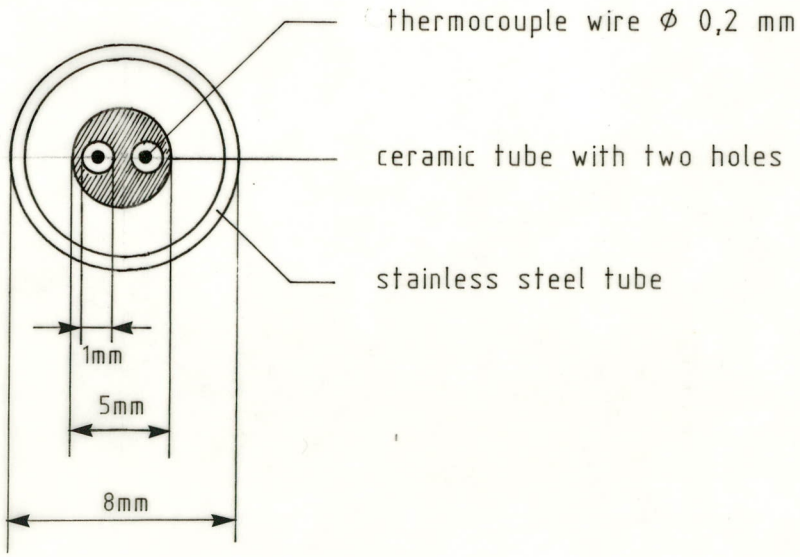


Diagram of the pyrometer.

IMET – TNO
91 – 422

Fig. 2

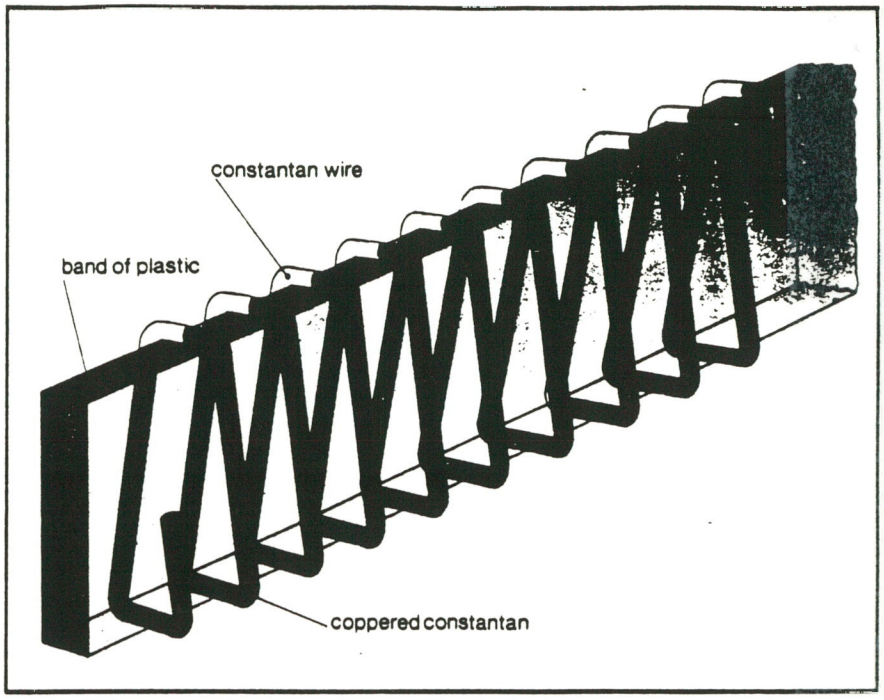


*Constantan wire is wound around a plastic strip and after half a winding has been copper-plated, it forms a thermopile.*

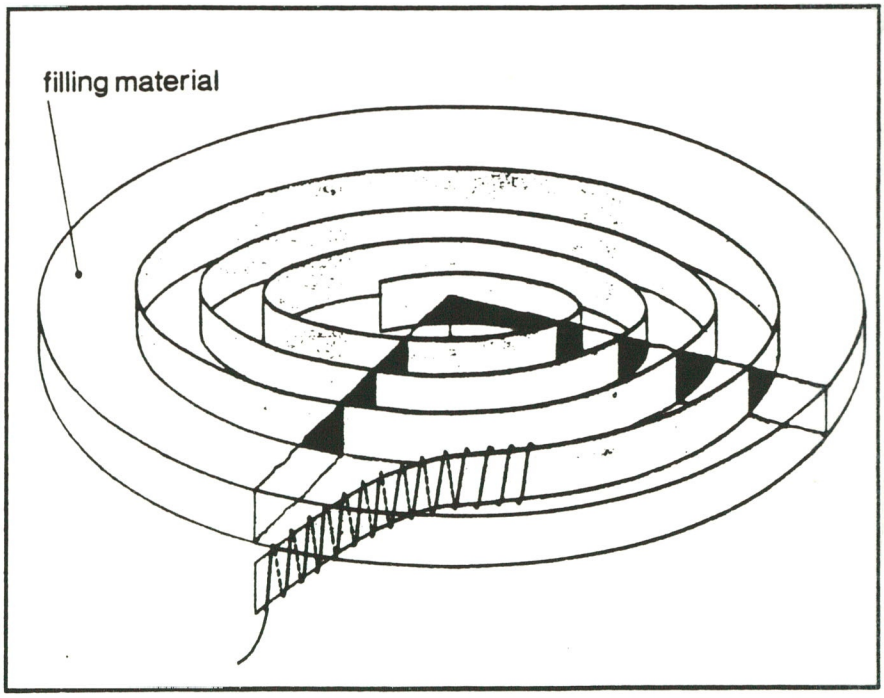


*The thermopile is wound into a spiral and embedded into a filling and enclosing material.*

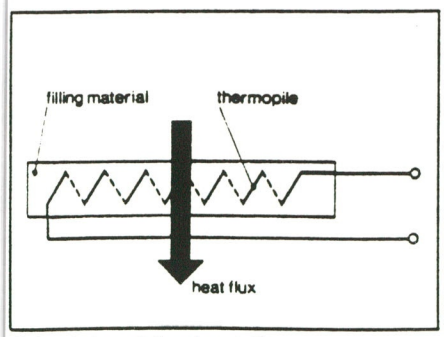


*Principle of the heat flux sensor.*

A heat flux sensor and its principle.

IMET – TNO
91 – 422

Fig. 3

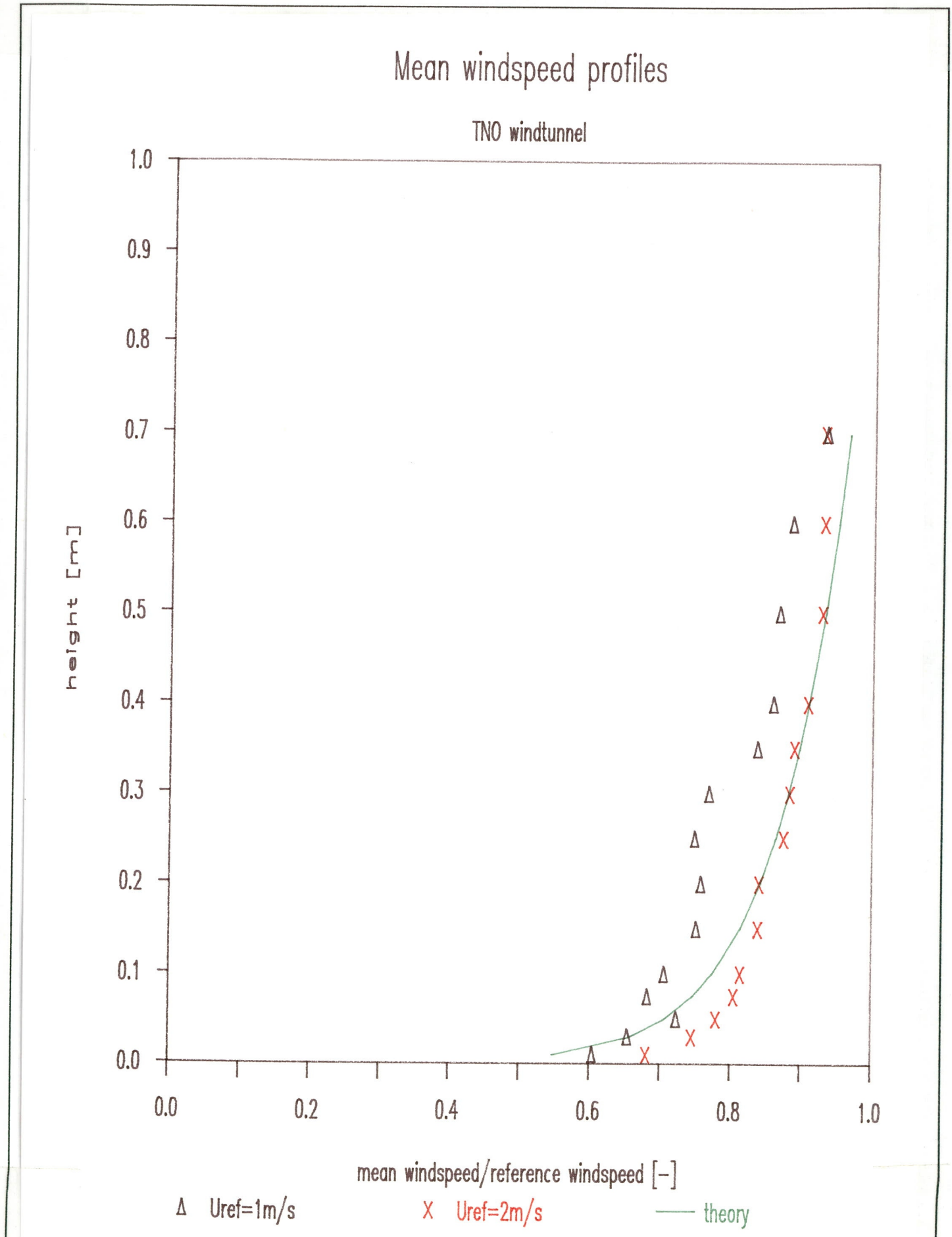


Mean windspeed profiles measured in the TNO windtunnel at two different reference windspeeds.

IMET – TNO
91 – 422

Fig. 4

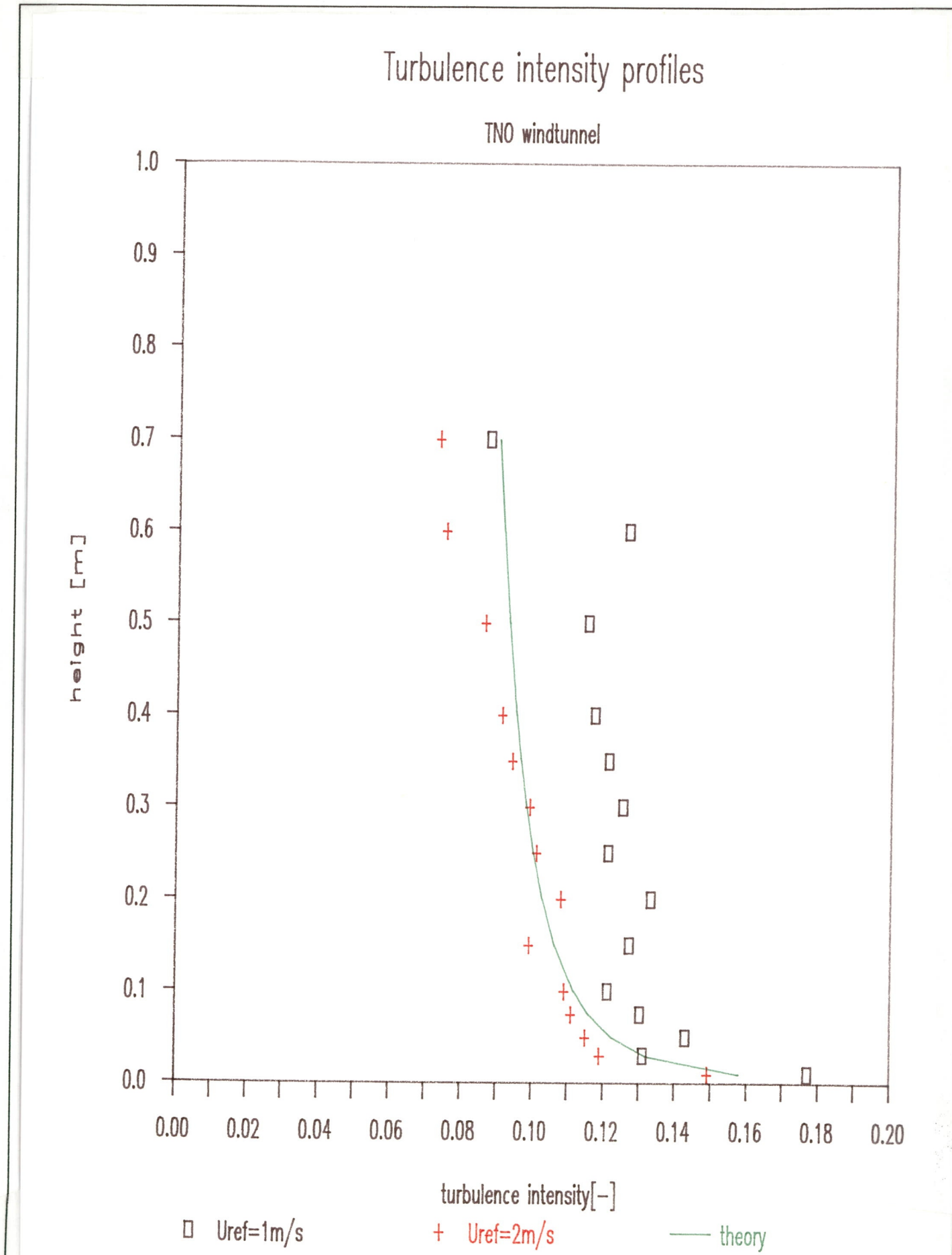


Turbulence intensity profiles measured in the TNO windtunnel at two different reference windspeeds.

IMET - TNO
91 - 422

Fig. 5

Model 1 : 10

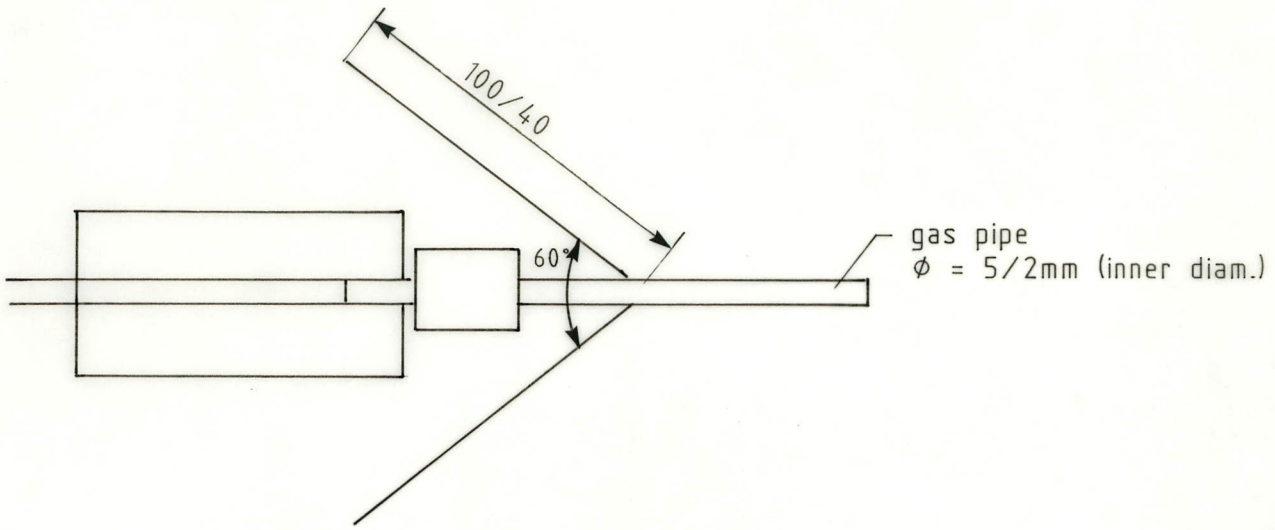


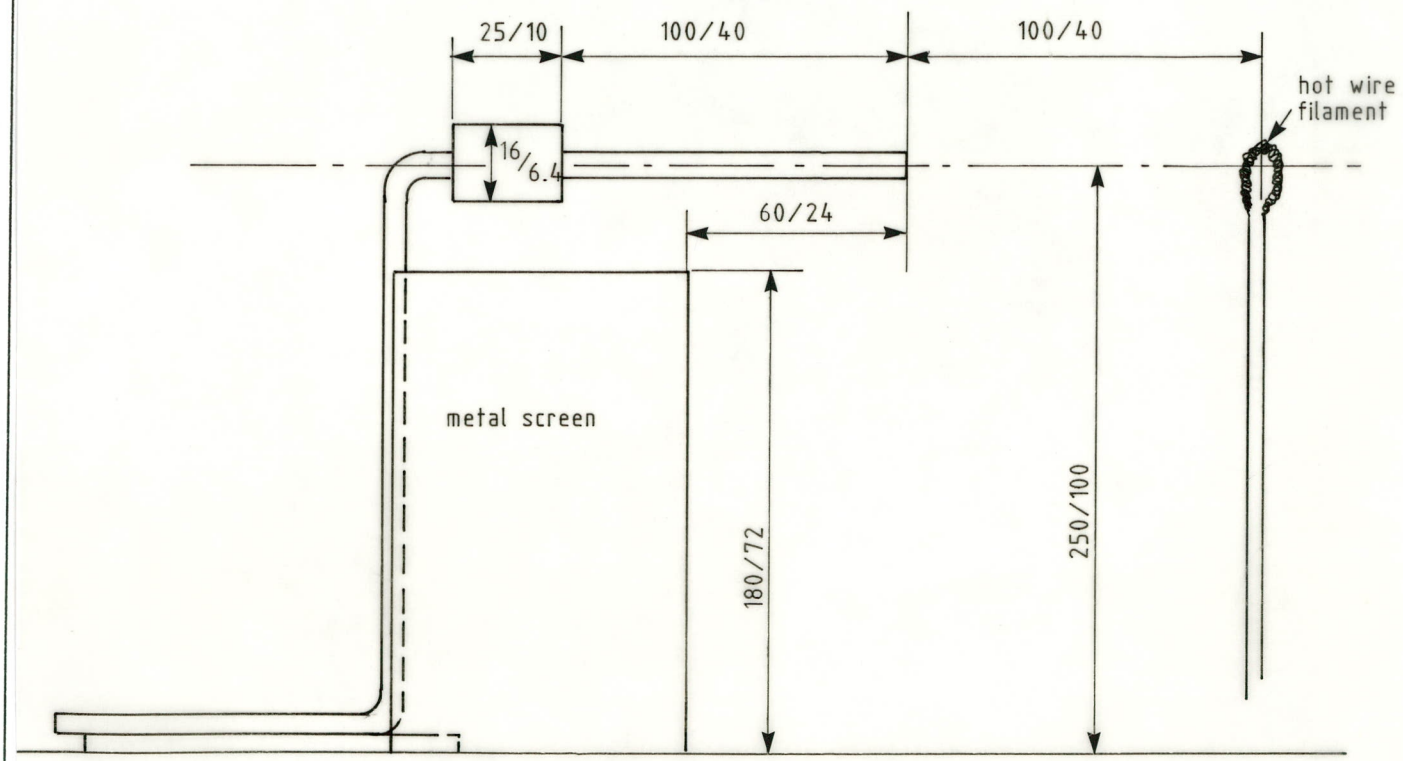


Lay-out of the burner configuration. Dimensions for 1:10 / 1:25 scale model, respectivily.

IMET - TNO
91 - 422

Fig. 6

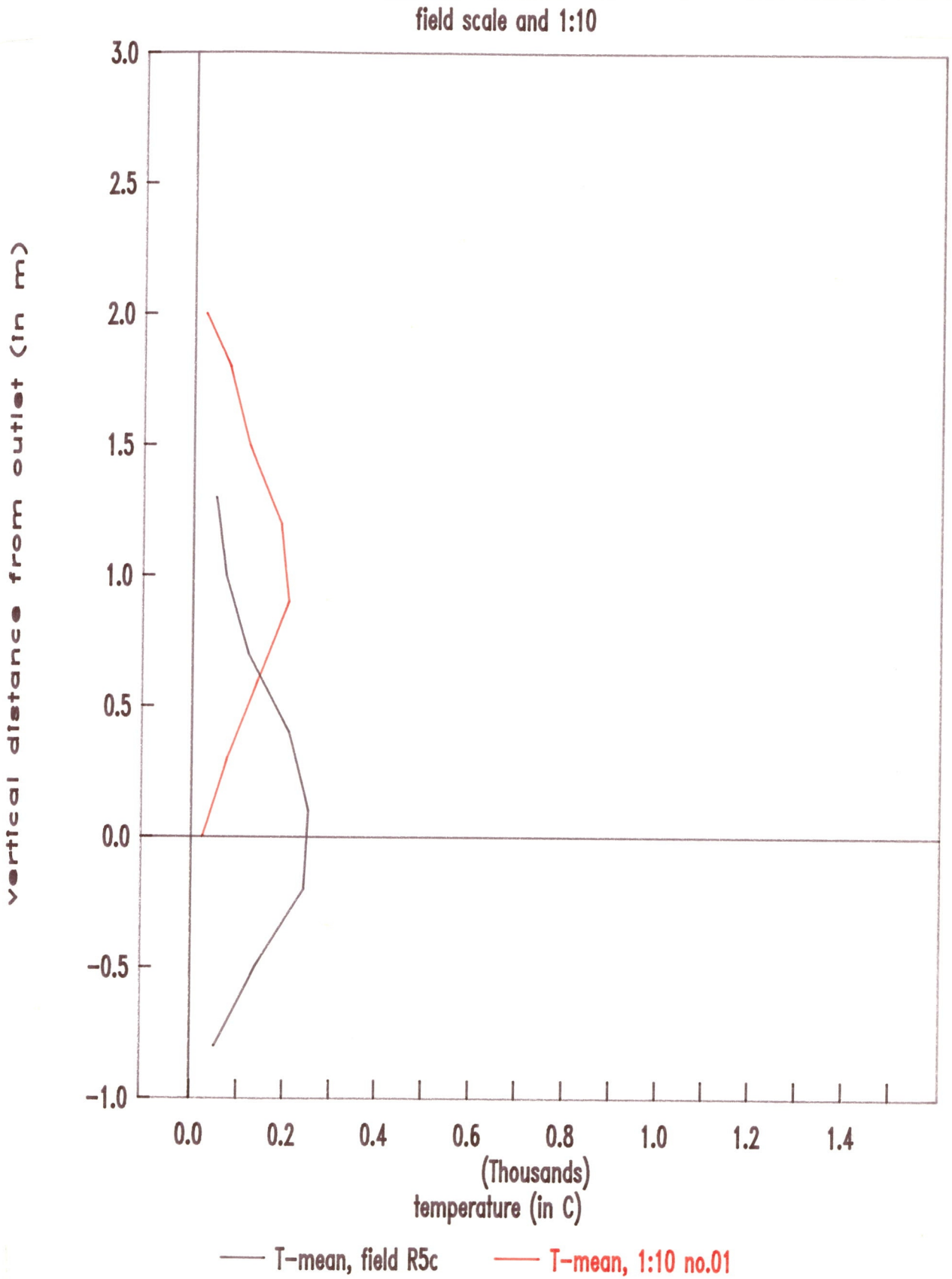


Vertical temperature profiles of field and windtunnel scale.
Windtunnel test no. 01.

IMET - TNO
91 - 422

Fig. 7

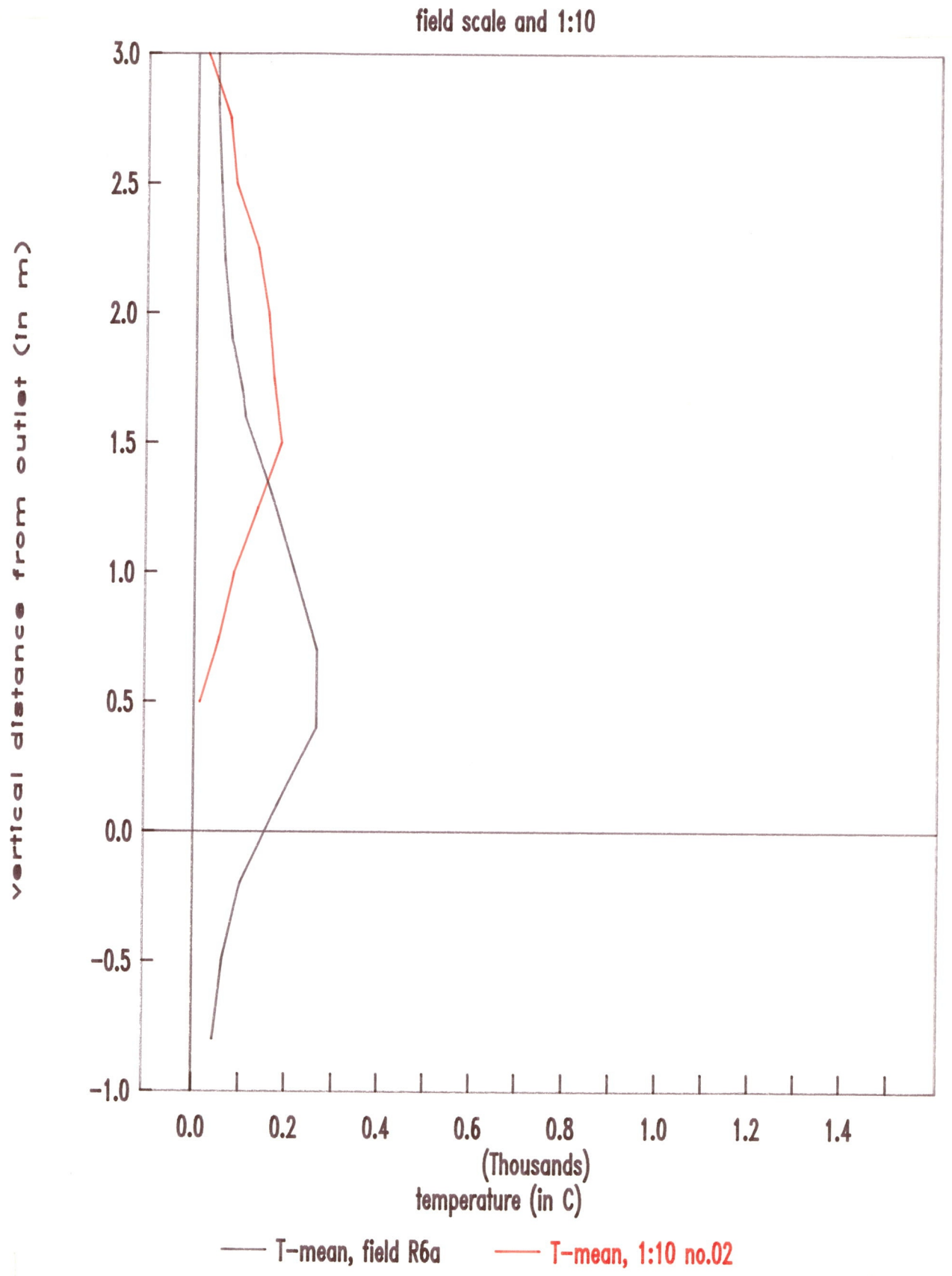


Vertical temperature profiles of field and windtunnel scale.
Windtunnel test no. 02.

IMET - TNO
91 - 422

Fig. 8

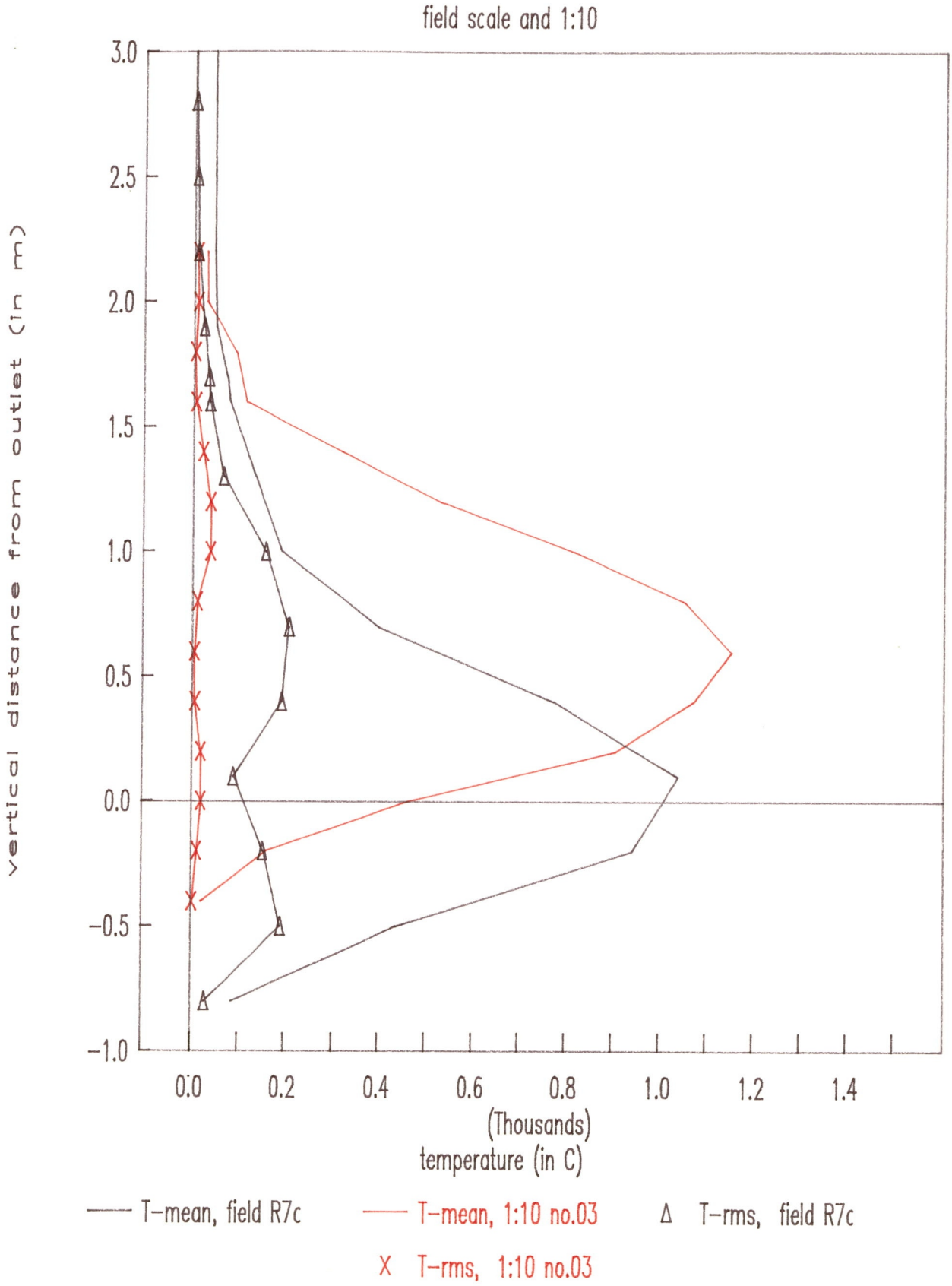


Vertical temperature profiles of field and windtunnel scale.
Windtunnel test no. 03.

IMET - TNO
91 - 422

Fig. 9

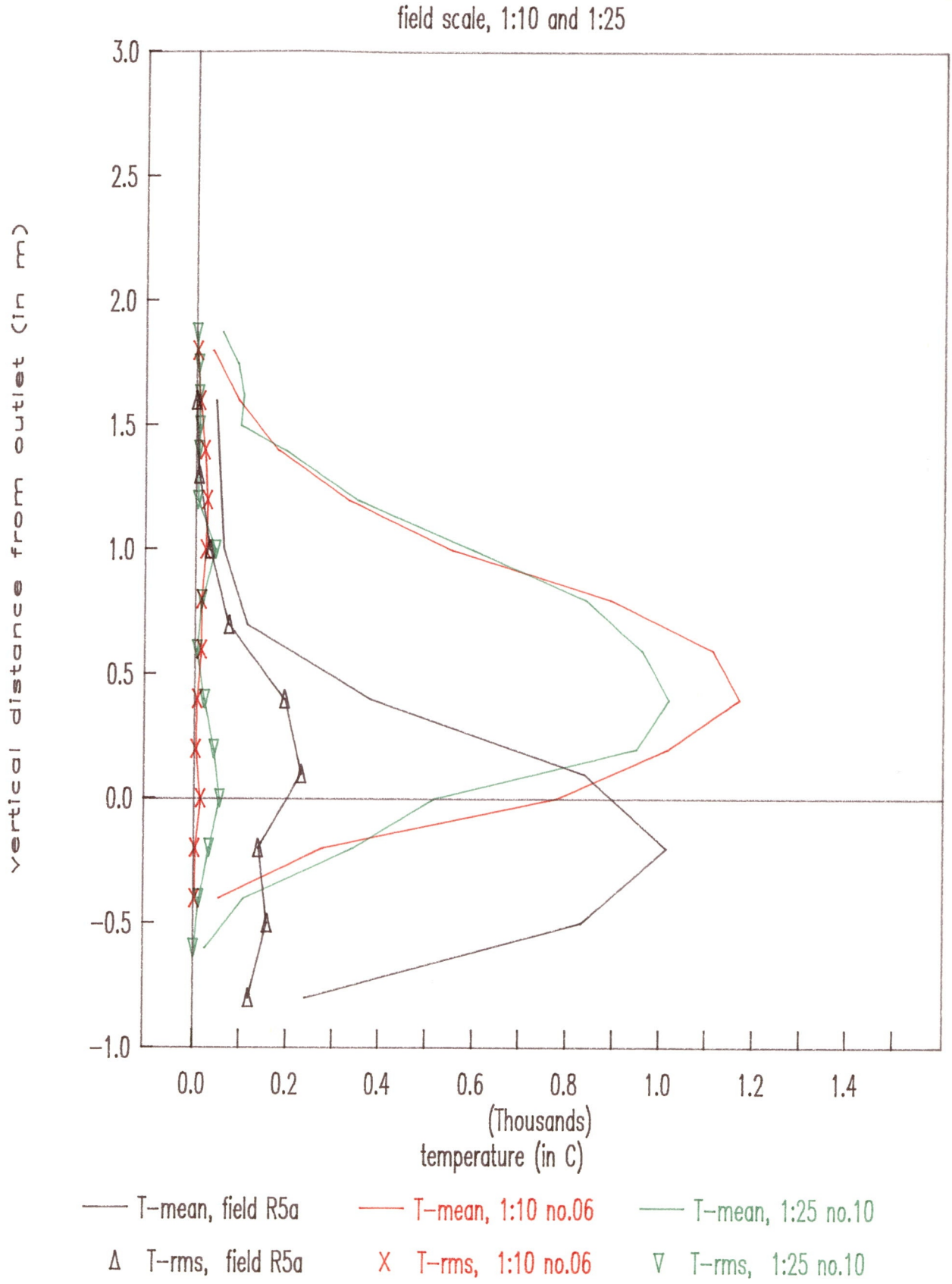


Vertical temperature profiles of field and windtunnel scale.
Windtunnel test no. 06.

IMET - TNO
91 - 422

Fig. 10

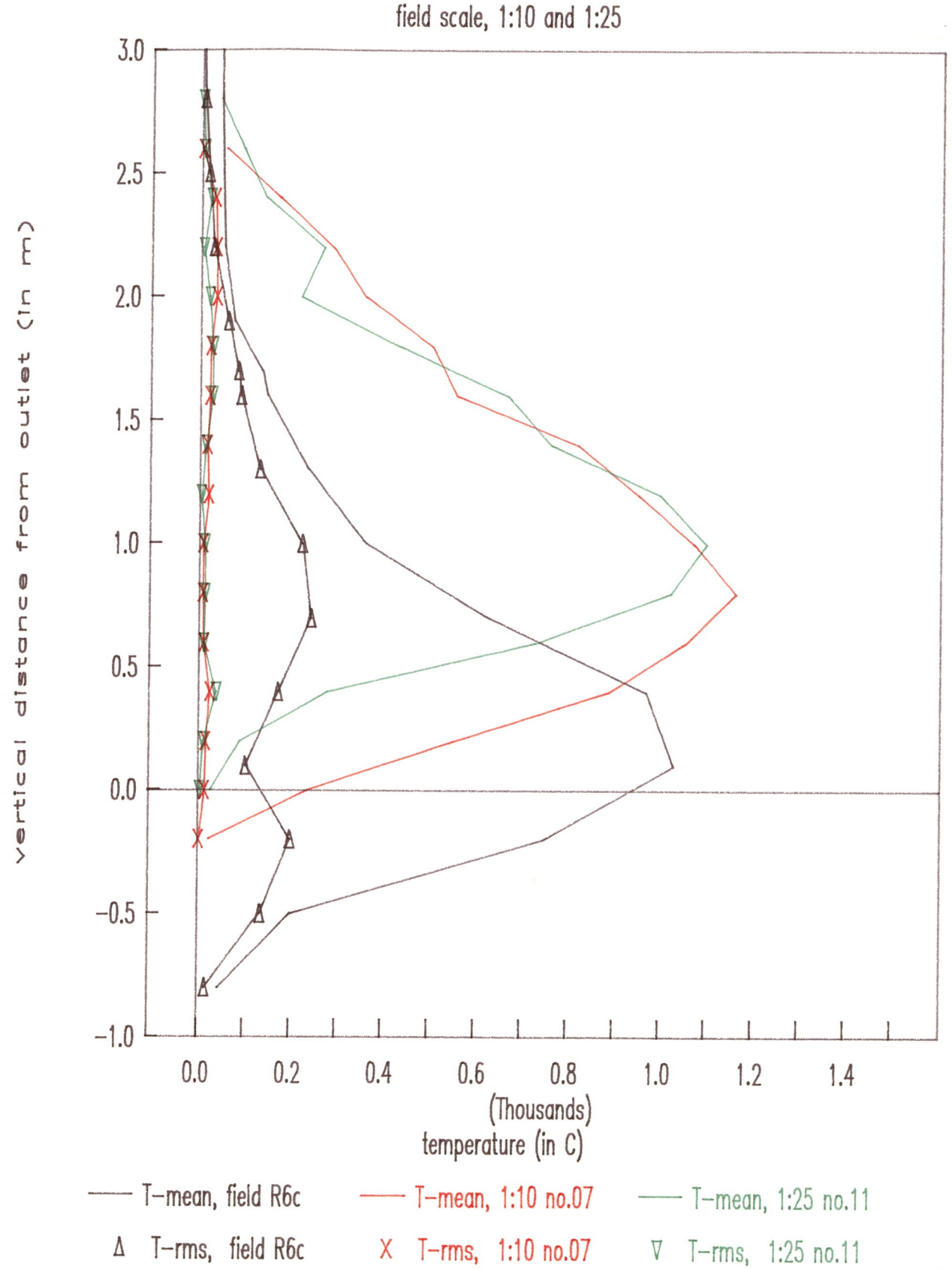


Vertical temperature profiles of field and windtunnel scale.
Windtunnel test no. 07.

IMET - TNO
91 - 422

Fig. 11

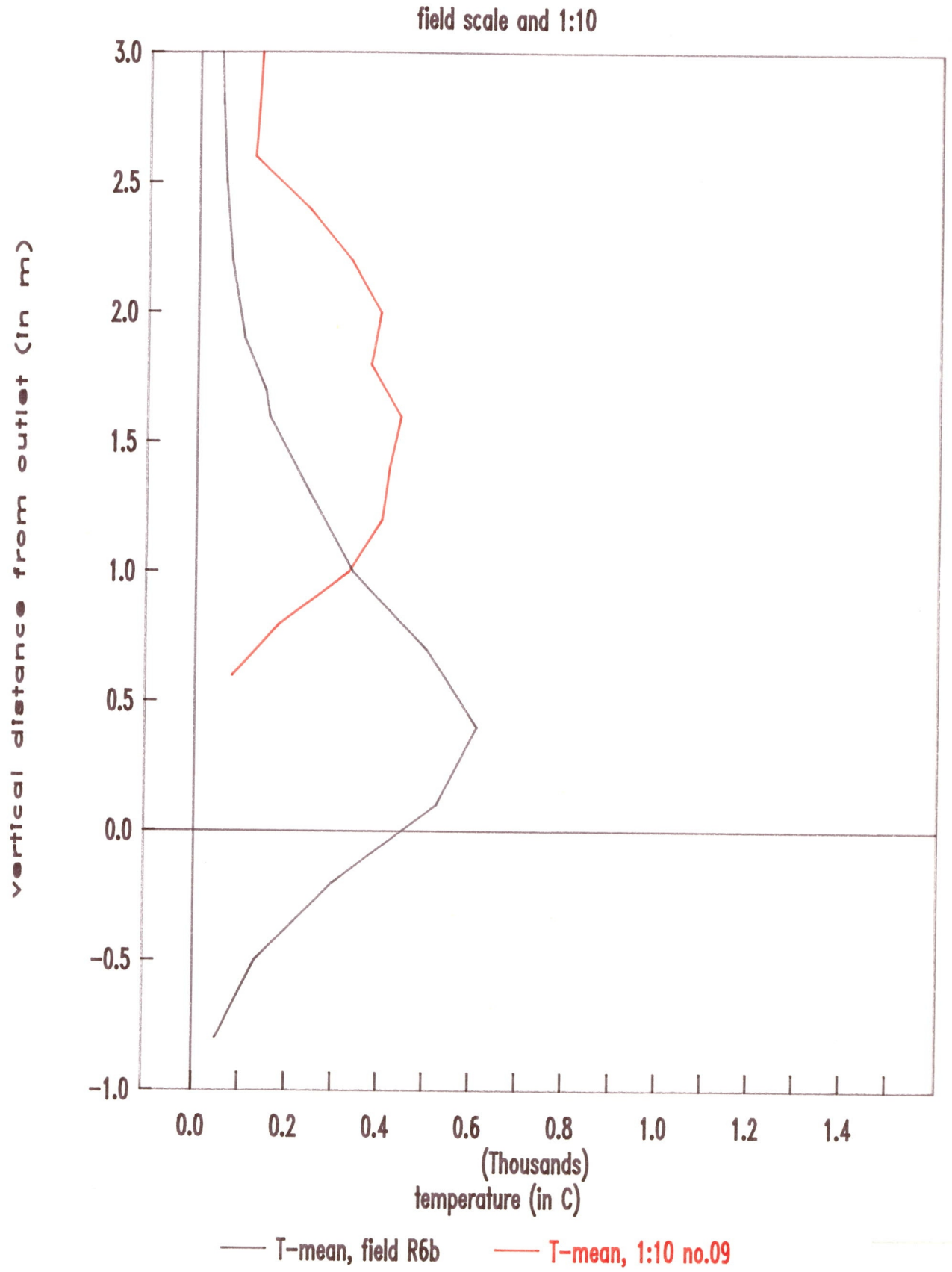


Vertical temperature profiles of field and windtunnel scale.
Windtunnel test no. 09.

IMET - TNO
91 - 422

Fig. 13

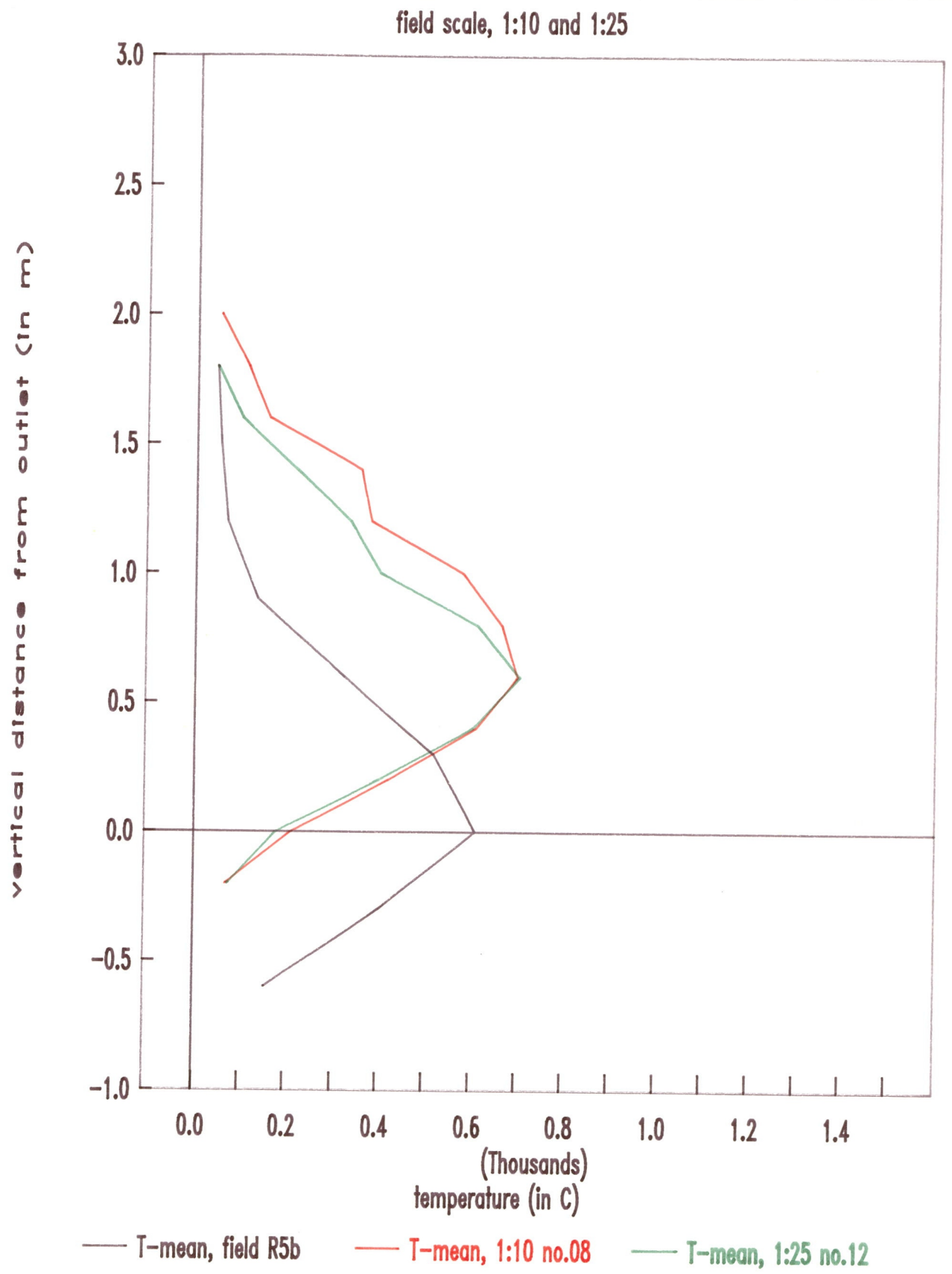


Vertical temperature profiles of field and windtunnel scale.
Windtunnel test no. 08.

IMET - TNO
91 - 422

Fig. 12

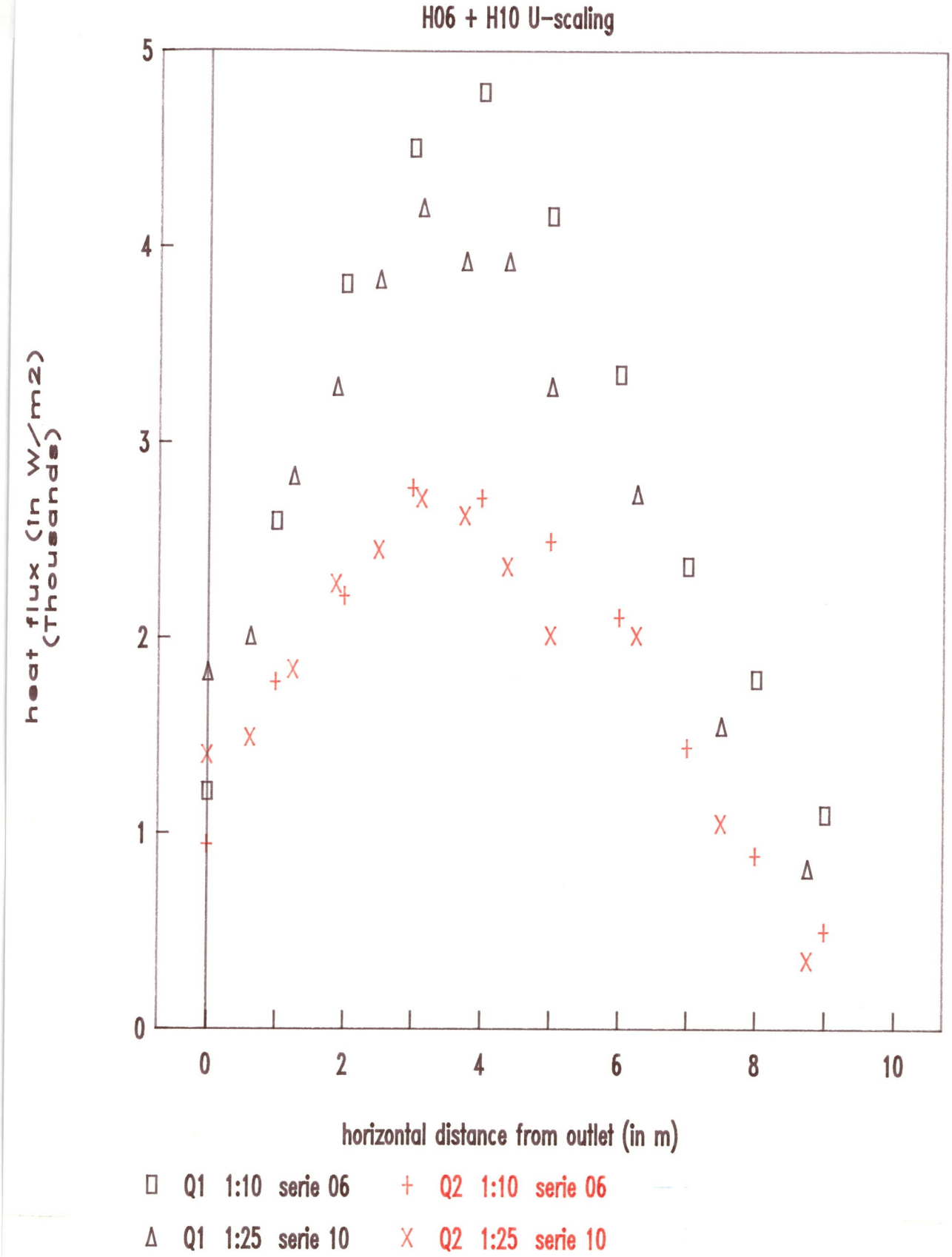


Windtunnel heat flux measurements at 1:10 and 1:25 scales. Comparison using the 'U-scaling' approach.

IMET - TNO
91 - 422

Fig. 14

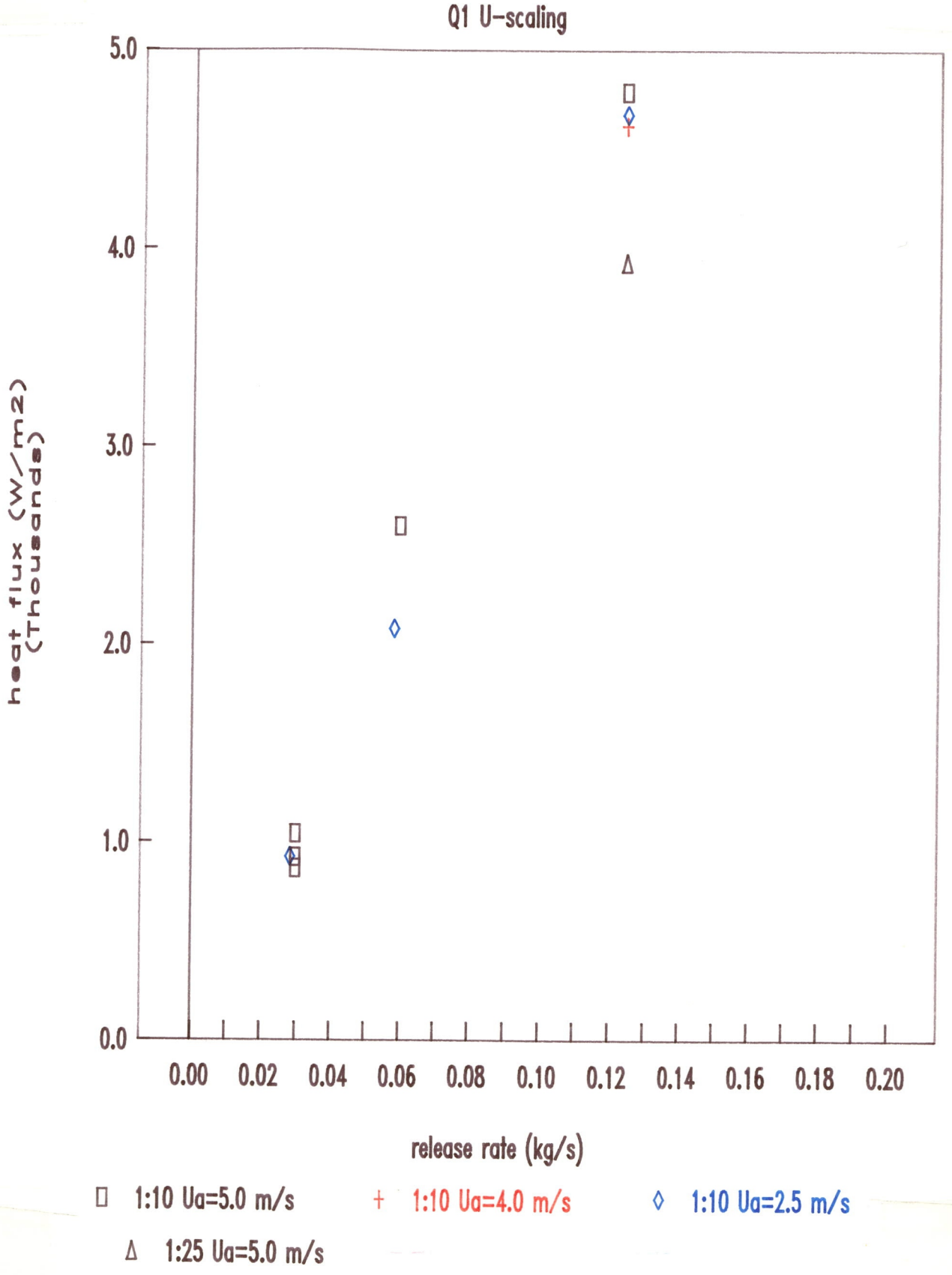


Heat flux Q1 measured at X = 4m (field scale) as a function of the gas release rate using the 'U-scaling' approach.
The measured windspeed values $U_a$ has been rounded off.

IMET – TNO
91 – 422

Fig. 15

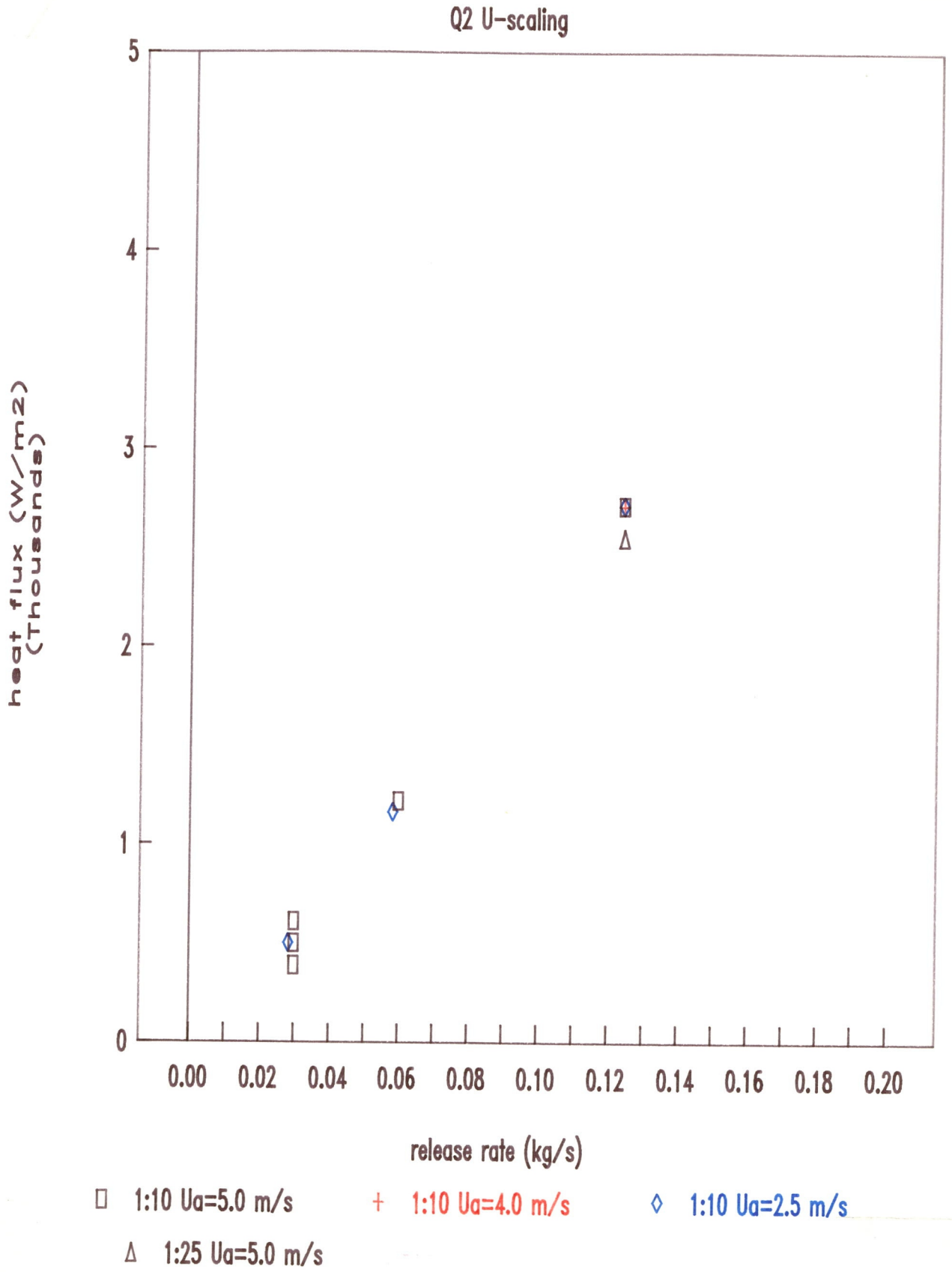


Heat flux Q2 measured at X = 4m (field scale) as a function of the gas release rate using the 'U-scaling' approach.
The measured windspeed values $U_a$ has been rounded off.

IMET - TNO
91 - 422

Fig. 16

# Appendix B Contour plots of the flame temperature in the along wind direction

This appendix contains the result of the flame temperature measurements at the centre line of the flame in the along wind direction presented as contour plots. The plots have been created using a plot program.

The contour plots have been made of all the windtunnel experiments.

Although the density of the measurement grid is relatively high interpolation between data points sometimes show a somewhat rectangular flame shape. Temperatures in the vicinity of the burner exit have not been measured in all cases. This causes non realistic flame shapes around this exit.

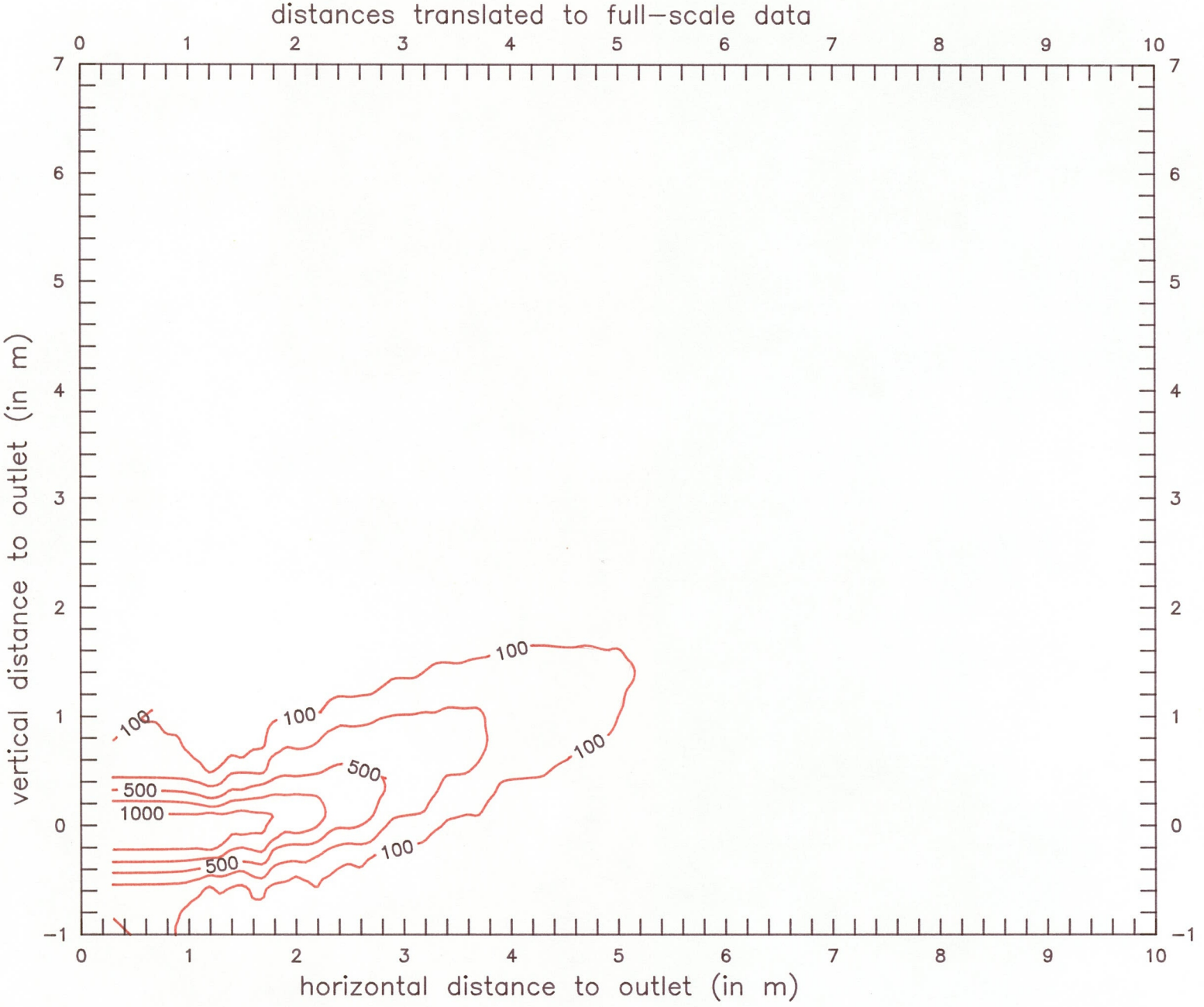


TOF01 along 1:10 Ua=1.4 Uf=6.1

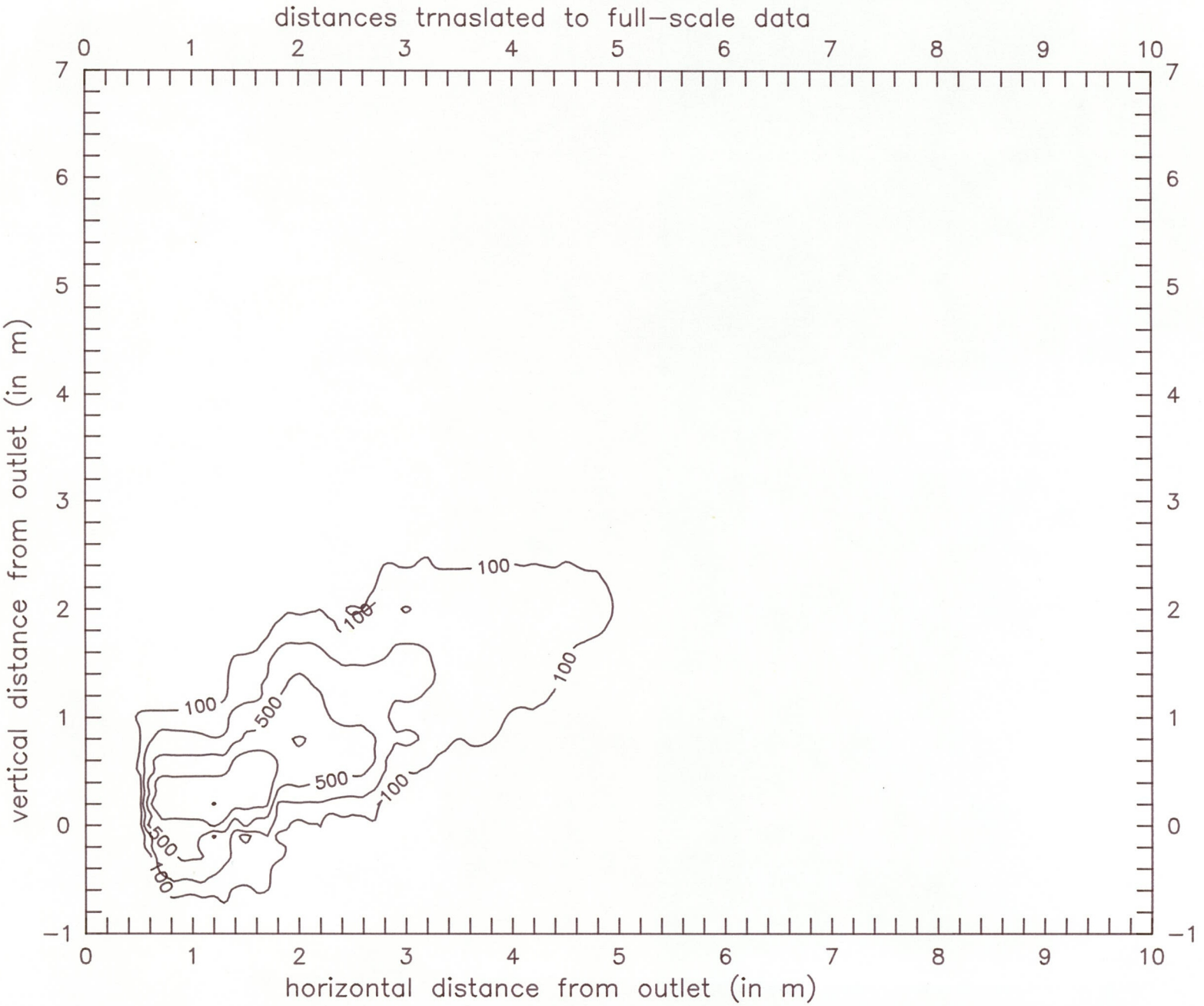


TOF02 along 1:10 Ua=0.7 Uf=6.1

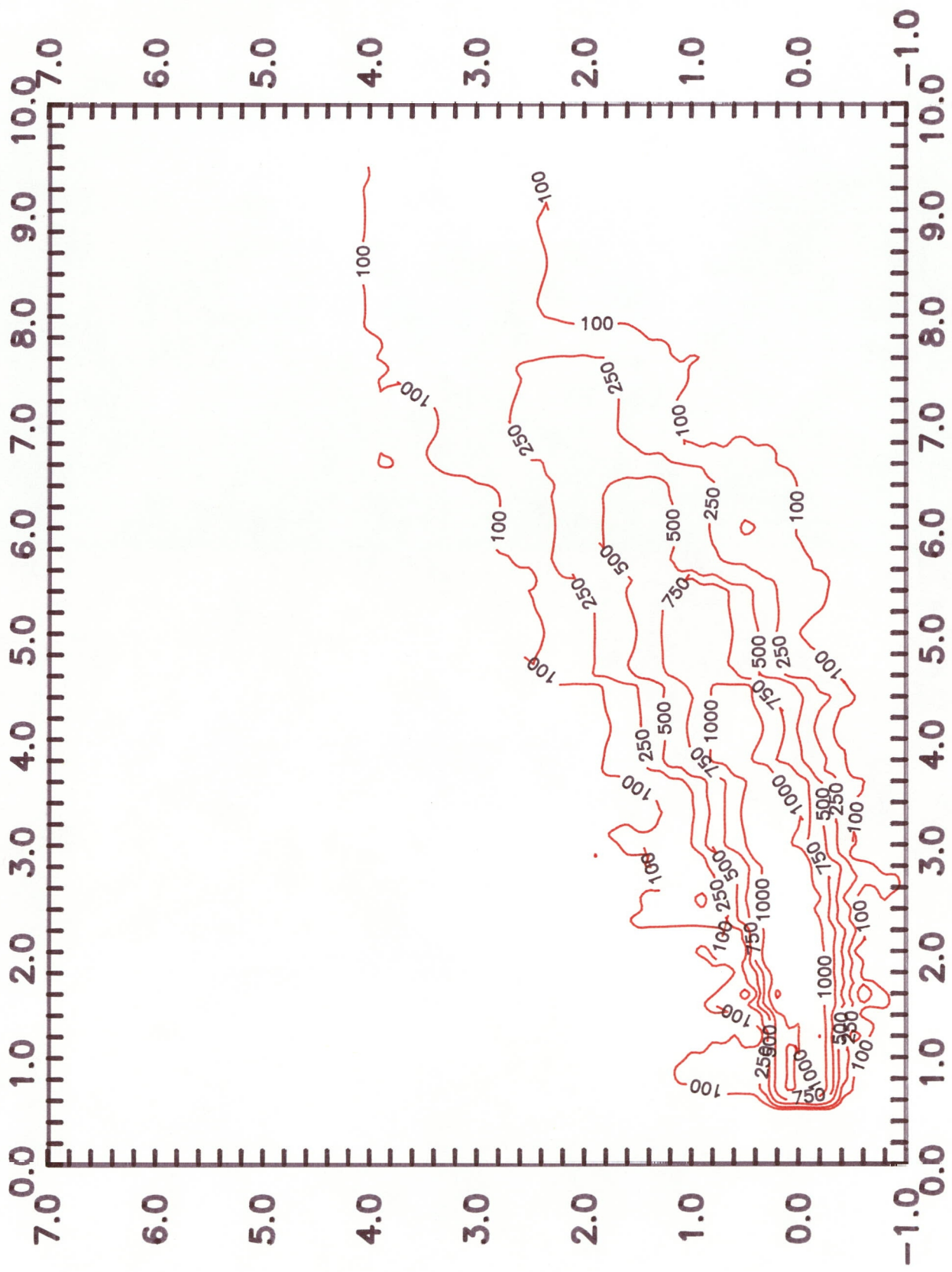
TOF03 ALONG 1:10 Ua=1.20 Uf=26.48
0.0
1.0
2.0
3.0
4.0
5.0
6.0
7.0
8.0
9.0
10.0
-1.0
100
250
500
750
1000

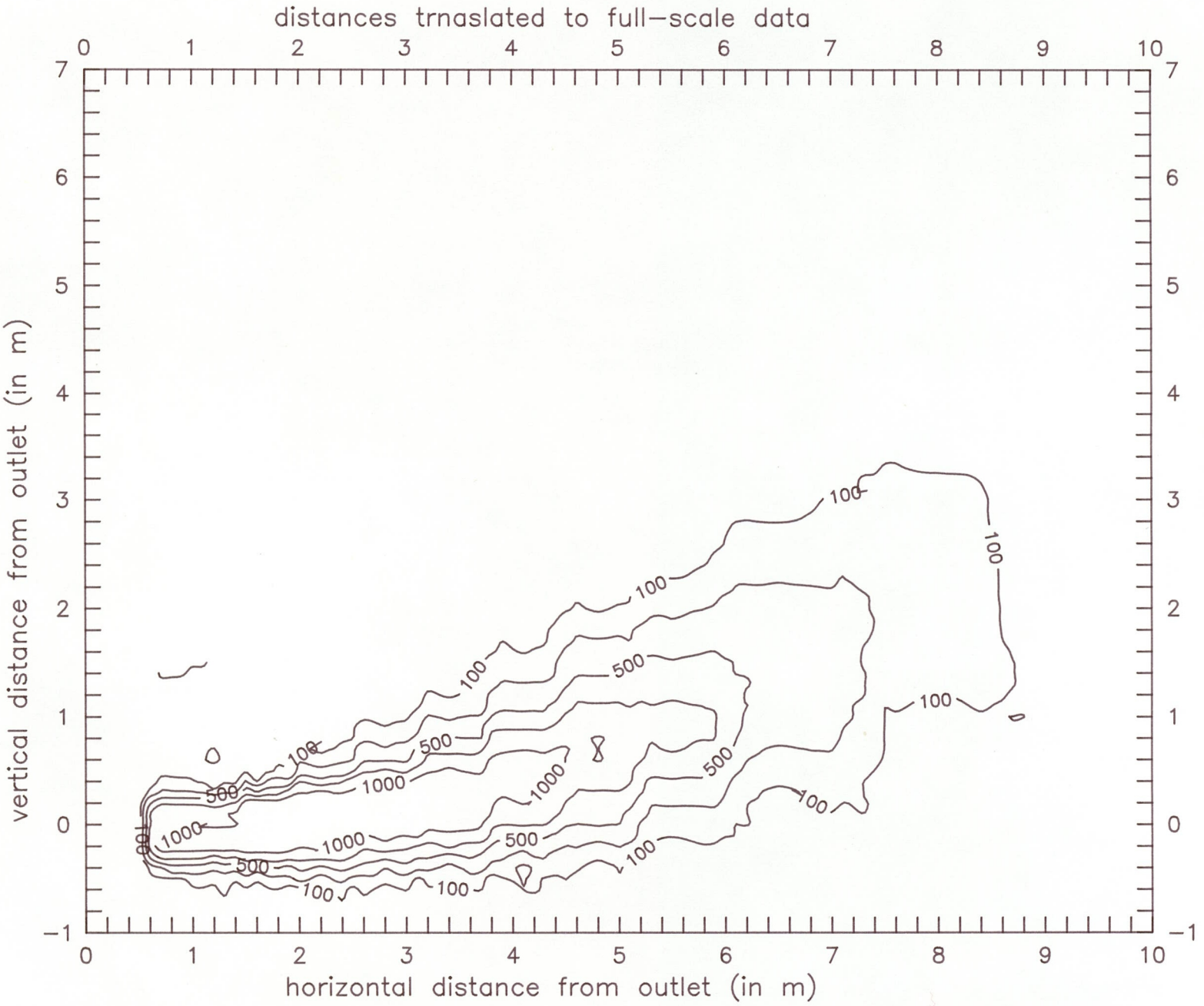


TOF06 along 1:10 Ua=1.5 Uf=26.5

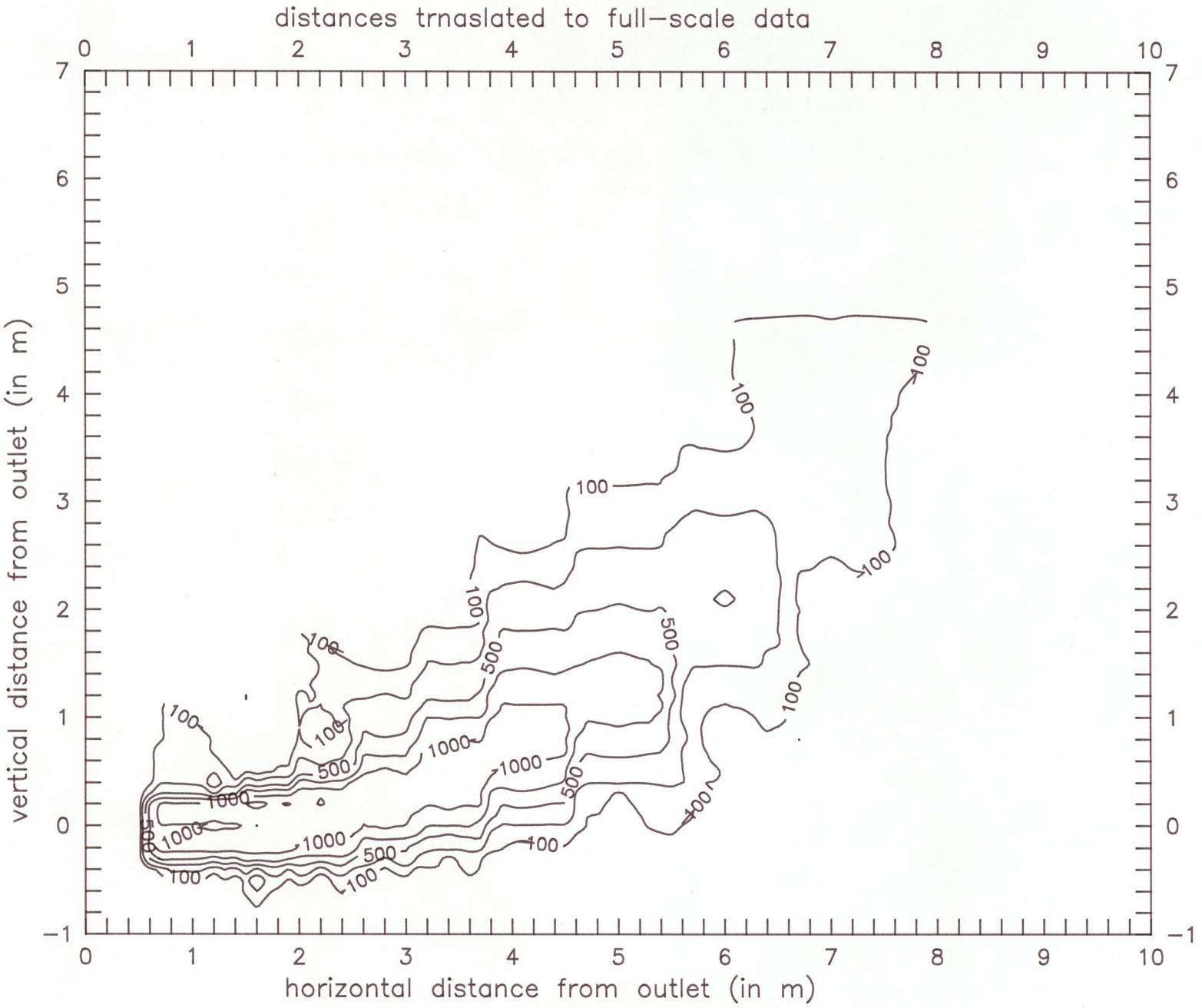


TOF07 along 1:10 Ua=0.8 Uf=26.5

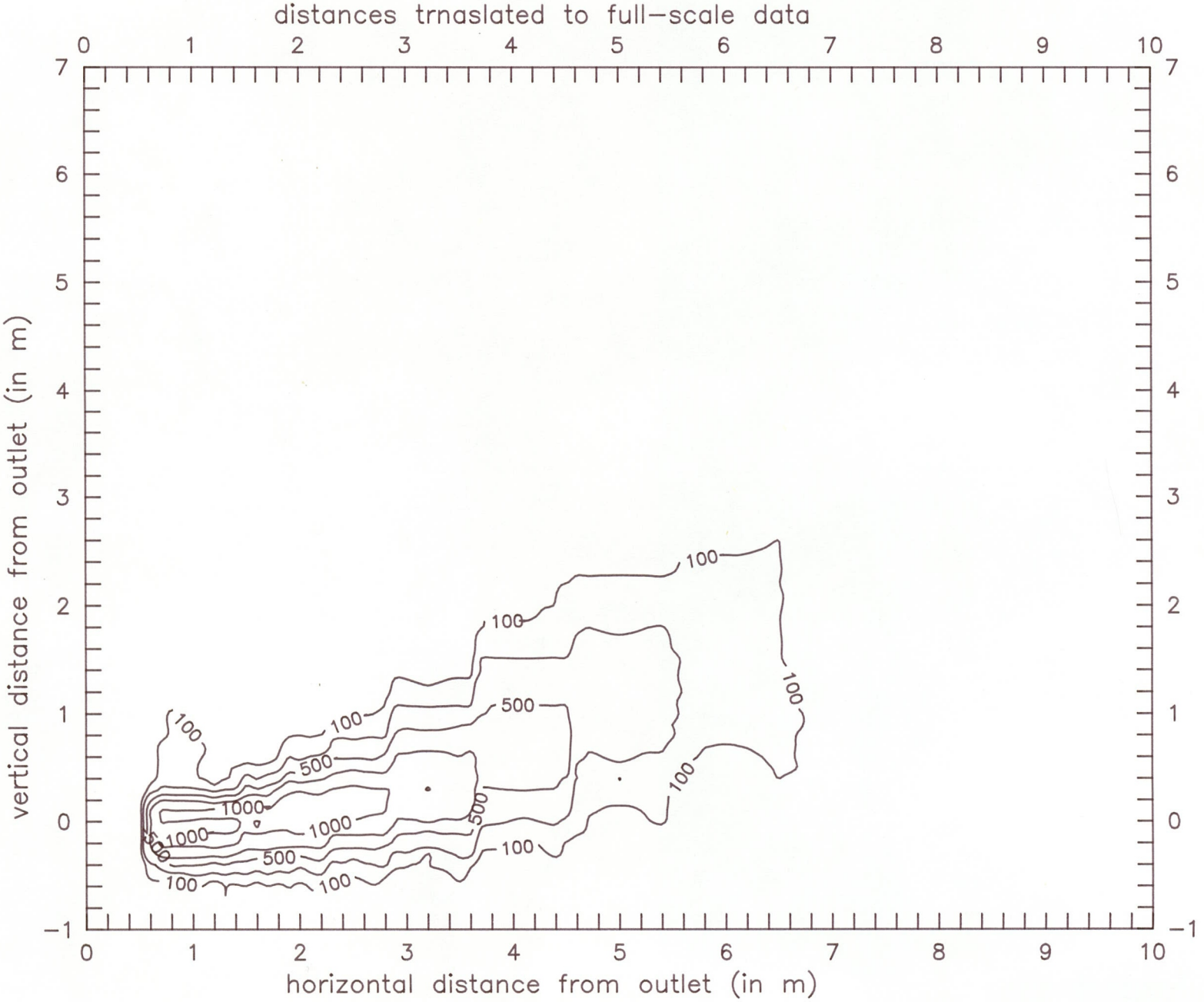


TOF08 along 1:10 Ua=1.6 Uf=12.7

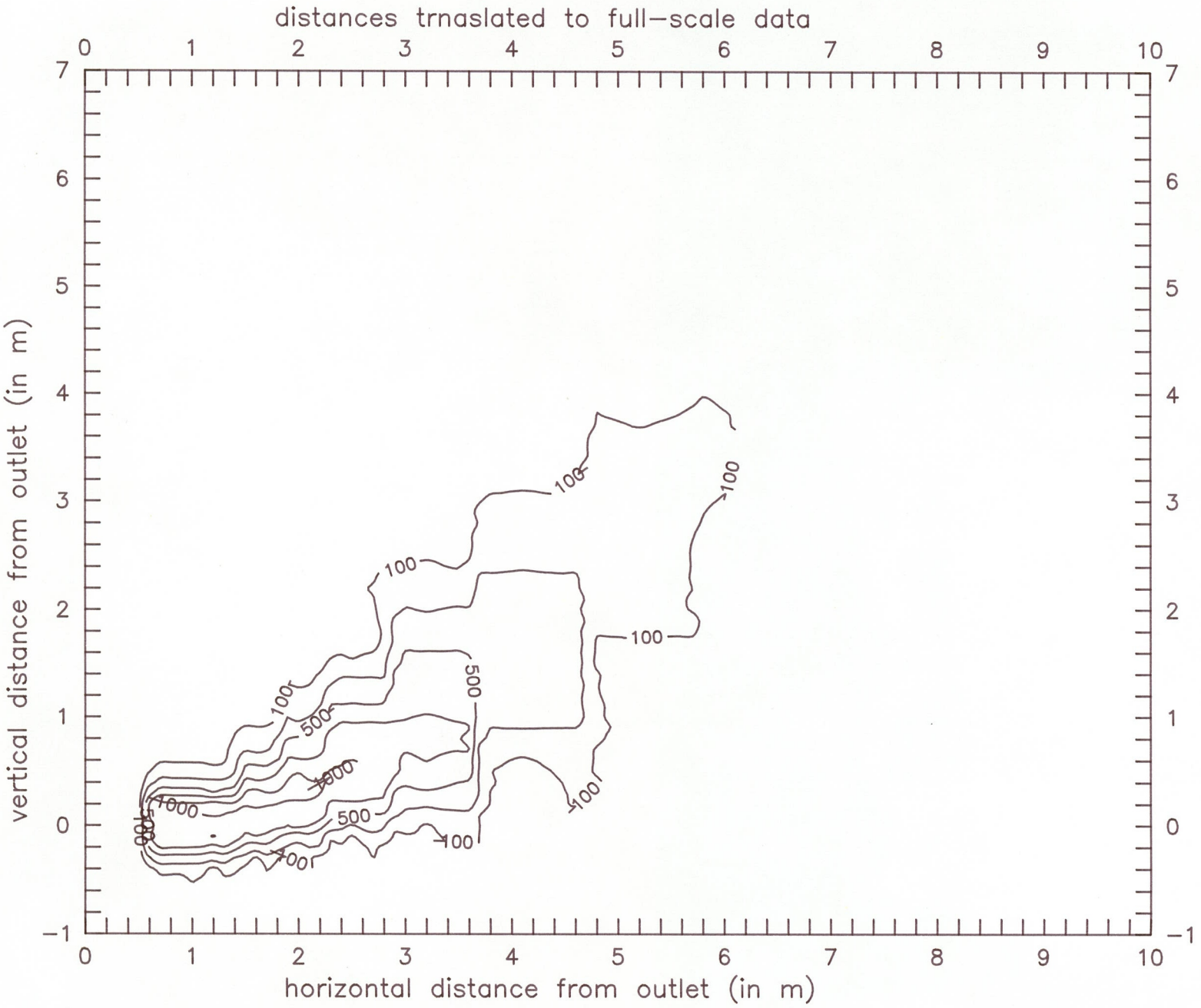


TOF09 along 1:10 Ua=0.8 Uf=12.2

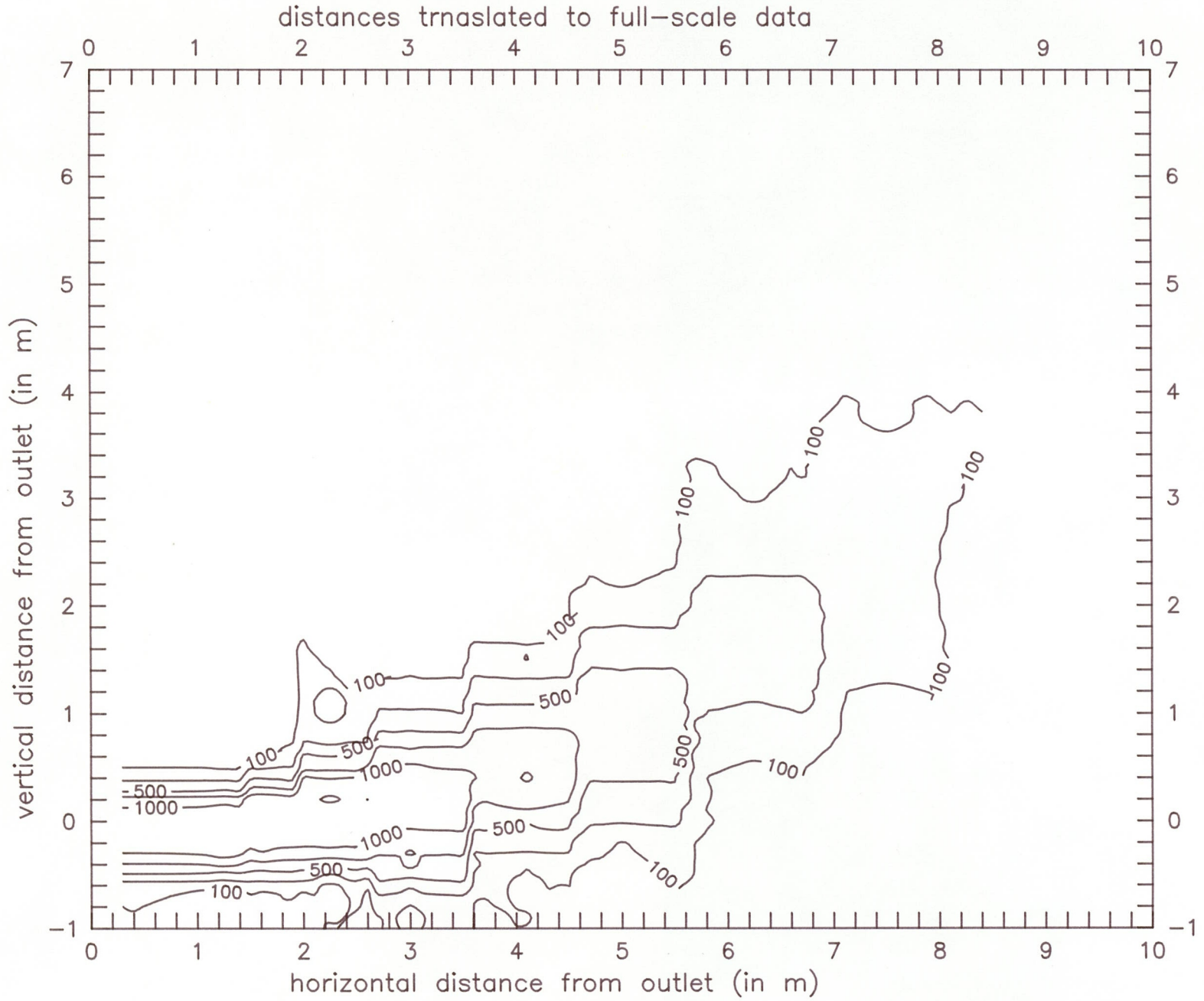


TOF10 along 1:25 Ua=1.0 Uf=16.5

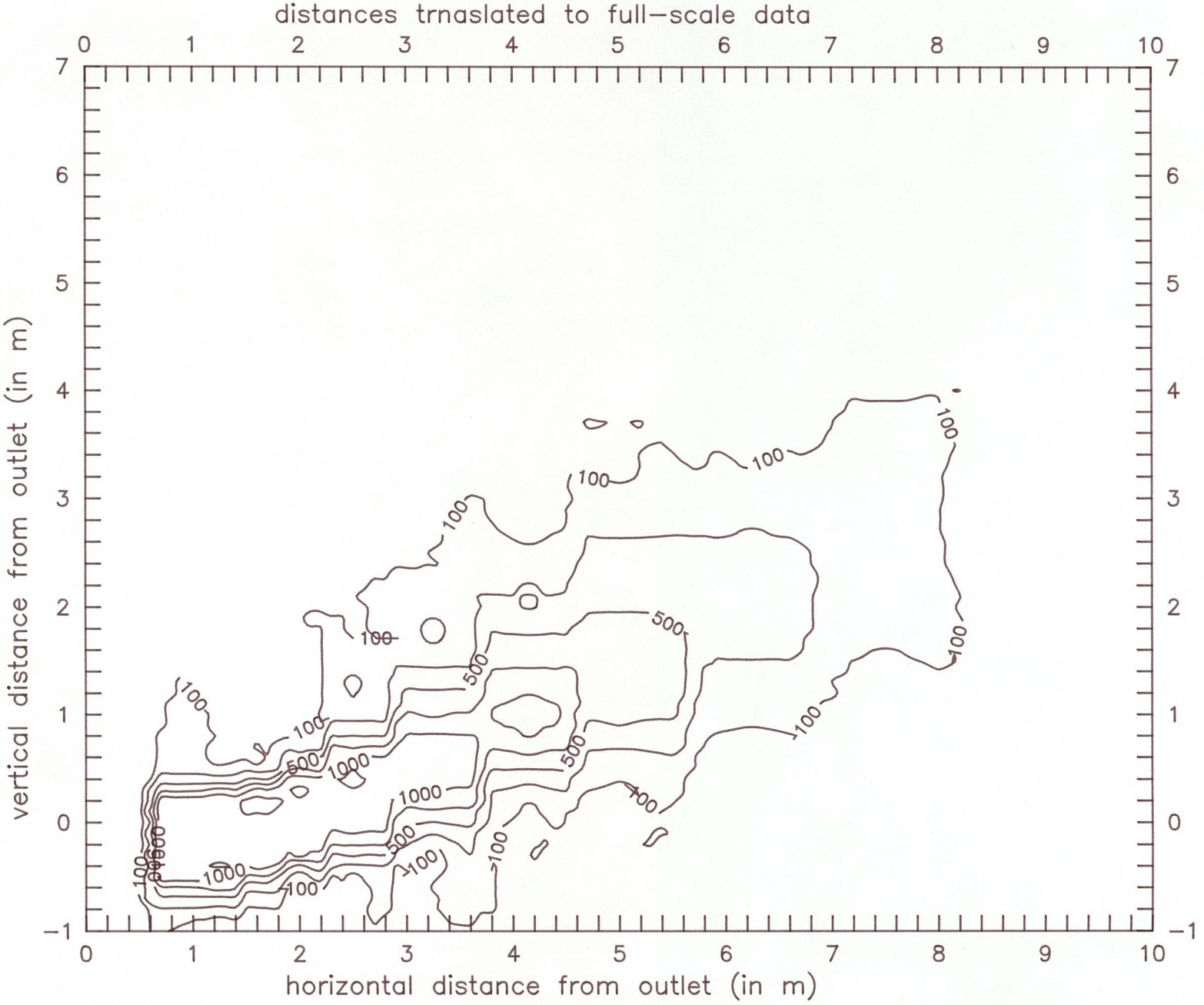


TOF11 along 1:25 Ua=0.5 Uf=16.5

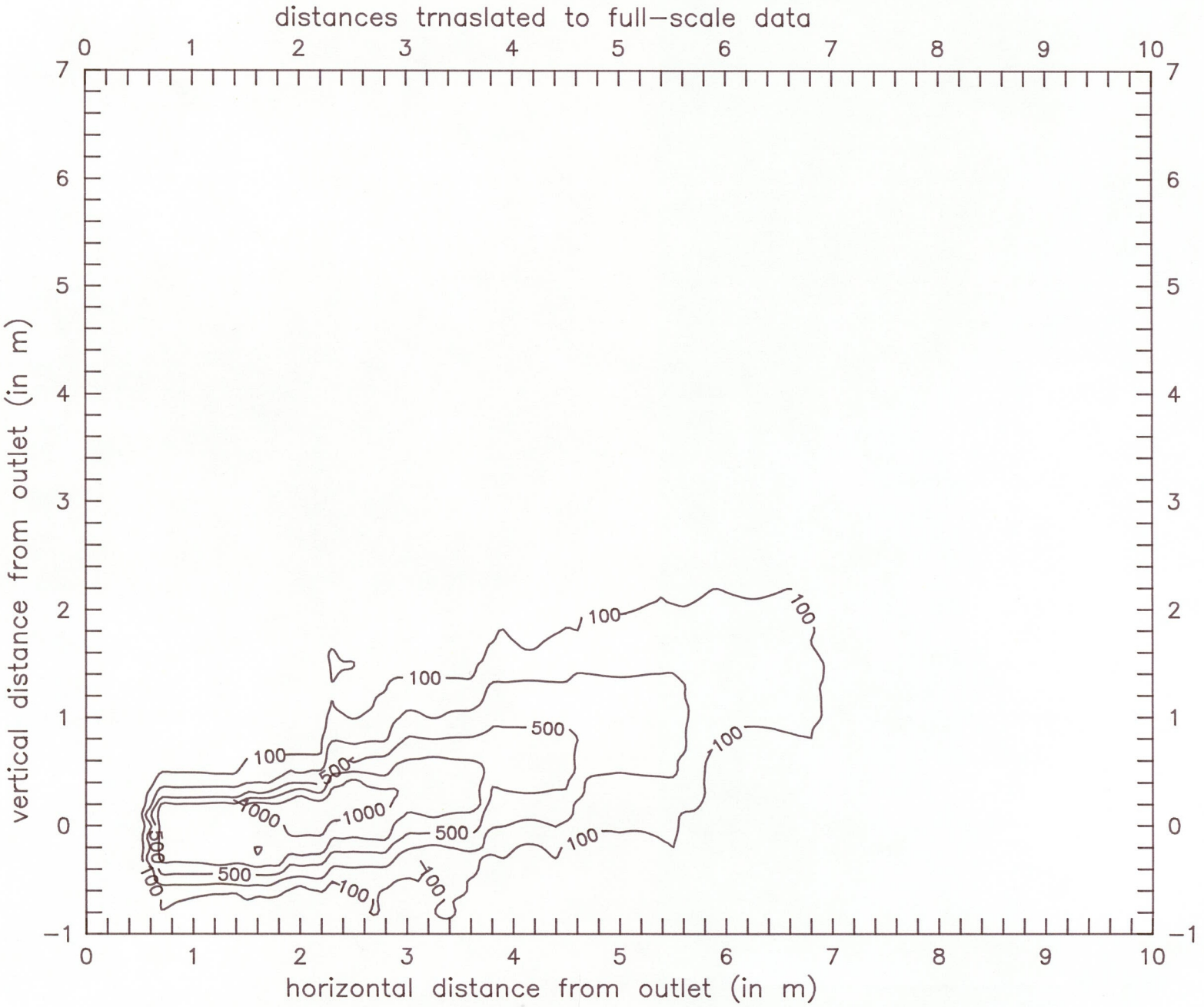


TOF12 along 1:25 Ua=1.0 Uf=8.0

# Appendix C Vertical temperature profiles at X=4.1 m

This appendix contains the results of the flame temperature measurements at X=4.1 m (field scale) on a vertical line perpendicular at the flame centre line. The results are presented as graphs.
The graphs also show the measured values of the field scale experiments.

Graphs have been made of all the windtunnel experiments.

For the windtunnel experiment number 3 (TOF03) vertical temperature measurements have also been performed at horizontal distances X=2 and X=3 m. Three of the graphs show mean and rms values of the measured temperatures.

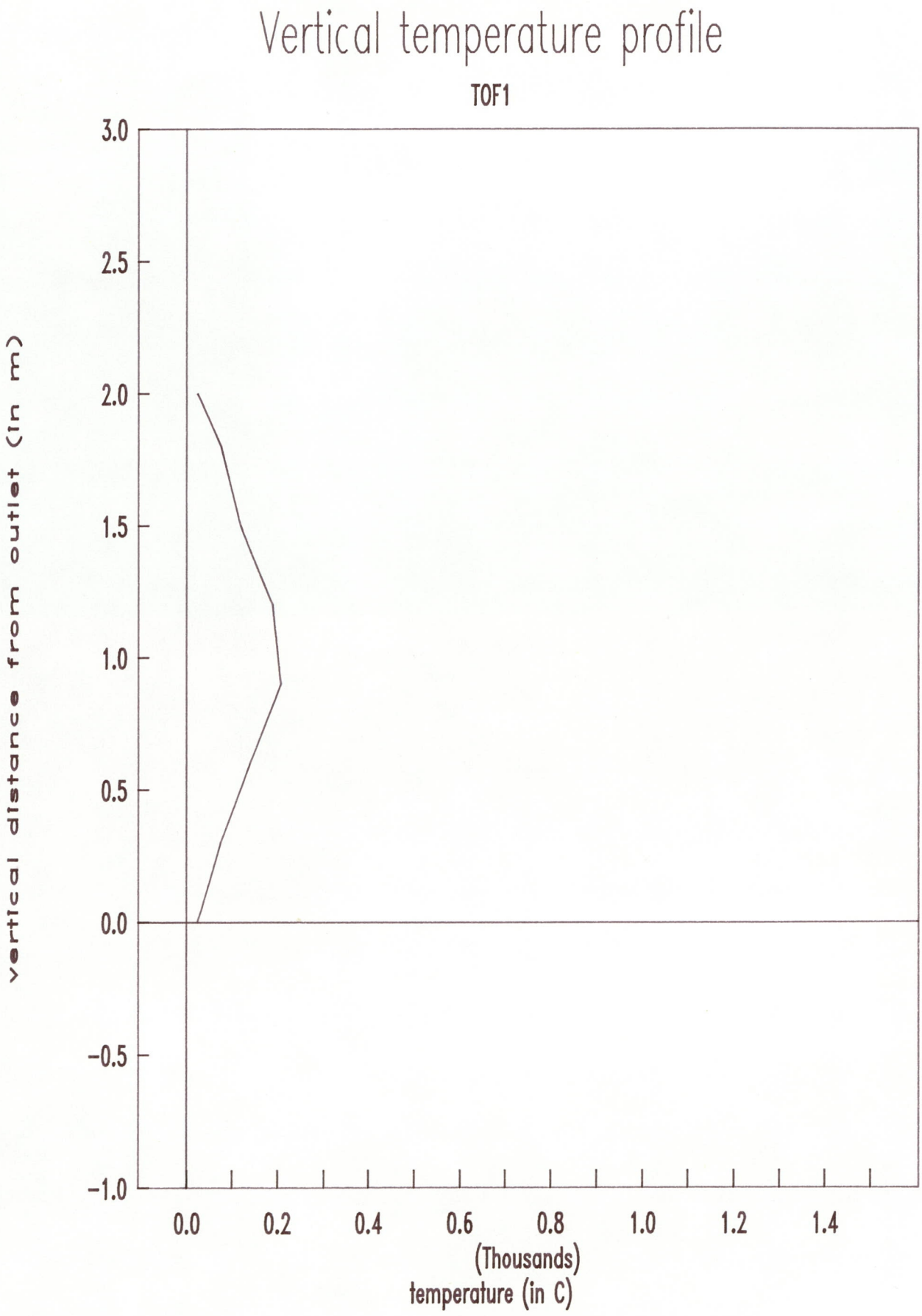
Vertical temperature profile
TOF1
3.0
2.5
2.0
1.5
1.0
0.5
0.0
-0.5
-1.0
vertical distance from outlet (in m)
0.0
0.2
0.4
0.6
0.8
1.0
1.2
1.4
(Thousands)
temperature (in C)

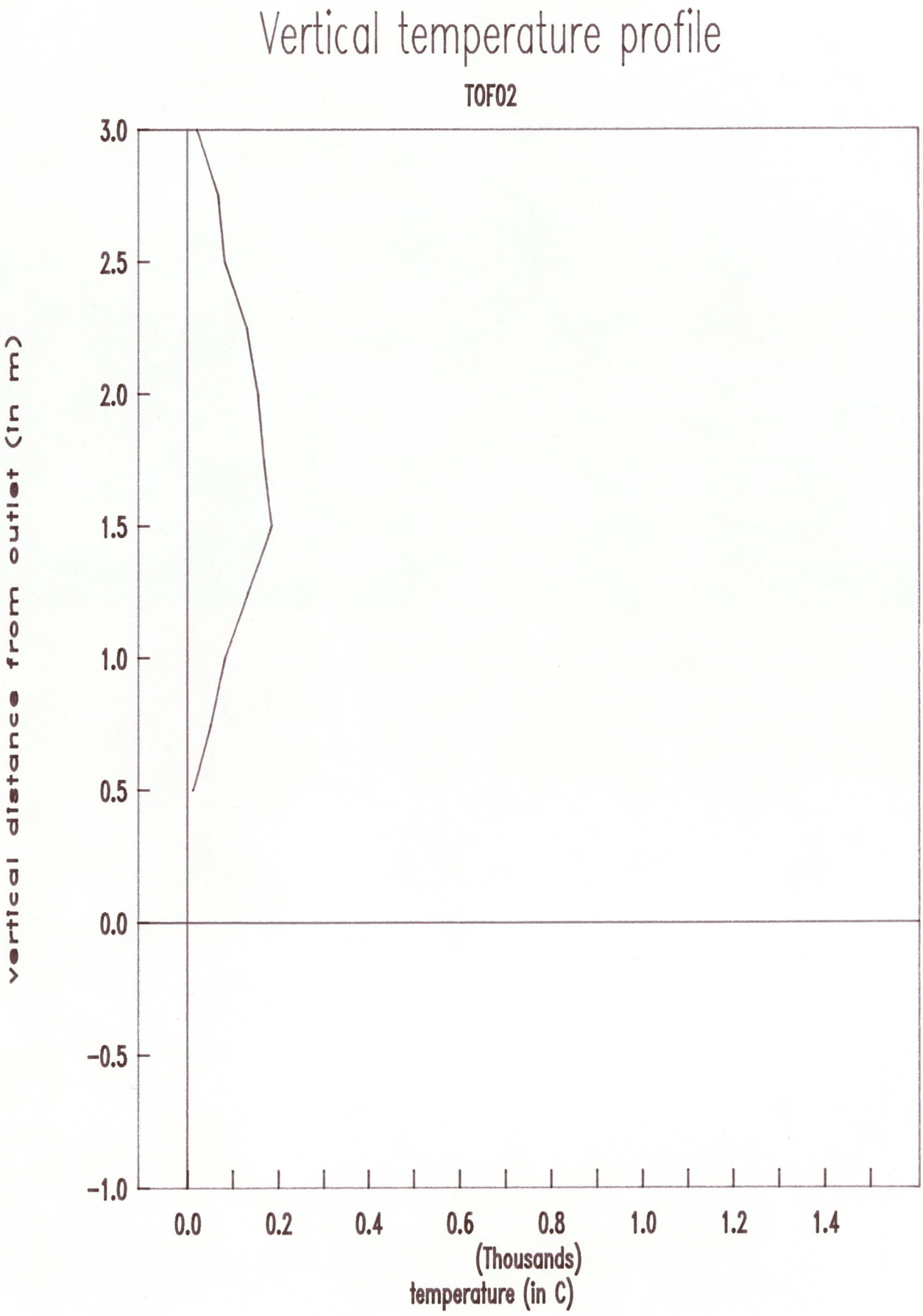
Vertical temperature profile
TOF02
3.0
2.5
2.0
1.5
1.0
0.5
0.0
-0.5
-1.0
vertical distance from outlet (in m)
0.0
0.2
0.4
0.6
0.8
1.0
1.2
1.4
(Thousands)
temperature (in C)

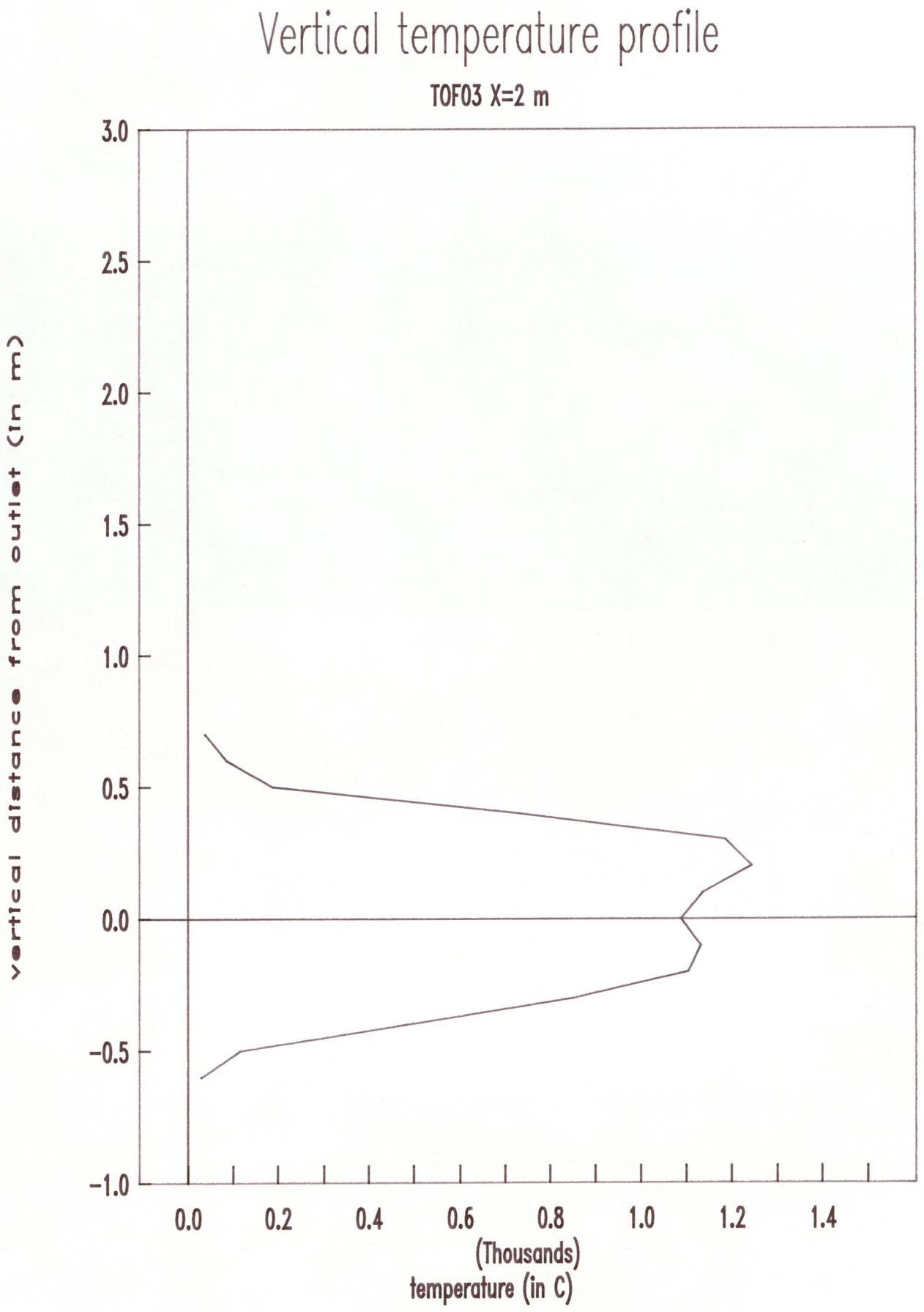
Vertical temperature profile
TOF03 X=2 m
vertical distance from outlet (in m)
3.0
2.5
2.0
1.5
1.0
0.5
0.0
-0.5
-1.0
0.0
0.2
0.4
0.6
0.8
1.0
1.2
1.4
(Thousands)
temperature (in C)

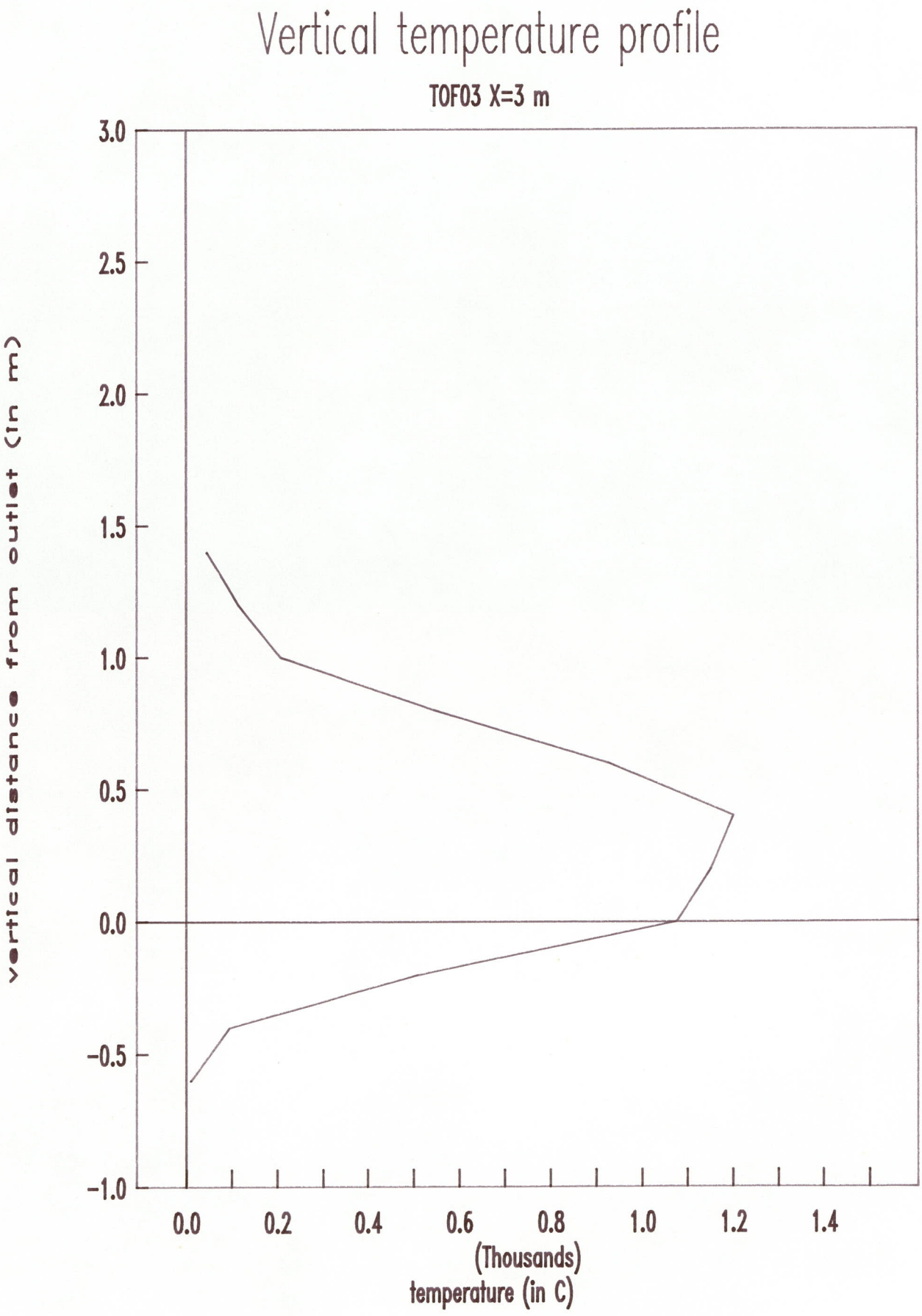
Vertical temperature profile
TOF03 X=3 m
vertical distance from outlet (in m)
3.0
2.5
2.0
1.5
1.0
0.5
0.0
-0.5
-1.0
0.0
0.2
0.4
0.6
0.8
1.0
1.2
1.4
(Thousands)
temperature (in C)

# Vertical temperature profile

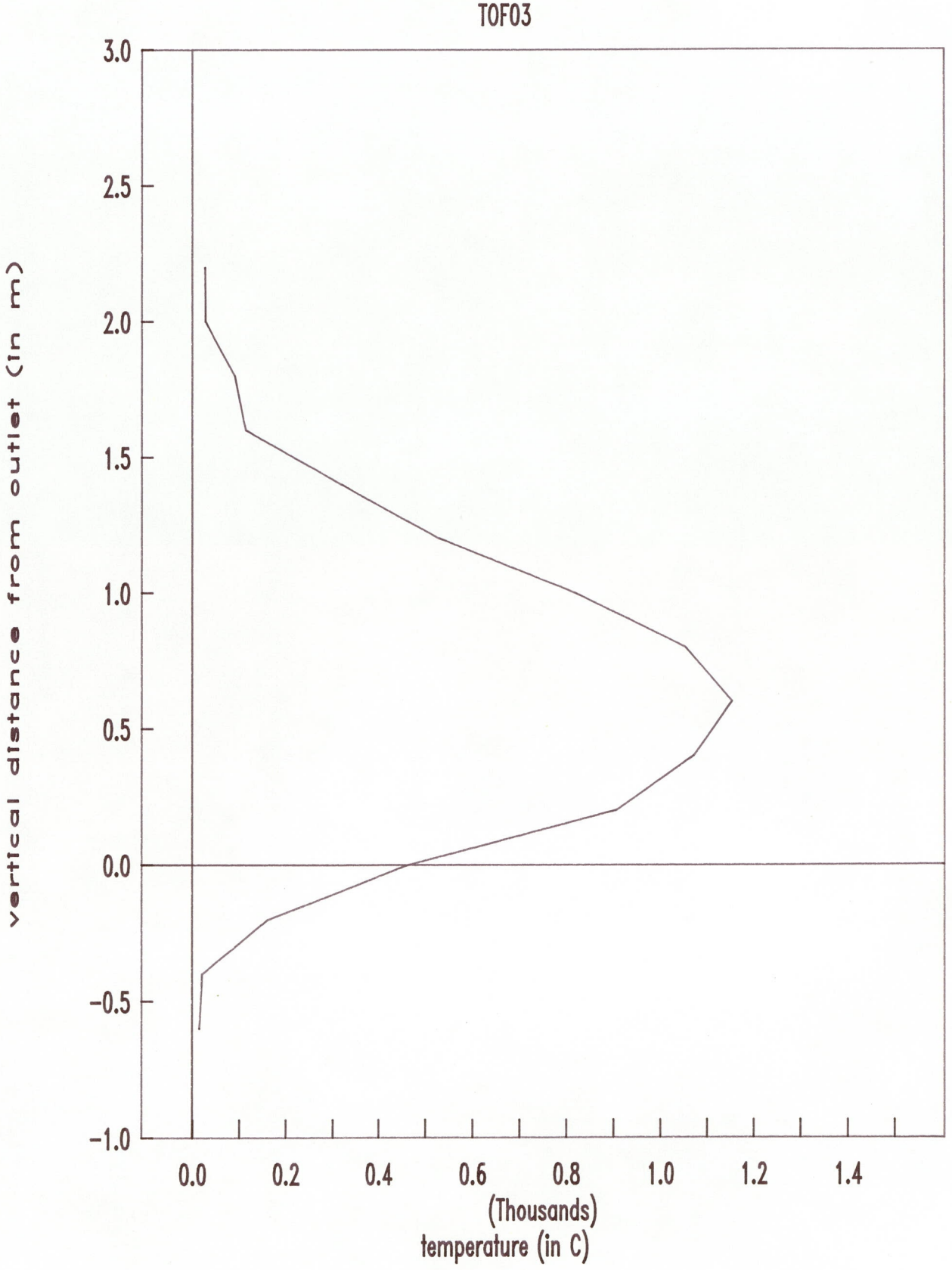

# Vertical temperature profile

TOF06

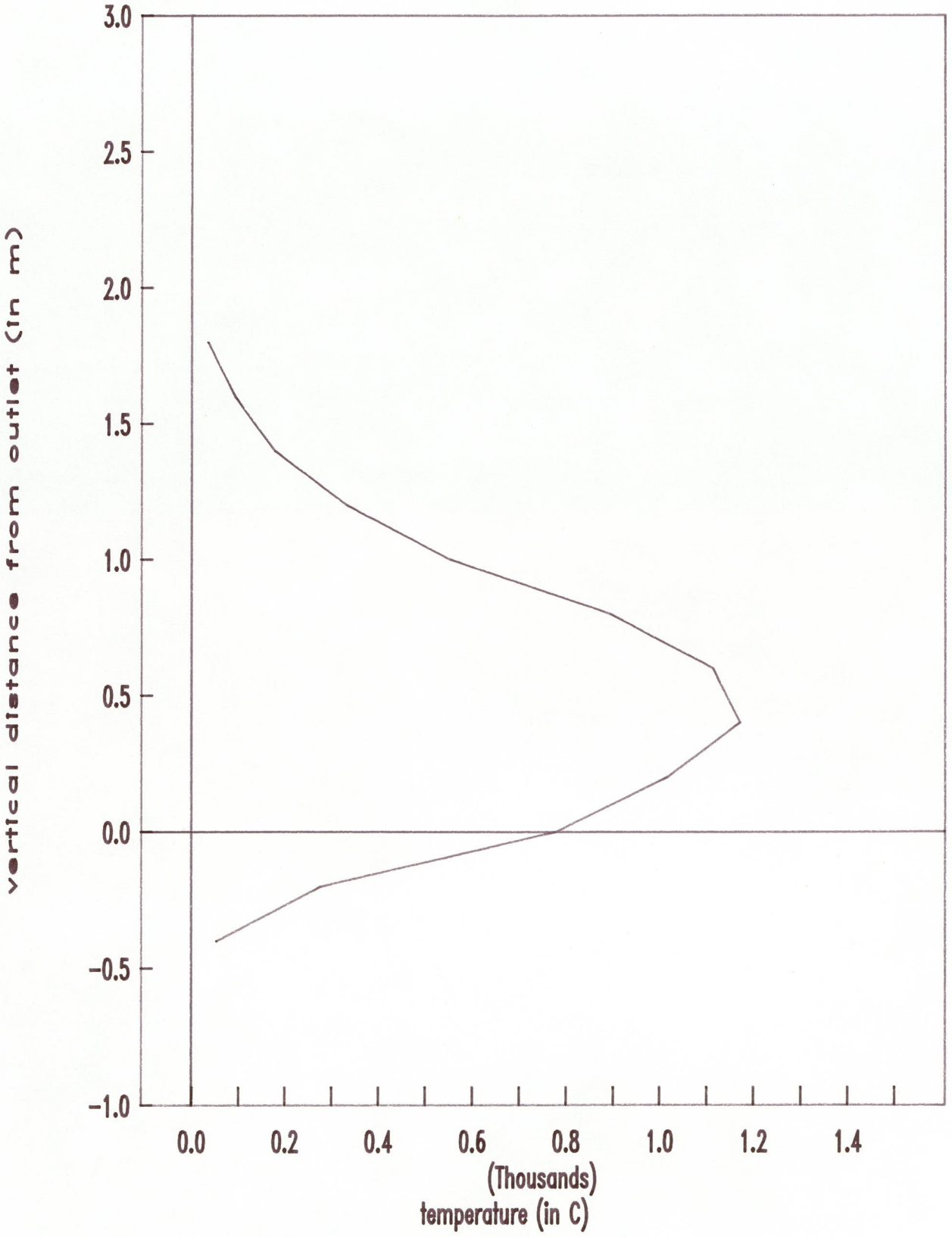

# Vertical temperature profile

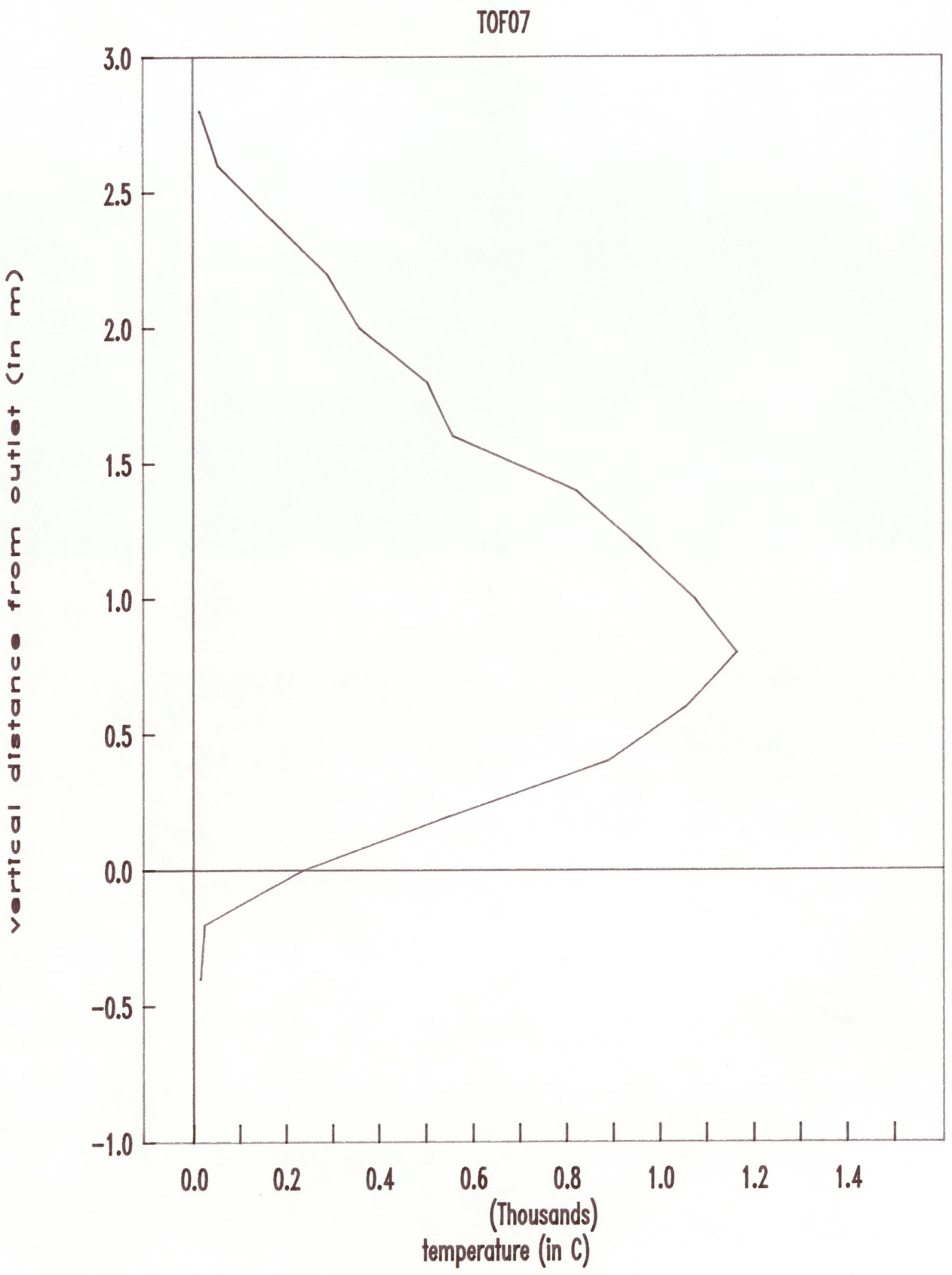

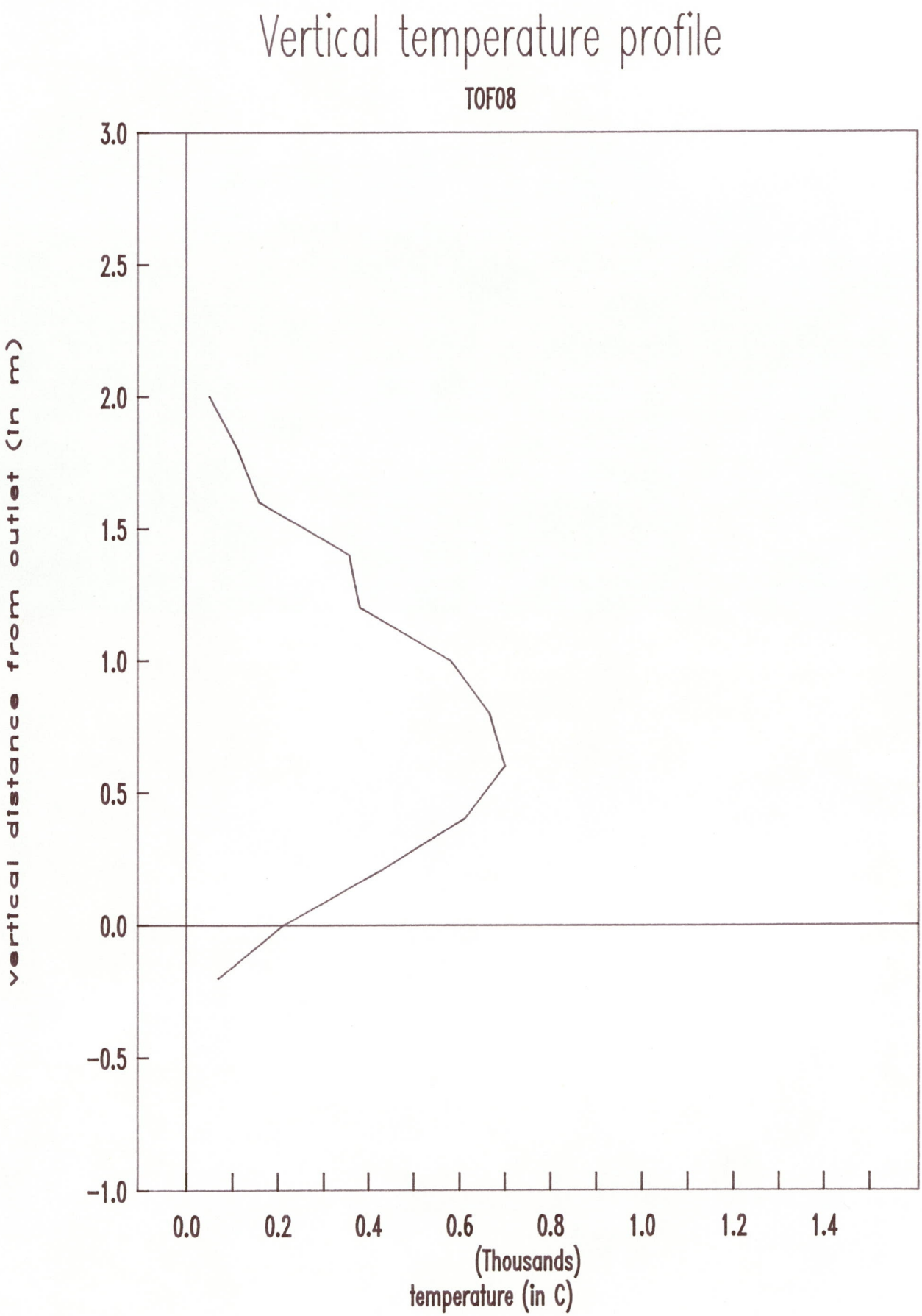
Vertical temperature profile
TOF08
3.0
2.5
2.0
1.5
1.0
0.5
0.0
-0.5
-1.0
vertical distance from outlet (in m)
0.0
0.2
0.4
0.6
0.8
1.0
1.2
1.4
(Thousands)
temperature (in C)

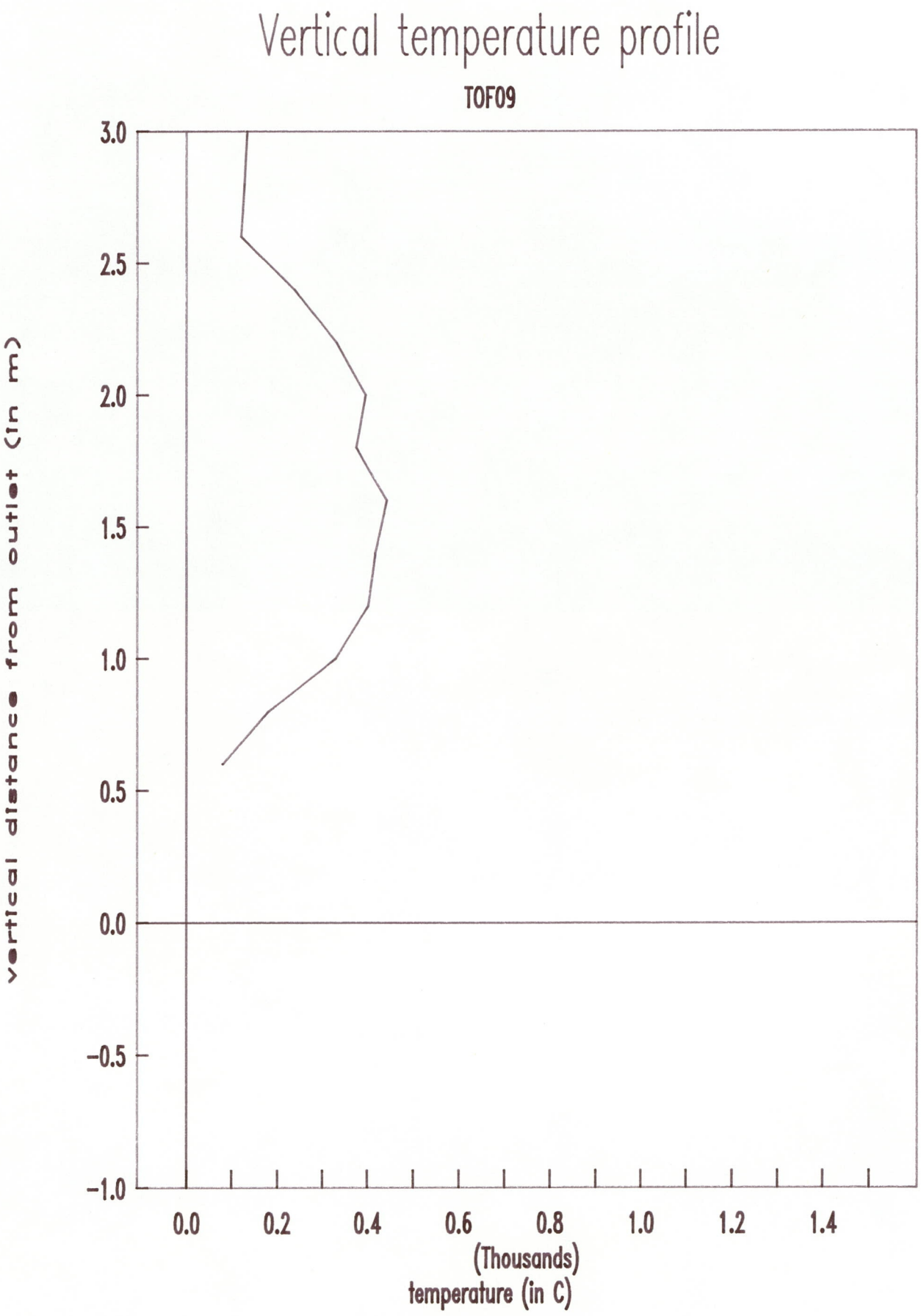
Vertical temperature profile
TOF09
3.0
2.5
2.0
1.5
1.0
0.5
0.0
-0.5
-1.0
vertical distance from outlet (in m)
0.0
0.2
0.4
0.6
0.8
1.0
1.2
1.4
(Thousands)
temperature (in C)

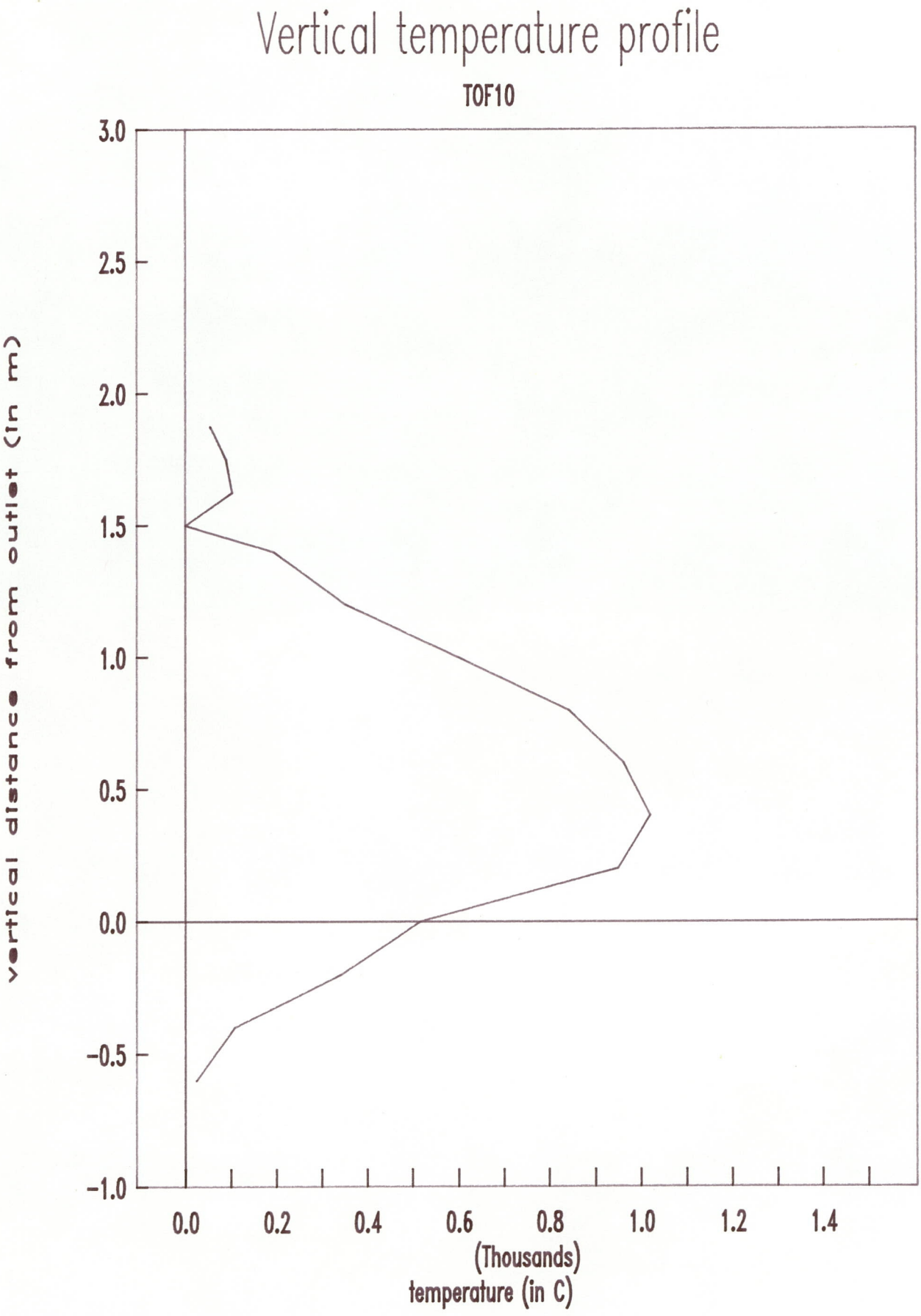
Vertical temperature profile
TOF10
3.0
2.5
2.0
1.5
1.0
0.5
0.0
-0.5
-1.0
vertical distance from outlet (in m)
0.0
0.2
0.4
0.6
0.8
1.0
1.2
1.4
(Thousands)
temperature (in C)

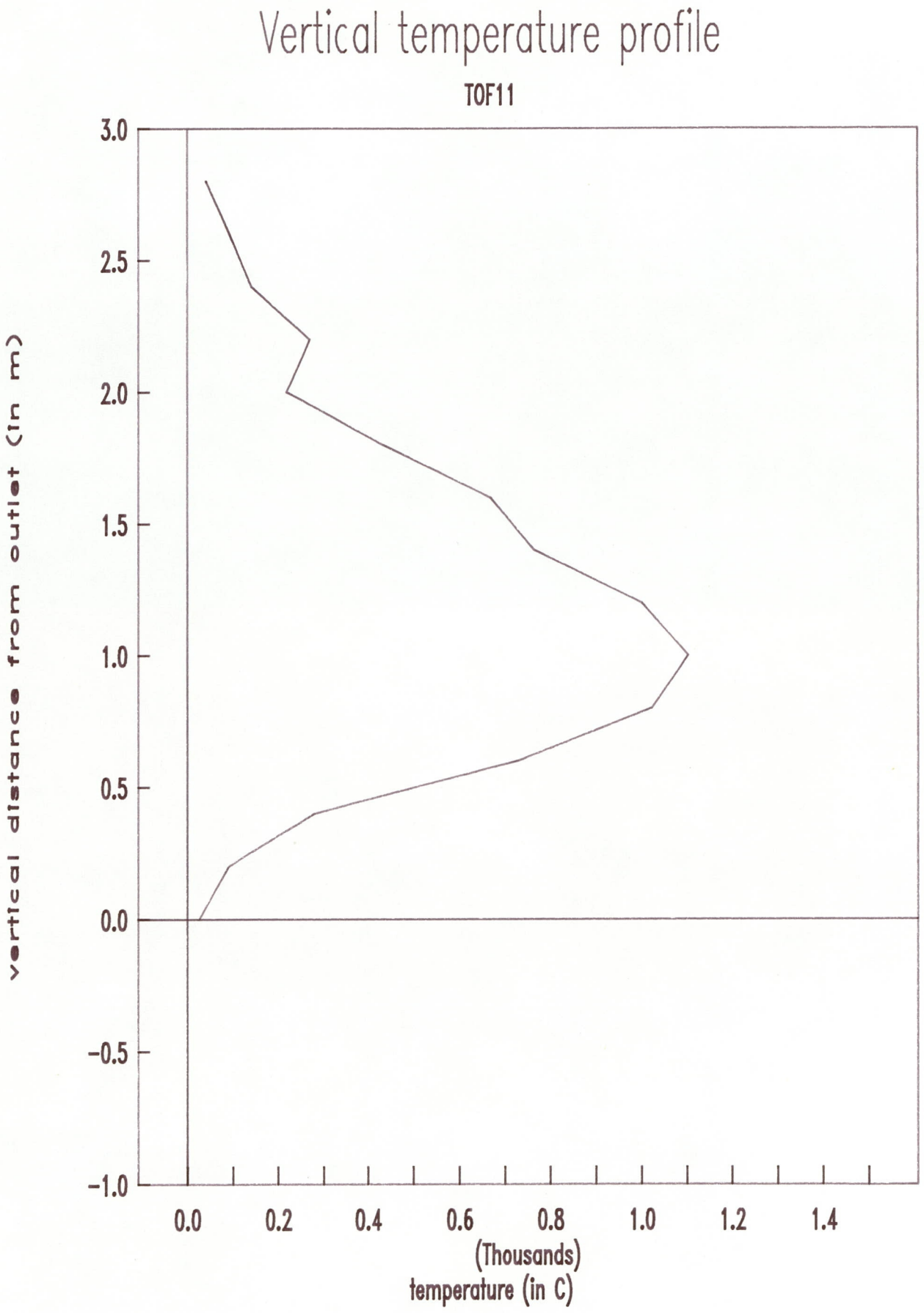
Vertical temperature profile
TOF11
vertical distance from outlet (in m)
3.0
2.5
2.0
1.5
1.0
0.5
0.0
-0.5
-1.0
0.0
0.2
0.4
0.6
0.8
1.0
1.2
1.4
(Thousands)
temperature (in C)

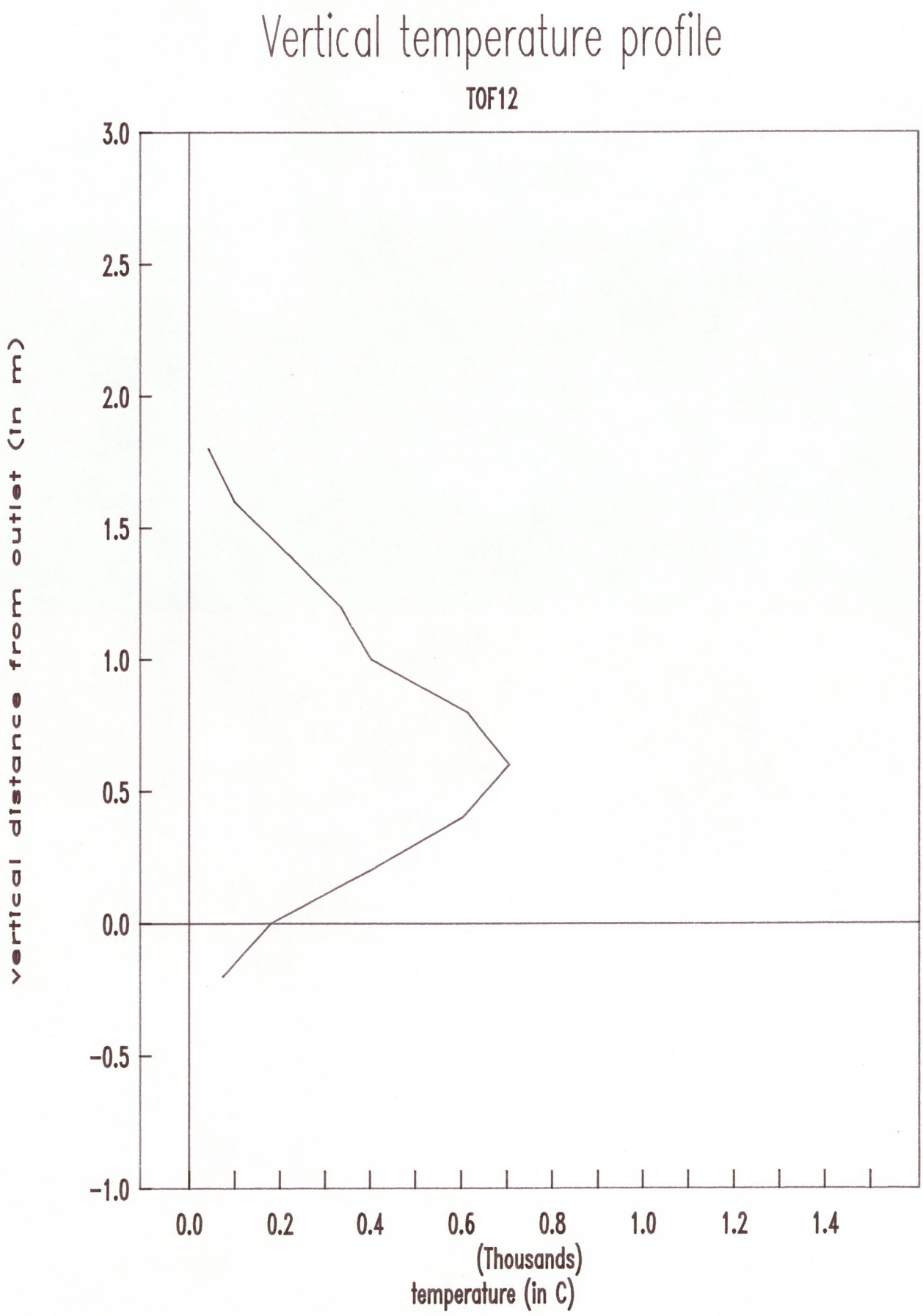
Vertical temperature profile
TOF12
3.0
2.5
2.0
1.5
1.0
0.5
0.0
-0.5
-1.0
vertical distance from outlet (in m)
0.0
0.2
0.4
0.6
0.8
1.0
1.2
1.4
(Thousands)
temperature (in C)

# Appendix D Contour plots of the flame temperature at X=4.1 m (across)

This appendix contains the results of the flame temperature measurements at X=4.1 m (field scale) of the flame in the across wind direction presented as contour plots. Because of the symmetry measurements have been performed of only half of this plane. The plots have been created using a plot program.

The contour plots have been made of the windtunnel experiments 1, 3, 7, 10, 11 and 12.

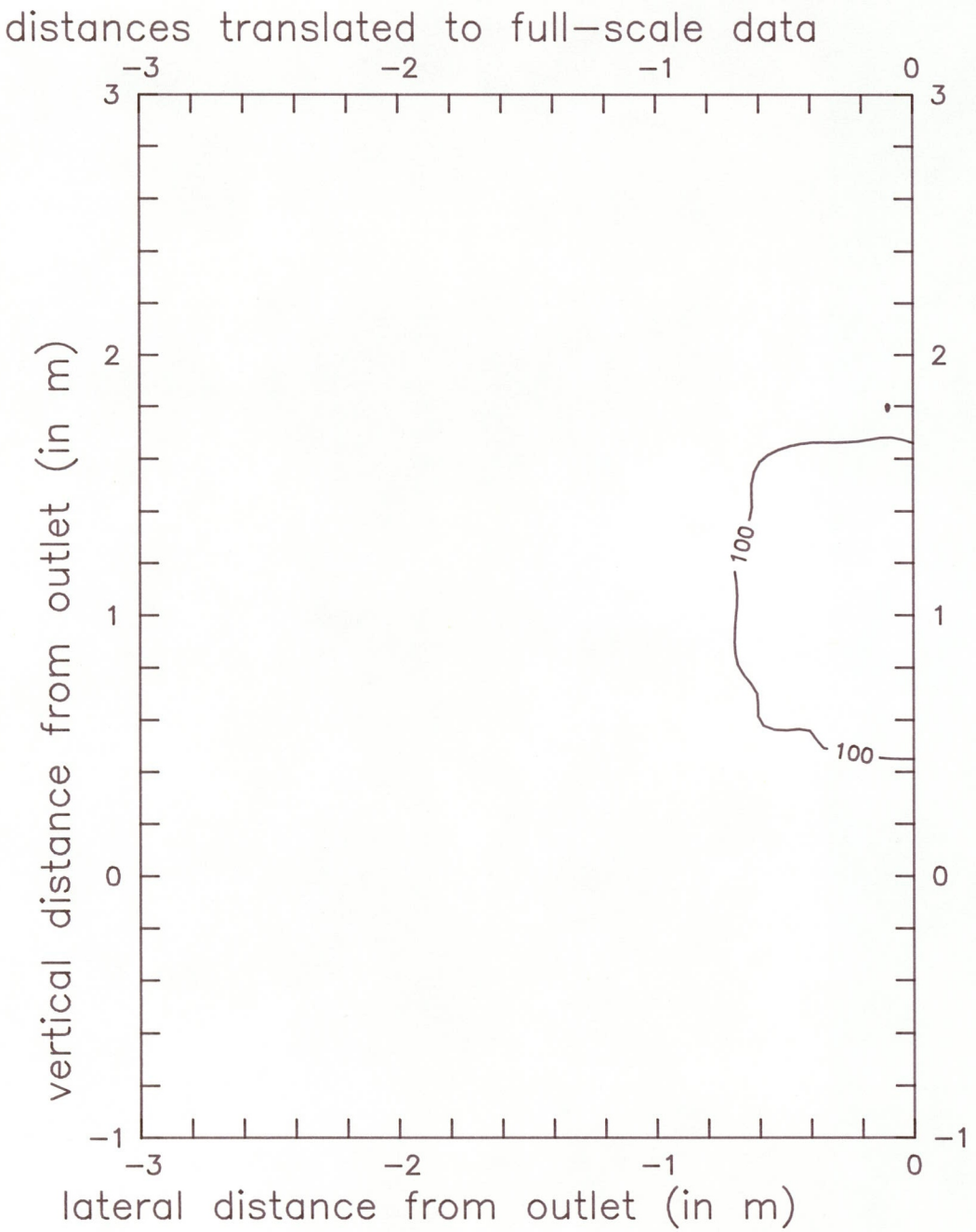


TOF01 across 1:10 Ua=1.4 Uf=6.1

distances translated to full-scale data
TOF03 across X=2 m 1:10 Ua=1.4 Uf=6.1
vertical distance from outlet (in m)
lateral distance from outlet (in m)
-3
-2
-1
0
3
2
1
0
-1
100
500
100

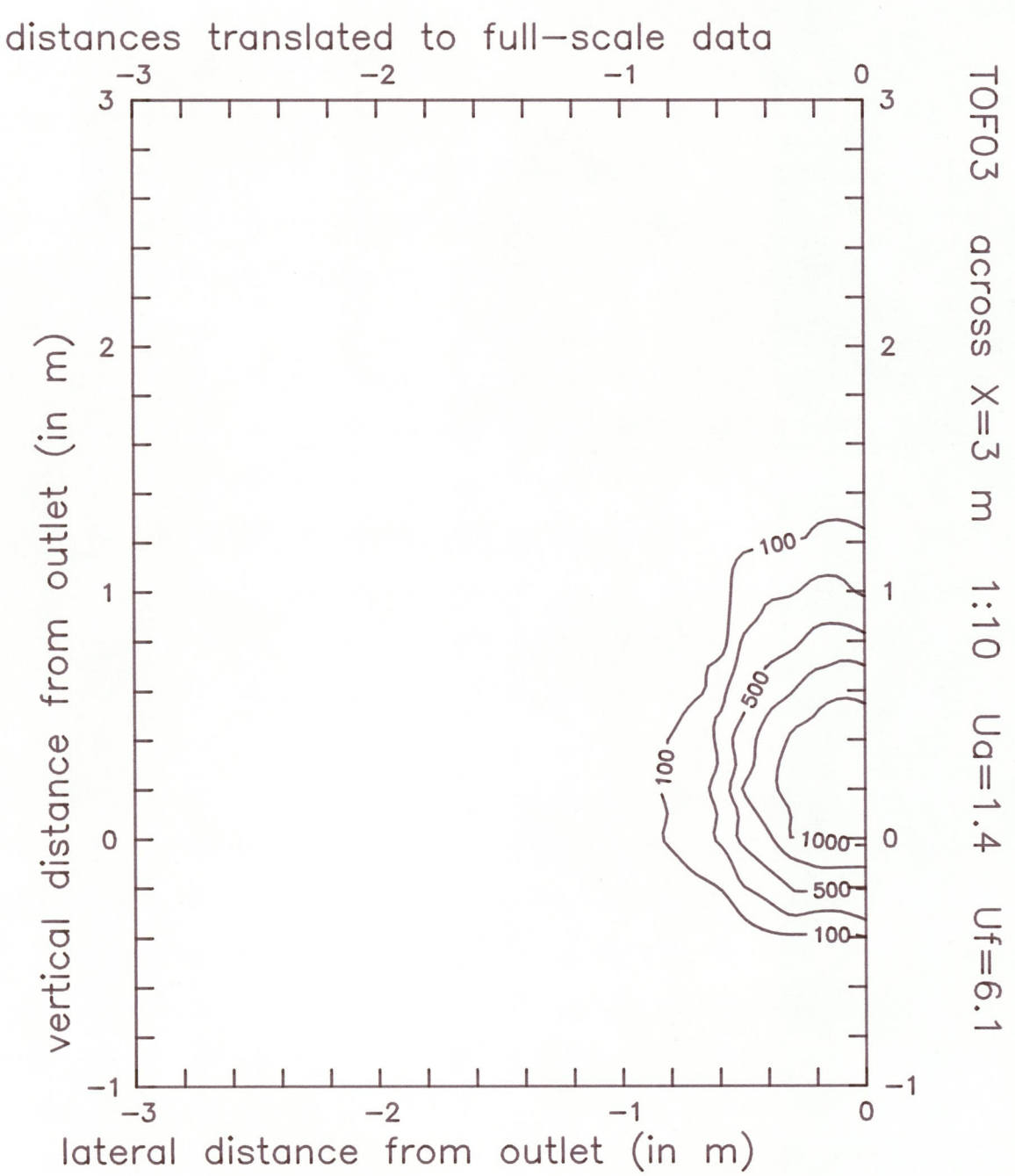
distances translated to full-scale data
TOF03 across X=3 m 1:10 Ua=1.4 Uf=6.1
vertical distance from outlet (in m)
lateral distance from outlet (in m)
-3
-2
-1
0
3
2
1
0
-1
100
500
1000
100
500
100

TOF03 across 1:10 Ua=1.2 Uf=26.5

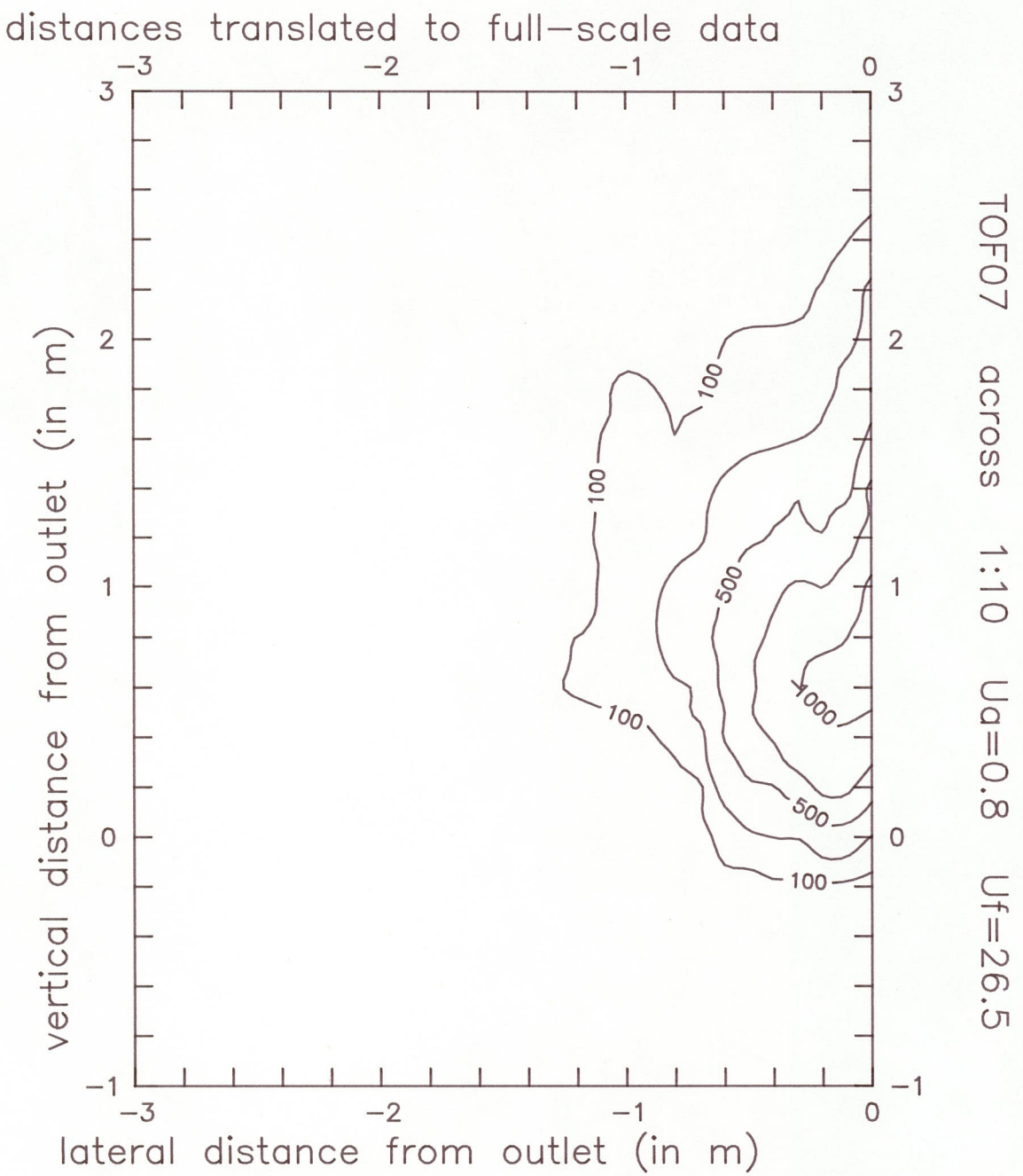


TOF07 across 1:10 Ua=0.8 Uf=26.5

TOF10 across 1:25 Ua=1.0 Uf=16.5

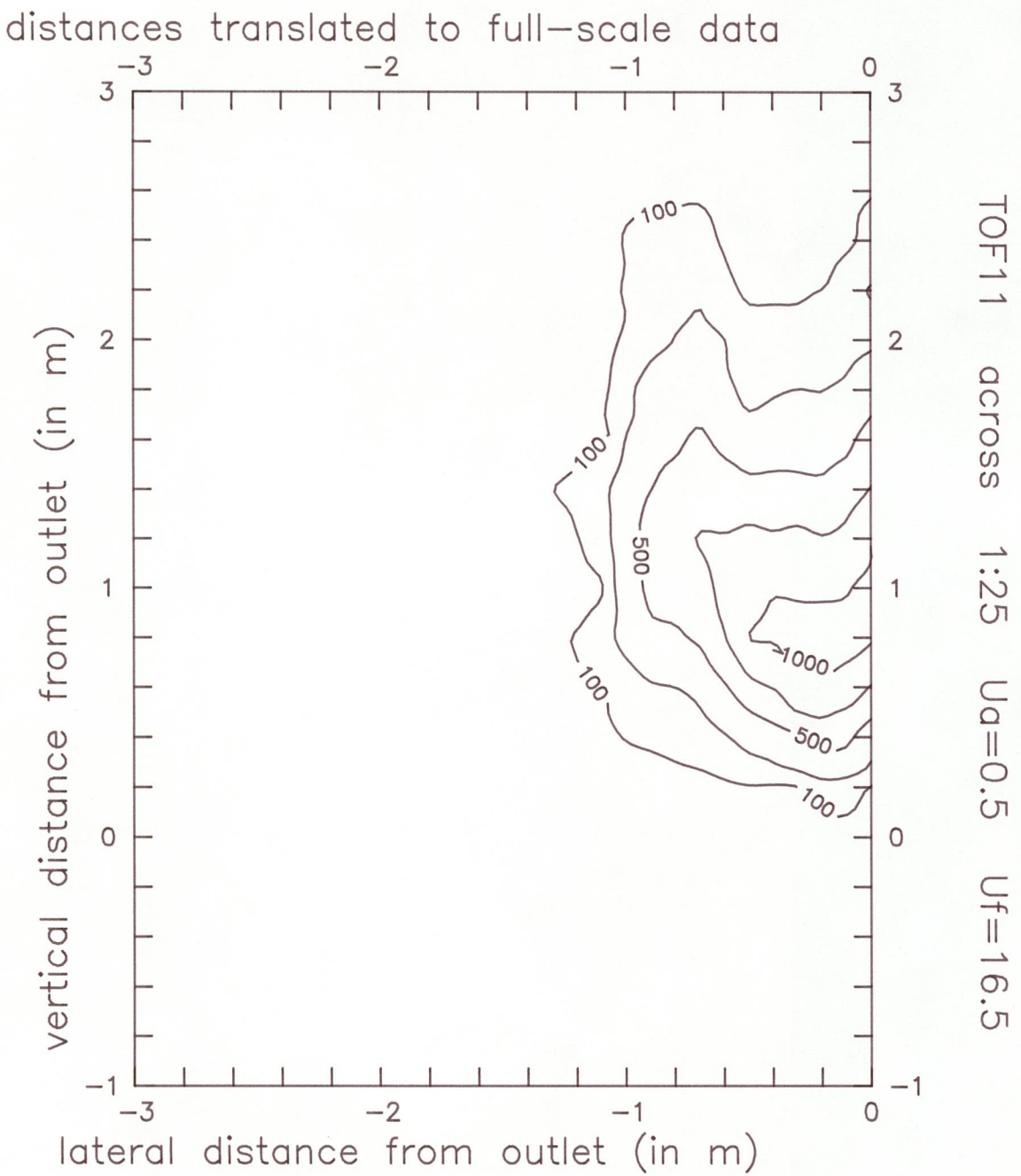


TOF11 across 1:25 Ua=0.5 Uf=16.5

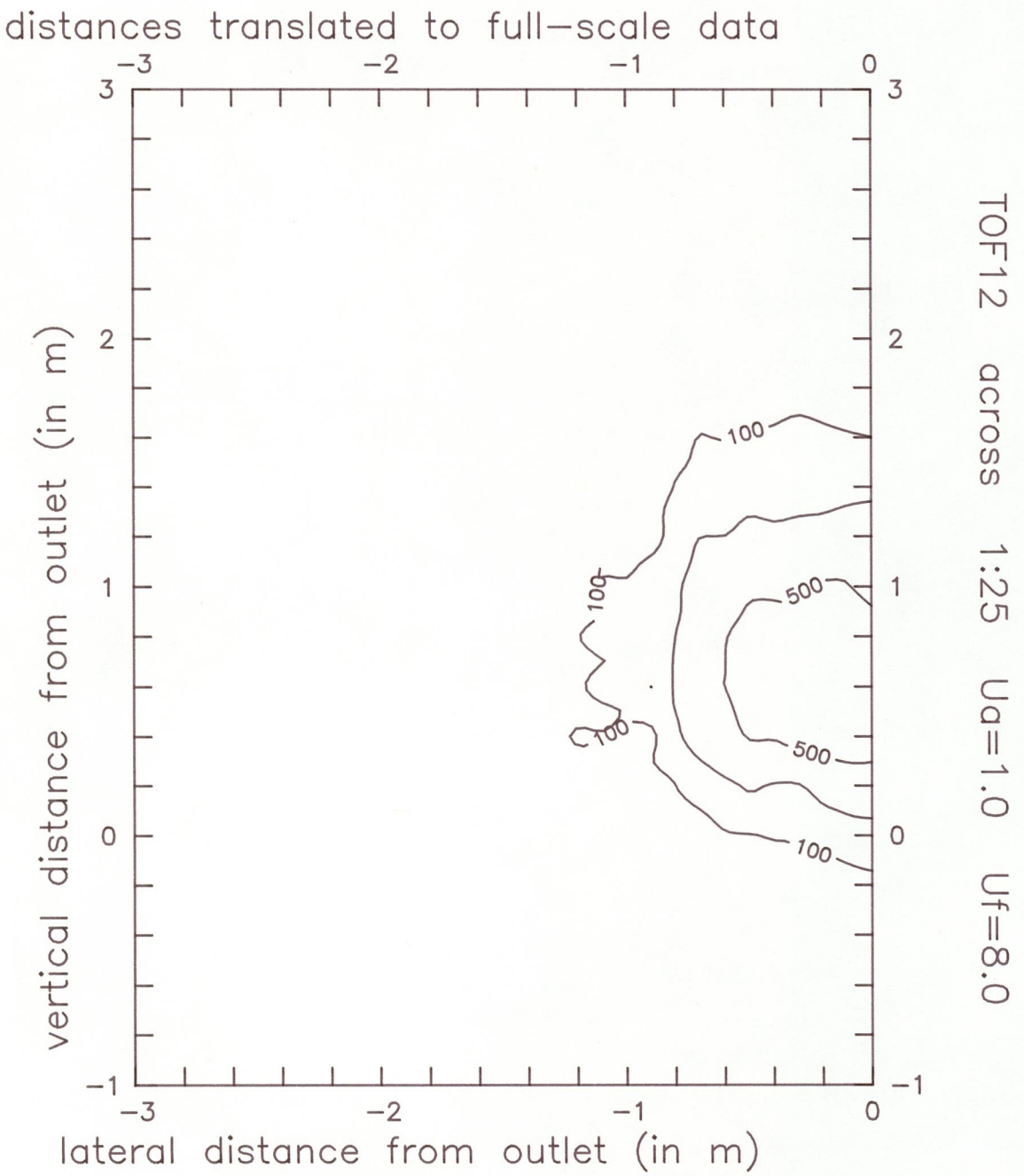


TOF12 across 1:25 Ua=1.0 Uf=8.0

# Appendix E Heat flux profiles

This appendix contains the results of the heat flux temperature measurements at the lines 2.5 m below the centre line of the flame (Q1) and at a lateral distance of 2.5 m from this line (Q2).
The values of the heat fluxes are those measured in the TNO windtunnel, the length scales have been translated into the field scale lengths.

The contour plots have been made of all the windtunnel experiments except for the numbers 11 and 12.

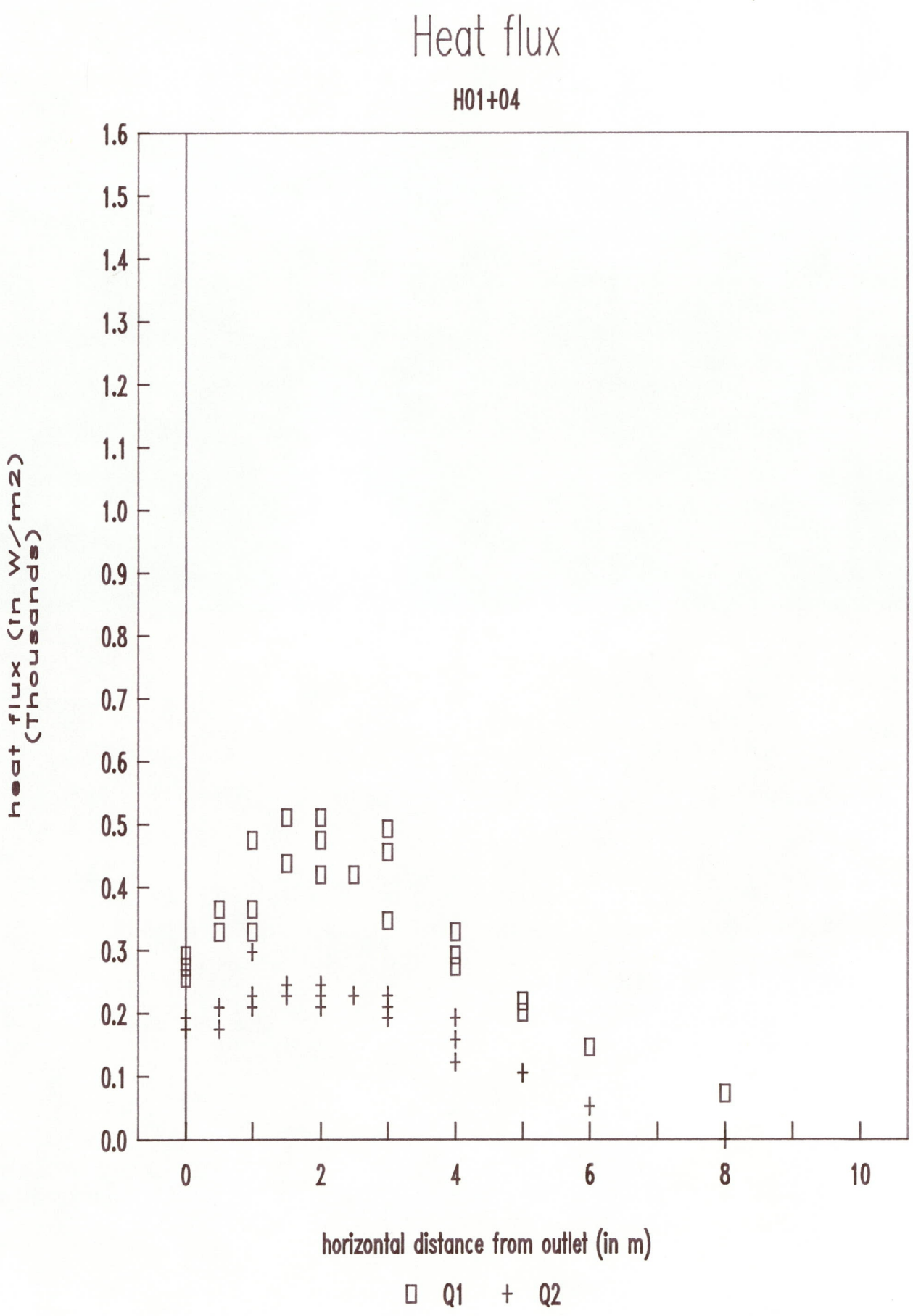
Heat flux
H01+04
heat flux (in W/m2)
(Thousands)
1.6
1.5
1.4
1.3
1.2
1.1
1.0
0.9
0.8
0.7
0.6
0.5
0.4
0.3
0.2
0.1
0.0
0
2
4
6
8
10
horizontal distance from outlet (in m)
Q1
Q2

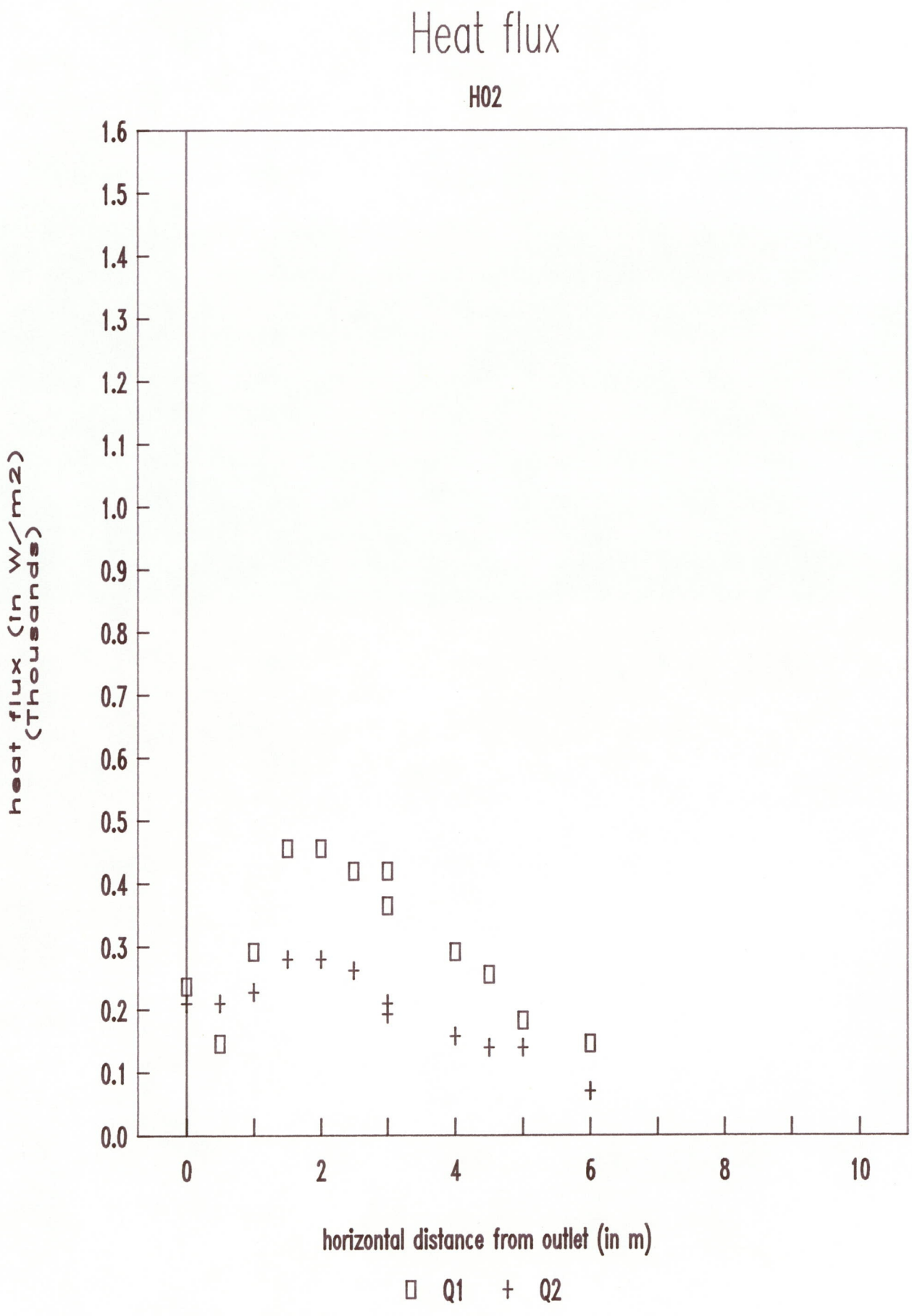
Heat flux
H02
heat flux (in W/m2)
(Thousands)
1.6
1.5
1.4
1.3
1.2
1.1
1.0
0.9
0.8
0.7
0.6
0.5
0.4
0.3
0.2
0.1
0.0
0
2
4
6
8
10
horizontal distance from outlet (in m)
Q1
Q2

# Heat flux

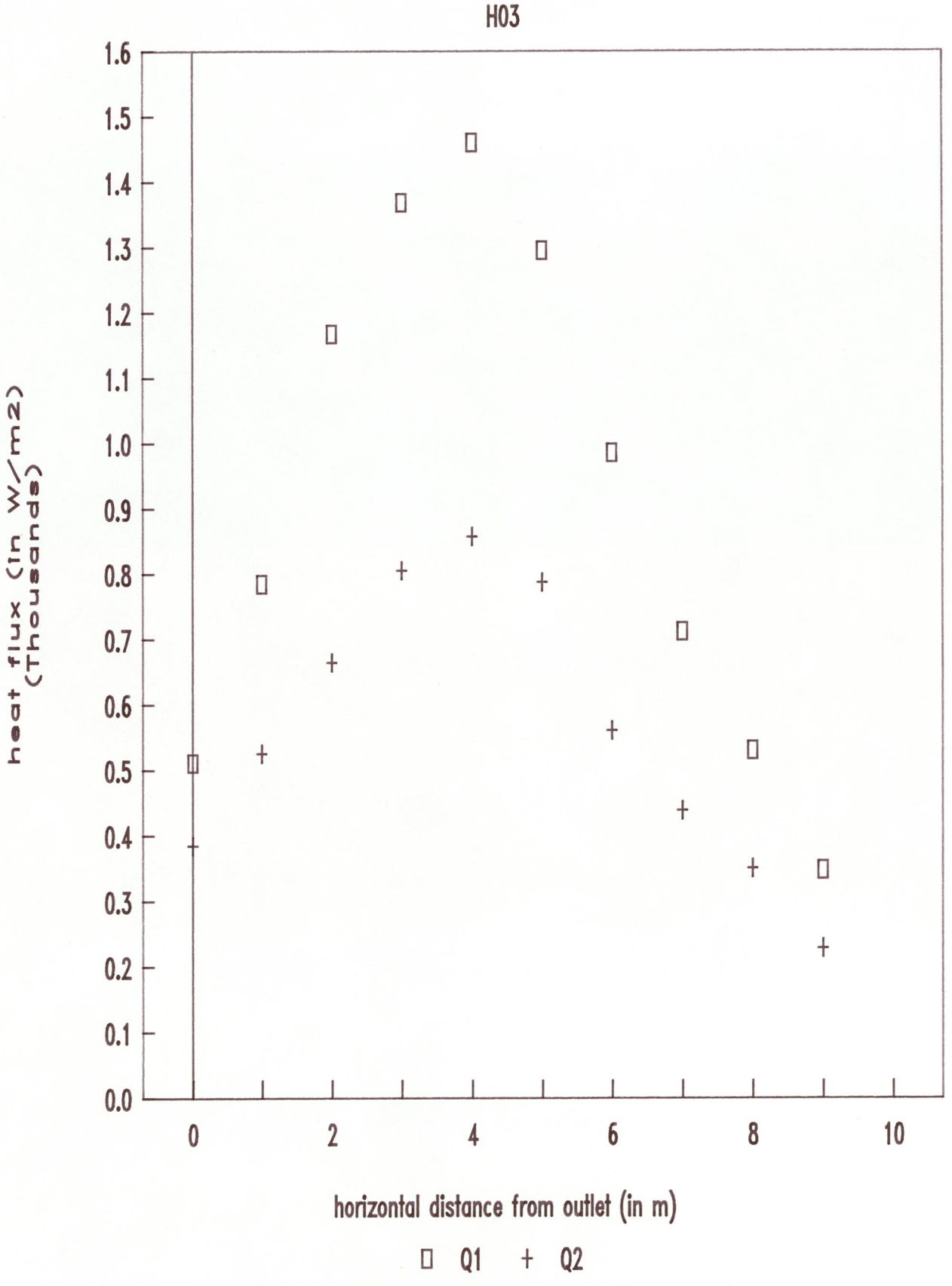
H03
heat flux (in W/m2)
(Thousands)
1.6
1.5
1.4
1.3
1.2
1.1
1.0
0.9
0.8
0.7
0.6
0.5
0.4
0.3
0.2
0.1
0.0
0
2
4
6
8
10
horizontal distance from outlet (in m)
Q1
Q2

# Heat flux

H06

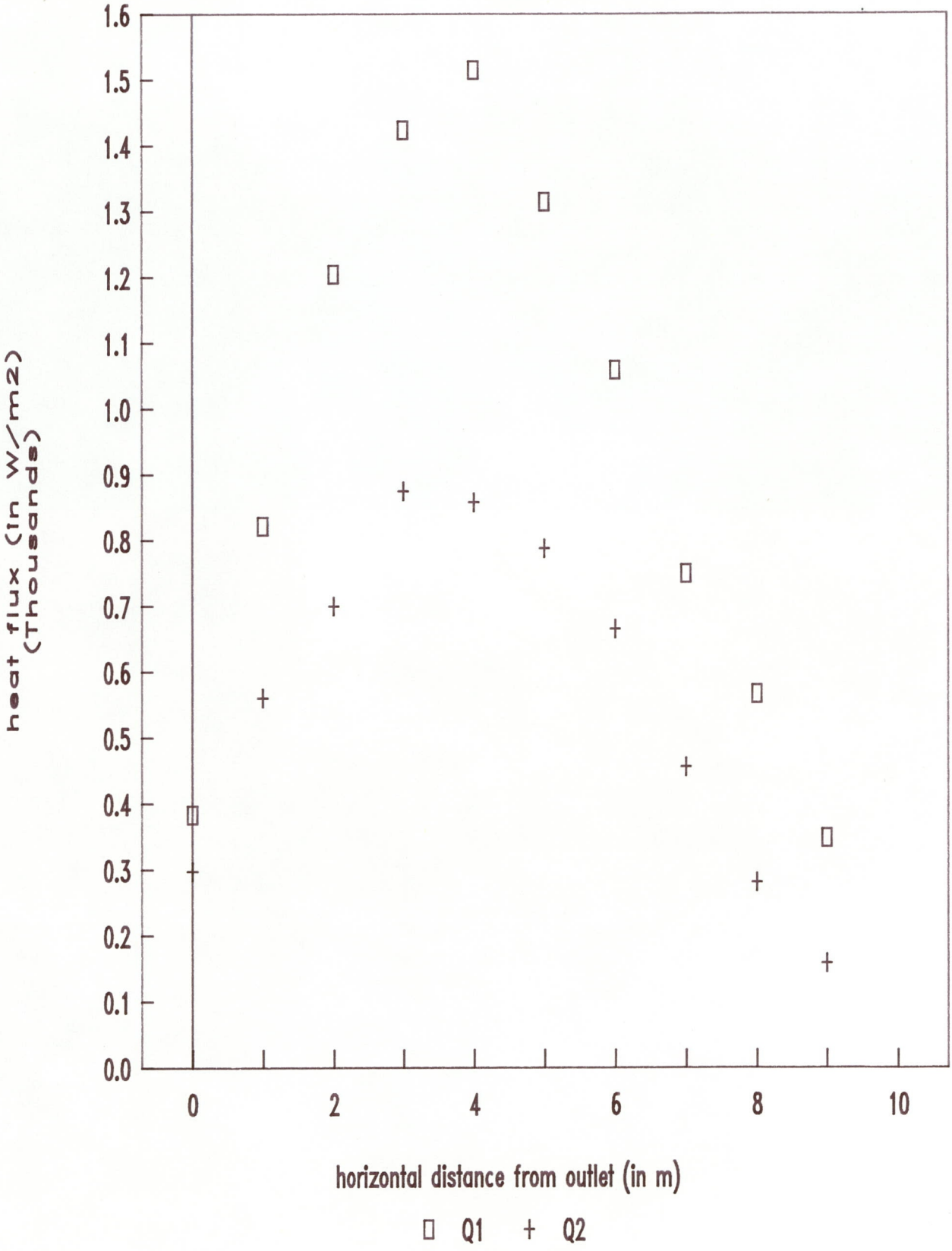

# Heat flux

H07

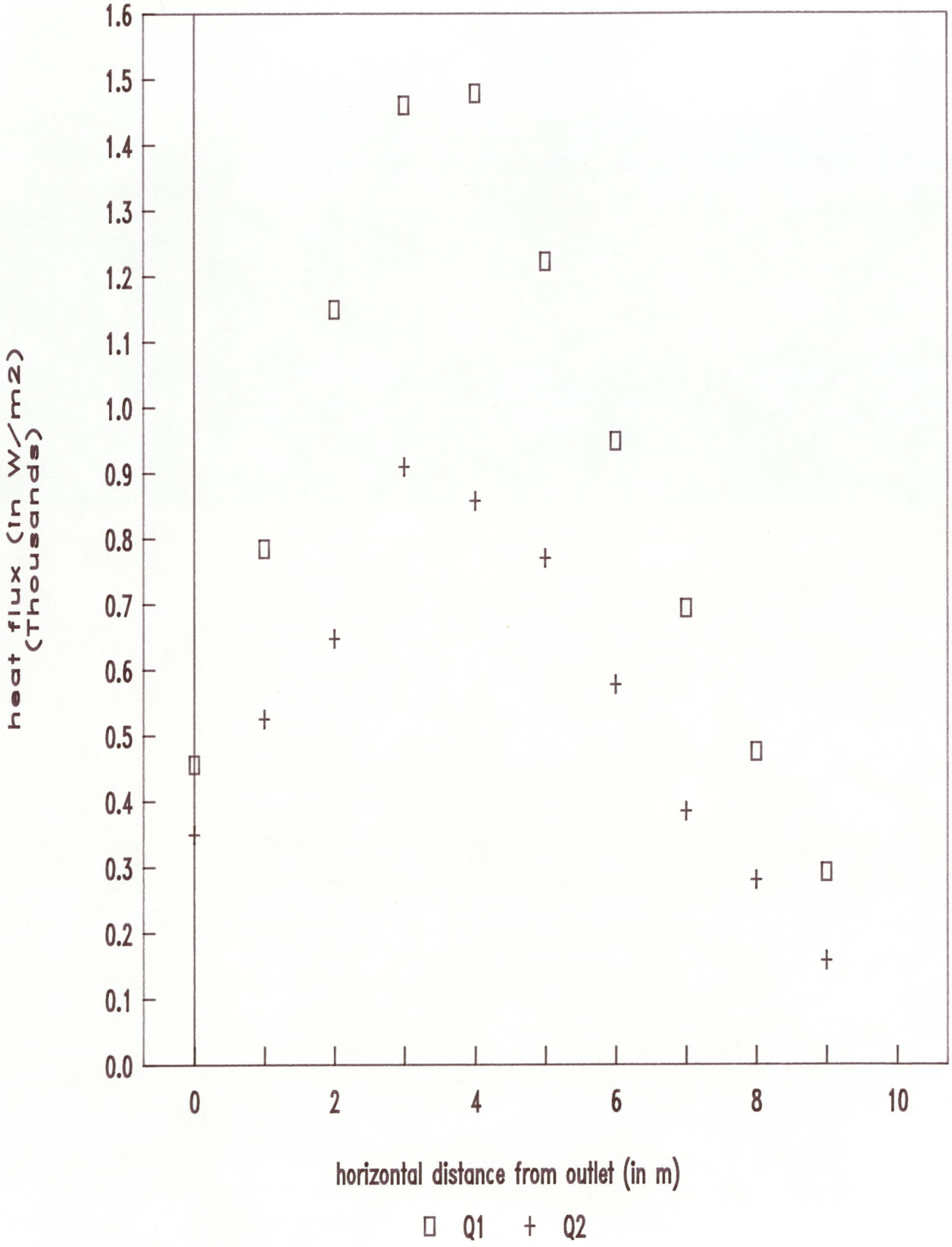

# Heat flux

H08

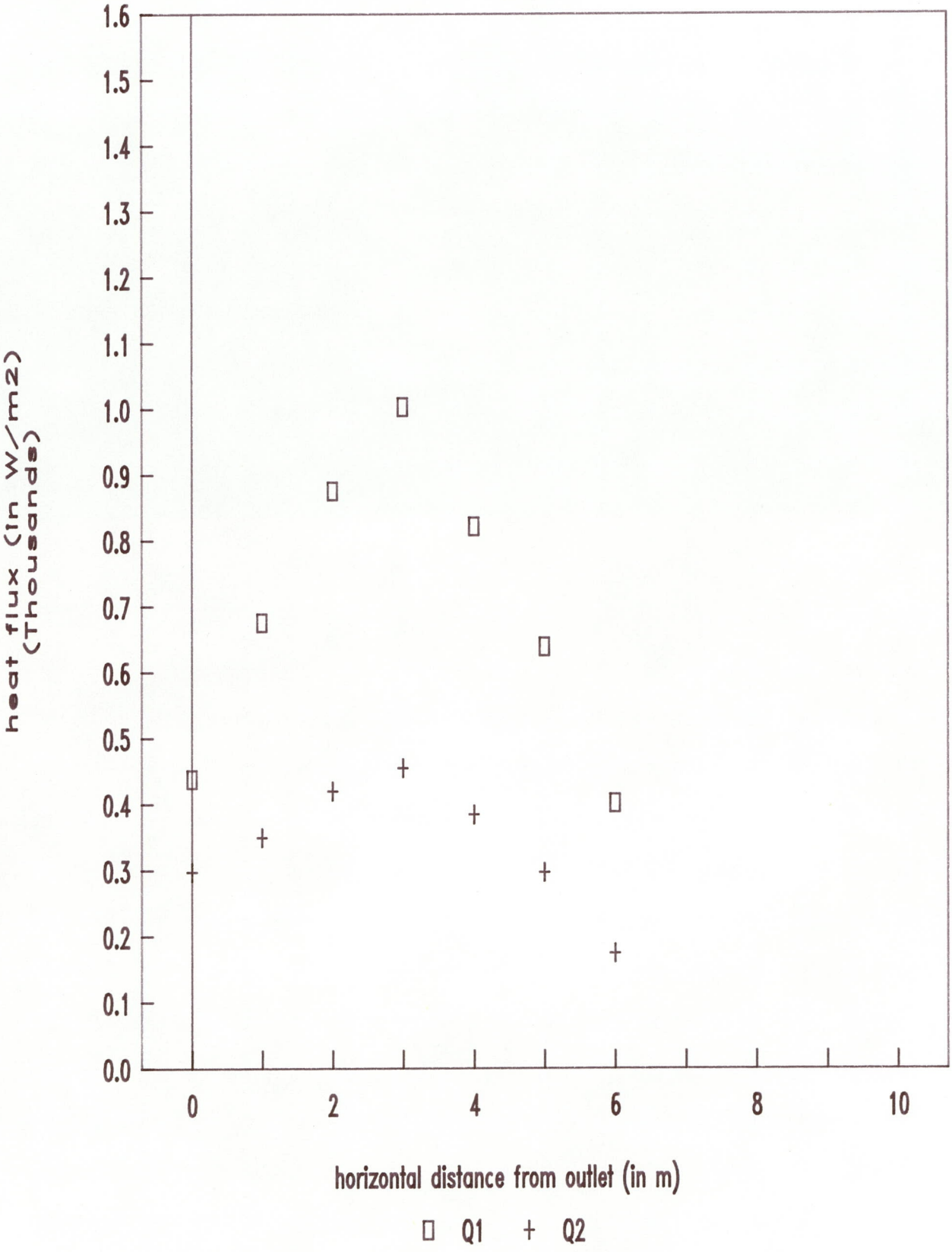

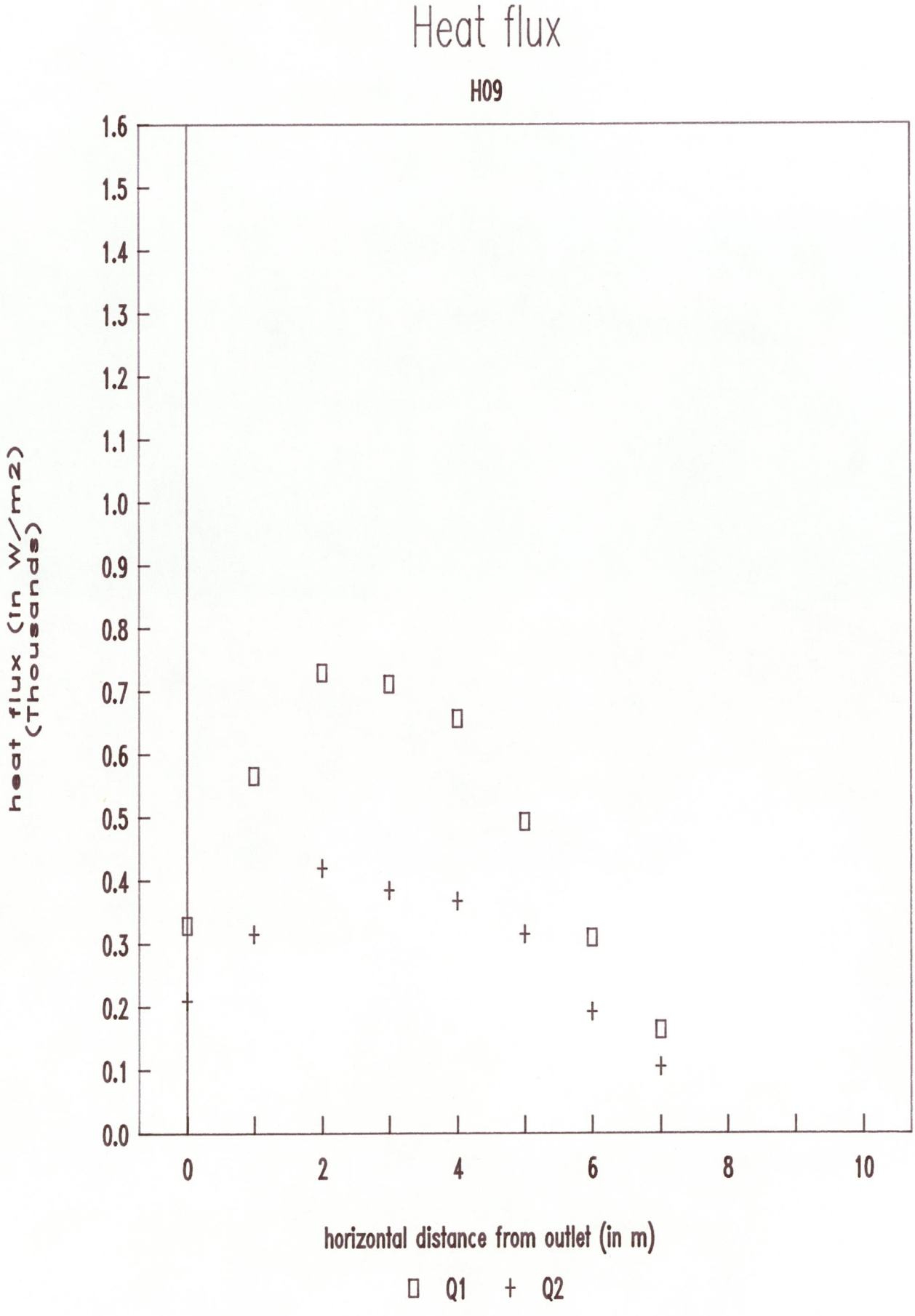
Heat flux
H09
heat flux (in W/m2)
(Thousands)
1.6
1.5
1.4
1.3
1.2
1.1
1.0
0.9
0.8
0.7
0.6
0.5
0.4
0.3
0.2
0.1
0.0
0
2
4
6
8
10
horizontal distance from outlet (in m)
Q1
Q2

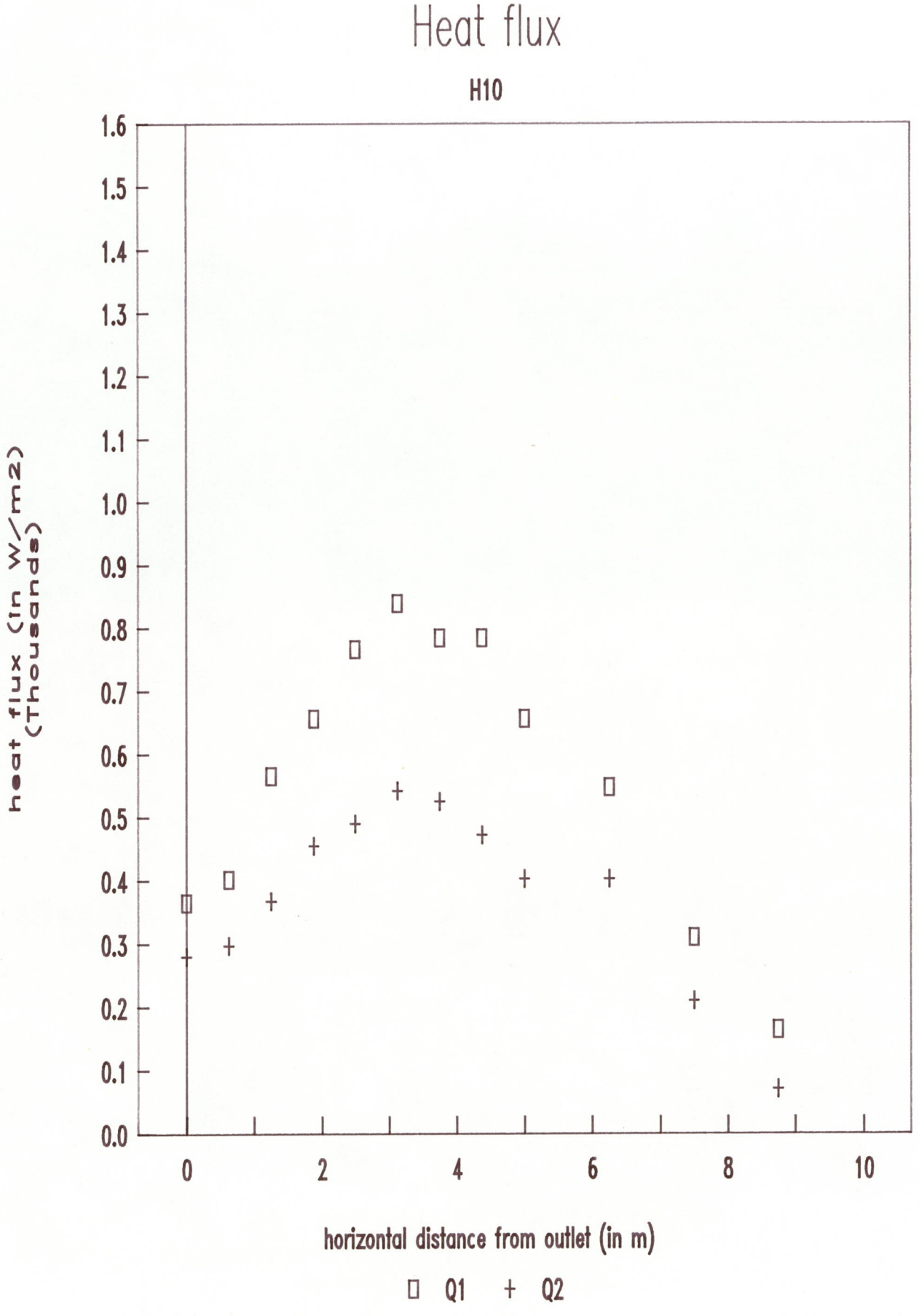
Heat flux
H10
heat flux (in W/m2)
(Thousands)
1.6
1.5
1.4
1.3
1.2
1.1
1.0
0.9
0.8
0.7
0.6
0.5
0.4
0.3
0.2
0.1
0.0
0
2
4
6
8
10
horizontal distance from outlet (in m)
Q1
Q2